論文 / 著書情報
Article / Book Information

題目(和文)	
Title(English)	A quick inspection method of U-shaped steel damper based on deformation behavior
著者(和文)	鄭皓文
Author(English)	ZHENG Haowen
出典(和文)	学位:博士(工学), 学位授与機関:東京工業大学, 報告番号:甲第12238号, 授与年月日:2022年9月22日, 学位の種別:課程博士, 審査員:吉敷 祥一,元結 正次郎,松岡 昌志,石原 直,佐藤 大樹
Citation(English)	Degree:Doctor (Engineering), Conferring organization: Tokyo Institute of Technology, Report number:甲第12238号, Conferred date:2022/9/22, Degree Type:Course doctor, Examiner:,,,,
学位種別(和文)	博士論文
Type(English)	Doctoral Thesis

A thesis submitted for the degree of

Doctor of Engineering

A quick inspection method of U-shaped steel damper based on deformation behavior

Zheng Haowen

Supervisor: Prof. Kishiki Shoichi

Department of Architecture and Building Engineering

Tokyo Institute of Technology

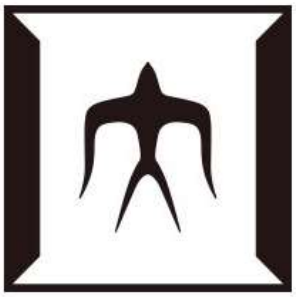

Contents

Acknowledgements

I would like to express my sincere thanks to all those who help me to compete my doctoral thesis:

Shoichi KISHIKI, Professor in Tokyo Institute of Technology, my academic advisor, for helping me formulate the research topic, methodology and guiding me through each stage of the process. I have learnt a lot from him, not only how to be a qualified researcher but also the way to be a nice man. It is my honor to receive his guidance.

Nobuhiko TATSUMI, Associate professor in Aichi Institute of Technology. I am deeply grateful for his patience and time in teaching me the precautions in experimental study. He is the most reliable partner I have ever seen.

Takanori ISHIDA, Associate professor in Yokohama National University, for his kind comment on my paper writing, both in English and Japanese.

Motoko OKUBO, Secretary of Kishiki lab, for her sincere kindness and consideration I have always been treated with, as well for helping me with all the paper work.

Atsushi WATANABE, Nippon steel, for giving me the opportunity to conduct an experimental study on U-shaped steel damper and for providing me the specimen tested in the dynamic cyclic loading experiment. I am also deeply grateful for his valuable comments on my paper writing.

Yang XIANG, Associate professor in Tongji University, for his help on establishing the data base of earthquake ground record and for his guidance to me on numerical simulation.

Jiaxi LI, Xiaoyu YNAG, Yang DONG, my friends in Kishiki lab, for their support and tolerance. It is my pleasure to meet you. I am willing to share happiness and sorrow with you in the rest of my life.

Miku KUROSAWA, my doctoral colleague in Kishiki lab, for teaching me a lot about the life in Japan and for your kind comment on my presentations.

In the end, I would like to thank my parents for their wise counsel and sympathetic. There is no doubt that I cannot make this without their understanding and support. I will try to live up to their exceptions and be a better me in the future.

Chapter 1

Introduction

1. Introduction

1.1. Seismic isolation technique

In August 1909, a medical doctor, J. A. Calantarients submitted a patent application to the British patent office for his construction method. He proposed an approach to reduce the force transmitted to the building itself by separating the building from its foundation with a layer composed of fine sand, mica, or tale that would allow the building to slide in earthquakes. This is the first well-documented example of an earthquake-resistant design strategy that was later known as "seismic isolation" [1-1]. During the same era, J. Bechtold from Germany was issued a US patent for an Earthquake Proof Building supported on a rigid plate that is mounted on balls of hard material such as loose pebble gravel. In his explanation, the rigid foundation of the conventional buildings is regarded as the main source of danger in the case of earthquakes. A rigid plate with suitable carrying power can prevent the building from being damaged by carrying the building freely [1-2]. The patents of Calantarients and Bechtold revealed the two key functions of seismic isolation system: 1), sufficient load-carrying capacity; and 2), capacity to uncouple the motion of the structure from the ground shaking. The third key function was introduced by R. W. de Montalk from New Zealand in the late 1930s. Montalk was issued a US patent for absorbing or minimizing the buildings' earthquake-induced vibration [1-2]. To achieve this, he described a bed composed of materials that will absorb or minimize shocks. Placing and retaining the bed between the base of the building and its solid foundation can prevent the building from earthquake-induced excitation. The term "absorb" revealed the third key feature of seismic isolation system—energy dissipation

capacity.

In the late 1960s, R. Ivan Skinner from New Zealand systematically expounded the theory of seismic isolation for civil structures [1-3]. Their findings are soon adopted in the design of a tall railway concrete bridge with base isolation [1-2]. Thereafter, the implementation of this earthquake protection strategy of buildings grew slowly but stably worldwide. People truly recognize that seismic isolation is an extremely effective means for buildings to fight against earthquake-induced damage in the 1990s. The performance of seismic isolated structures under catastrophic events was verified with the occasions of a series of severe earthquakes. The University of Southern California (USC) hospital building experienced strong vibration in the 1994 Northridge earthquake. However, due to the effectiveness of base isolation, the peak roof acceleration was reduced to nearly 50% of the peak ground acceleration, and the peak drift was controlled under 30% of the code specification. It is confirmed that the bearings worked normally and the superstructure remained elastic in the subsequent studies [1-4]. As in another earthquake-prone developed country Japan, the implementation of seismic isolation started in the early 1980s. less than a decade later, the excellent performance of two base isolation buildings (the Matsumura-Gumi Research Laboratory and the West Japan Postal Savings Computer Center (West-1)) in the 1995 Kobe earthquake kicked off a new era for seismic isolation technique [1-5]. The growth of base-isolated buildings increased to 150 buildings per year after 1995, making Japan a leading country in the number of base-isolated buildings [1-6].

The explosion of seismic isolation applications promotes the rapid maturity of new techniques. A large variety of seismic isolation devices are developed to fulfill the aforementioned functions of seismic isolation system. The high compressive strength and

low lateral stiffness of isolators provide the building with sufficient load-carrying capacity and freely moving capacity. The energy dissipation capacity of dampers is helpful to reduce the displacement experienced by the superstructure in the case of severe earthquakes and promotes the building to recover from shaking. The present study focuses on the relationship between the shape change induced by in-plane cyclic loading and cumulative damage of U-shaped steel dampers—one type of hysteretic dampers that is widely applied in the design practice of base-isolated structures in Japan—and establishing a quick inspection approach for it.

1.2. U-shaped steel damper and seismic isolation devices

1.2.1. seismic isolation devices

The majority of seismic isolation system's features are achieved rely on the devices known as "seismic isolation devices". Taking the base-isolated structure, for instance, isolators and energy dissipation devices have composed the main body of its base-isolated layer.

As aforementioned, the function of isolators includes 1) supporting the superstructure; and 2) reducing and inhibiting the transmission of vibrations by uncoupling the motion of ground and building. whereas, when an earthquake strikes, the building might crash into the around buildings if isolators cannot put the building back promptly. Isolators are always designed with the following characteristics to satisfy these requirements.

1). Sufficient compressive carrying capacity. The superstructure is connected with the ground surface only through isolators, which means isolators must be capable to hold up

the whole weight of the building.

2). Low lateral stuffiness. Reduces the response of the building by allowing the superstructure to move freely to a certain extent, and provides the structure with a longer natural vibration period to mitigate the potential threat from long-period ground motions. Otherwise, the base-isolated structure will be indistinguishable from the conventional ones.

3). Sufficient restoring force (re-centring capability). Prompt the building to get back to its original position.

The displacement experienced by a structure without damping tends to be relatively large. It is not conducive to the design practice of base-isolated structures in space-limited urban areas. Meanwhile, low damping makes it difficult for the structure to soon recover from swaying, and earthquake-induced energy can only be dissipated through the dynamics of the whole system. This results in significant challenges for structural damage control and gravely threatens the security of the people and equipment inside. Energy dissipation devices referred to as “dampers” are induced in the system to prevent the load-resisting structural elements from inelastic behavior by concentrating the input energy dissipation at pre-defined locations and consequently reduce the displacement experienced by the system. To achieve these purposes, dampers are generally fabricated with the following two characteristics:

1). Excellent energy dissipation capacity. As supplementary to the system’s energy dissipation capacity, dampers have to ensure reliable and stable performance in any extreme environments.

2). High initial stiffness. Ensure the building would not sway severely when suffering from wind load.

As a country devastated by natural disasters such as earthquakes and tsunamis, seismic isolation design has been a high priority in Japan. Thus, seems in comparison with the structural engineers from other regions of the world, Japanese structural engineers tend to be more concerned about the seismic-resistant capacity of the structure and are willing to consider more costly designs. In recent years, Rubber bearings (RB) and Sliding Bearings (SB) have been the most commonly used types of isolators in Japan. In the years before 1944, Natural rubber bearings (NRB, [1-13]) are the best-known isolator (applied in over 65% of cases) [1-6]. Their validity against the earthquake-induced vibration had survived the test of the 1995 Kobe earthquake. With the rapid development of seismic isolation techniques, Rubber bearings with a subset of the features of energy dissipation devices are subsequently developed and taken into use. HDRB (High Damped Rubber Bearings) and LRB (Lead Rubber Bearings, [1-13]) are outstanding representatives. Sliding Bearings such as Friction Pendulum bearings (Figure. 1-3) are normally applied in combination with these Rubber bearings.

Although the advent of isolators with energy dissipation capacity such as HDRB and LRB gives the designers more options, advantages such as using flexible, convenient replacement make dampers cannot be replaced completely. Takayama et al. (1993) reported that the seismic isolation devices that integrate the function of isolators and dampers have disadvantages in striking a balance between the system's re-centring and damping capability [1-7]. That is why incorporating various types of isolators and dampers in the design practice of base-isolated structures is becoming more and more popular in recent years. Furthermore, take Lead Rubber Bearings, for instance. The earthquake-induced energy is dissipated through the inserted lead plug's hysteretic behavior (Figure. 1-2 (a)). Therefore, the fatigue life of the metallic material would

seriously affect the service life of the whole system. Additionally, it is hard to evaluate the cumulative damage of the lead plug after years of use and the device cannot be fixed even though the lead plug is severely damaged because the lead plug is installed inside the device.

Dampers are conceived as and destined to a unitary function, meant to reduce the displacement experienced by the superstructure and protect the main components from irreparable plastic damage. In comparison with isolators, the variety of dampers is rather limited. Types of dampers commonly used include 1) hysteretic, and 2) fluid viscous dampers. Fluid viscous dampers such as oil dampers (Figure. 1-4) dissipate the energy through convert it to the kinetic energy of the high-pressure fluid [1-8]. Hysteretic dampers exercise the function of energy dissipation through frictional forces arising from the relative motion between two contacting surfaces (friction damper) or outstanding plastic deformation capacity of metallic materials (metallic damper (Figure. 1-5) [1-9]). U-shaped steel damper (Figure. 1-5(b)) is a type of metallic damper. The specially designed curved part greatly optimizes the dampers' plastic deformation capacity and extents its fatigue life [1-10]. Unlike another type of widely adopted metallic damper—lead damper (Figure. 1-5(a)) [1-11] [1-12], steel dampers demonstrate less dependence on temperature and loading speed. Stable performance promotes the rapid growth of the application of U-shaped steel dampers in recent years.

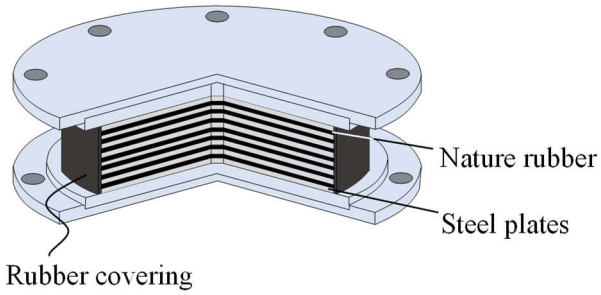

(a). Configuration (b). Photo [1-13]

Figure. 1-1 Natural Rubber Bearing

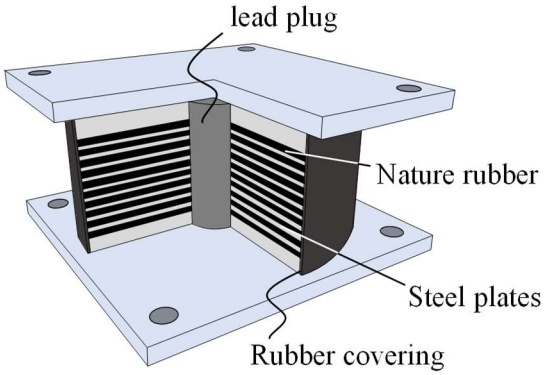

(a). Configuration (b). Photo [1-14]

Figure. 1-2 Lead Rubber Bearing

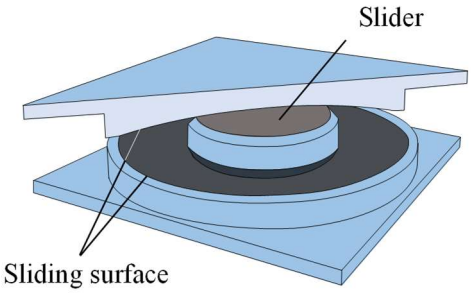

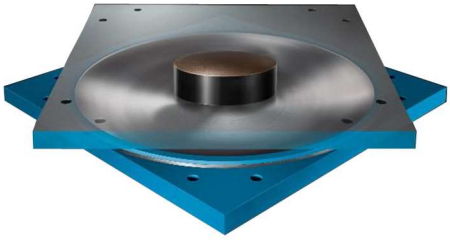

(a). Configuration (b). Photo [1-15]

Figure. 1-3 Simple friction pendulum friction

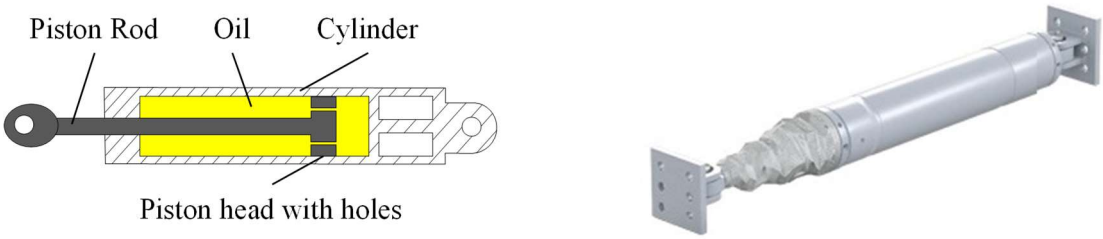

(a). Configuration (b). Photo [1-16]

Figure. 1-4 Oil damper

(a). U-shaped lead damper [1-17] (b). U-shaped steel damper [1-18]

Figure. 1-5 Metallic damper

1.2.2. U-shaped steel dampers

Research into U-shaped steel energy dissipation devices began in the early 1990s. Echavarría et al. proposed oval-shaped strips energy dissipation devices that dissipate energy through the rolling–bending motion of oval steel elements positioned horizontally [1-19]. This type of energy dissipation device is assumed to be adopted in "*one story, one-bay steel frames with inverted Y-shaped braces*". Varieties of U-shaped energy dissipation devices are developed since entering the new century. Kato et al. described a J-shaped metallic damper in 2004 (Figure. 1-6) [1-20]. Four energy dissipation plates are fixed

between the connection plates and a loading plate that is connected to the wall with two rollers. Consequently, energy dissipation would be achieved through the rolling–bending motion of the U-shaped plates caused by the relative motion between wall and connection plates.

Suzuki et al. conceived the idea of U-shaped steel dampers [1-10]. U-shaped steel dampers not only possess the general features of dampers such as using flexible and ease of maintenance but also enable the system to suit the different types and magnitudes of loads present at particular structural support locations through different configurations (Figure. 1-7) of dampers. To enhance the seismic energy dissipation and plastic deformation capability of U-shaped steel dampers, researchers are dedicated to optimizing the appearance of U-dampers. Deng et al. and Khatibinia et al. focused on the effect of the main influential dimensions such as the length, height, thickness of the dampers, and the shape of its parallel arms [1-21] [1-22]. Atasever et al. broke through the outline of commercially used U-shaped steel dampers and proposed new types with perforated and nonparallel arm configurations [1-23].

The object of the present research—the standardized products of U-shaped steel dampers manufactured by Nippon Steel (referred to here as U-dampers) —are engineered based on long-accumulated technologies in the fields of steel material and energy dissipation devices. The U-shaped element is fabricated by a type of high-quality rolled steel SN490B. The U-shaped curved part is built after a series of cold bending and heat treatment processes. The main features of U-dampers can be summarized as follows:

1). Specially designed U-shaped. The geometric proportions of U-dampers were determined based on numerous sets of loading tests. The resultant strain caused by cyclic loading tends to disperse all over a U-shaped element rather than concentrating on a

certain place. The fatigue life of the U-shaped element is greatly extended by this special design.

2). Stable performance in harsh environments. Cyclic loading tests conducted in the previous studies demonstrated U-dampers' low dependence on temperature and loading speed. Additionally, almost no strength deterioration was observed even though the damper was loaded under large deformation amplitude.

3). Differently sized U-shaped elements are similar in shape. Five commercially available sizes of the U-damper (Figure. 1-8 and Table 1-1) were designed to address different capacities. Previous experimental studies [1-24] indicated that the properties of differently sized dampers could be evaluated based on similarity principles. Therefore, it is much more flexible to determine the number or size of the damper to fit the design requirements, such as the required yield shear force of the system.

U-dampers have been among the most widely used energy dissipation devices in Japan for several types of seismic isolated structures due to the aforementioned advantages. After the 2011 Great East Japan Earthquake, almost none of the U-dampers used in base-isolated buildings were reported to be seriously damaged even in severely affected areas.

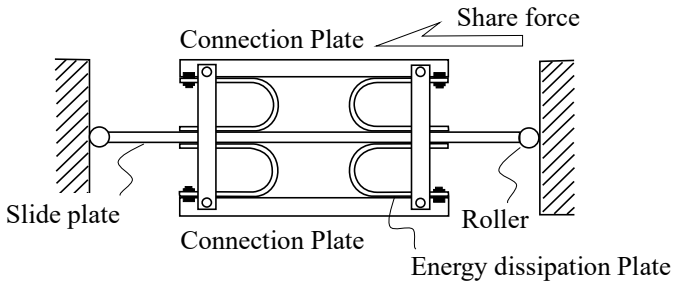

Figure. 1-6 The composition of a J-shaped metallic damper

Figure. 1-7 Example of U-shaped steel dampers' different configurations [1-15]

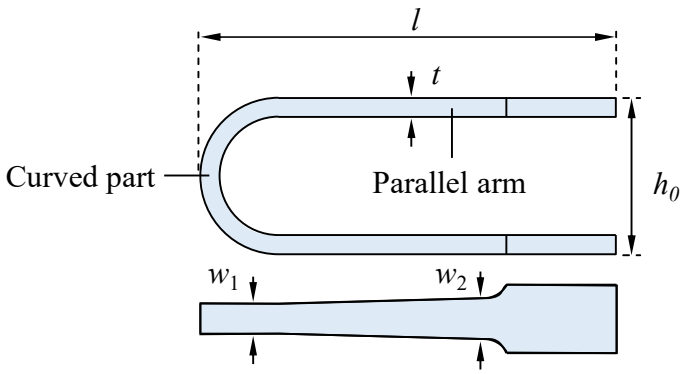

Figure. 1-8 Outline of the specimen

Table 1-1 Geometric characteristics

Damper size	L (mm)	h_0 (mm)	t (mm)	w_2 (mm)	w_1 (mm)
UD40	611	231	28	60	45
UD45	758	284	36	74	55*
UD50	882	335	40	87	65
UD55	983	374	45	97	72*
UD60	1199	453	55	118	88

(*: Calculated value based on the available data)

1.3. Research objectives

To minimize personal injury and property damage, conducting post-earthquake safety

assessments for building subjected to severe vibration as soon as possible has been a consensus. Damage evaluation approaches of structural components based on visible damage can usually provide speedy results and are relatively easy to implement. Thus, these damage estimation methods are ideal for the structure's quick inspection and can provide the primary mechanism for prohibiting secondary hazards. Kishiki et al. conducted a series of studies from 2014 to 2017 and proposed quick inspection methods for structural components such as exposed column bases, single angle braces, and steel columns based on visible damage such as the crack pattern initiating on the concrete foundation and the residual deformation caused by local buckling [1-25] [1-26] [1-27]. Ufuk described a seismic assessment method of buildings using post-earthquake residual displacement in his doctoral thesis [1-28]. Raghunandan et al. (2015) discussed in depth the correlation between the residual inter-story drift and the reduction in collapse capacity of reinforced concrete frame structures [1-29].

A series of dynamic cyclic loading tests confirmed a positive correlation between the residual plastic deformation and cumulative damage of U-dampers (Figure. 1-9). This finding reveals the possibility of establishing a cumulative damage evaluation approach for U-shaped steel dampers based on shape change. U-dampers loaded under in-plane loading normally deform in the way shown in Figure. 1-9. The most obvious residual plastic deformation initiates in the middle part of the parallel arms when deformation returns to 0 (the superstructure returns to its original location) (APPENDIX A), whereas the accumulation of residual plastic deformation would not be induced by the dampers' out-of-plane deformation. Therefore, the focus of the present study has been 1) the development of the in-plane cyclic loading induced residual plastic deformation that initiates in the middle part of parallel arms when deformation equals 0, and 2) how this

deformation behavior correlates to the dampers' cumulative damage. However, as aforementioned, it is unsafe to ignore the effect of the factors, such as the damper's out-of-plane and torsion deformation. The effect of these factors on the dampers' cyclic deformation capacity and quick inspection method composed in the present study is briefly discussed in APPENDIX C and will be systematically investigated in further study.

Kishiki et al. and Ene et al. had systemically discussed the cumulative damage evaluation of U-dampers from 2008 to 2016 [1-30] [1-31] [1-32] [1-33], the deformation behavior of U-dampers under cyclic loading remains uncharted territory. On the other hand, the quick inspection of U-dampers cannot rely solely on the residual plastic deformation initiating on the dampers' parallel arms. A U-damper loaded under relatively small amplitude deformation might be damaged more seriously than the one loaded under relatively large deformation amplitude, even though they are the same in residual plastic deformation. Other commonly available factors such as the maximum displacement experienced by base-isolated layers and duration of earthquake-induced vibration are found to be tightly correlated to the U-dampers' cumulative damage as well. How to use these factors to achieve the cumulative damage estimation of U-dampers has been the other pressing concern of the present study.

For this purpose, the objectives of the present study are targeted as follows (Figure. 1-10).

1). A set of dynamic cyclic loading tests of U-dampers are conducted to investigate the deformation behavior of the dampers loaded under constant deformation amplitude. The previously discussed cumulative damage evaluation method is adopted as a tool to describe the fatigue behavior of the dampers, while a new indicator—residual plastic deformation ratio—is introduced for quantifying the deformation behavior of the dampers.

Consequently, a set of evaluation equations are proposed to describe the correlation between the residual plastic deformation and the cumulative damage when the dampers are loaded under constant deformation amplitude **(Chapter 2)**.

2). Effect of random waves on the U-dampers' residual plastic deformation-cumulative damage relationship is indicated by a set of dynamic loading tests under complicated loading histories. Using the proposed residual plastic deformation-cumulative damage relationship evaluation equations, a precision verification approach for the previously discussed cumulative damage evaluation method is discussed **(chapter 3)**.

3). Assess the reliability of U-damper under various hazard levels of earthquakes by conducting a set of nonlinear time-history analyses. Based on the analytical results, indicators of visible damage such as the plastic deformation of the dampers and the maximum displacement experienced by base-isolated layers are adopted in the quick inspection method of U-damper **(chapter 4)**.

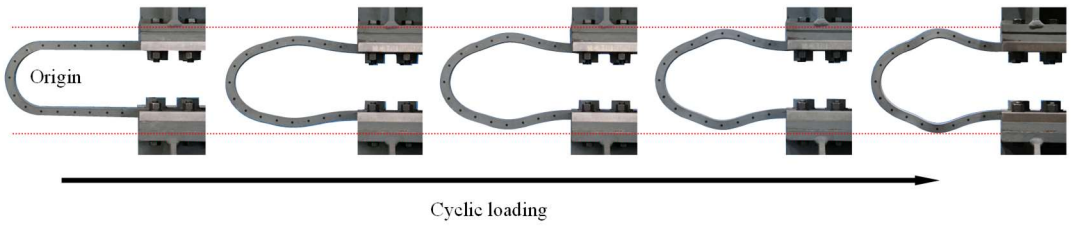

Figure. 1-9 Residual plastic deformation caused by cyclic loading

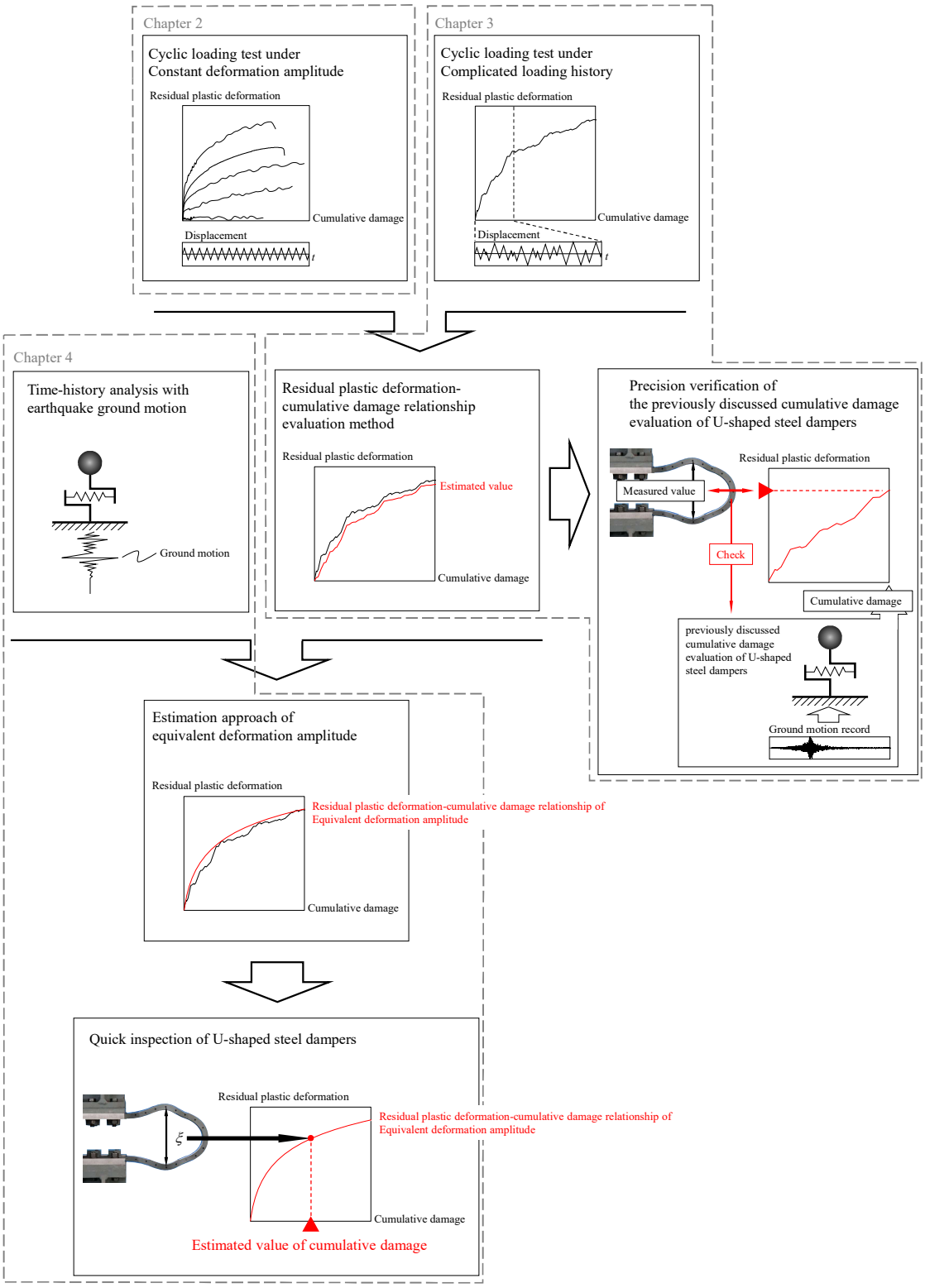

Figure. 1-10 Research objectives

1.4. Reference

[1-1] Naeim F, and Kelly J. Design of Seismic Isolated Structures — From Theory to Practice, Wiley, New York. 1-23.

[1-2] Nicos Makris. Seismic isolation: Early history, Earthquake Engineering & Structural Dynamics. 2019; 48:269-283.

[1-3] Skinner R, Robinson W, McVerry G. An Introduction to Seismic Isolation, Wiley, England. 1993.

[1-4] Nagarajaiah S, and Sun. Response of base-isolated USC hospital building in Northridge Earthquake, Journal of Structural Engineering. 126(10), 1177–1186.

[1-5] Clark P, Aiken I, Nakashima M, Miyazaki M, and Midorikawa M. “The 1995 Kobe (Hyogo-ken Nanbu) Earthquake as a trigger for implementing new seismic design technologies in Japan,” Lessons Learned Over Time, Learning From Earthquake Series; Earthquake Engineering Research Institute.

[1-6] Pan P, Zamifrescu D, Nakashima M, Nakayasu N, Kashiwa H. Base-isolated design practice in Japan: Introduction to the post-Kobe approach. Journal of Structural Engineering 2005;9(1):147–71.

[1-7] 森田慶子，高山峯夫，多田英之，積層ゴムアイソレータの設計上の諸問題について，日本建築学会大会学術講演梗概集(関東), pp.543-544, 1993.9

(Morita K et al. Considerations about the Basic Design of Rubber Bearing. Proceedings of Architectural Institute of Japan (AIJ) Annual Conference 1993;543-544.)

[1-8] Lee D, Taylor D. Viscous damper development and future trends. The structural

design of tall buildings 2011; 10:311-320.

[1-9] 多田英之，酒井 章，森田慶子，姫野多加男，免震ダンパーに関する研究，その 1, 2，日本建築学会九州支部研究報告, pp.133-140，昭和 61 年 3 月

[1-10] Suzuki K, Watanabe A, Saeki E. Development of U-shaped steel damper for seismic isolation system. Nippon Steel Tech Report No. 92 July 2005.

[1-11] 多田英之，酒井 章，高山峯夫，早川邦夫，免震構造に関する実物実験，その 12, 13，日本建築学会大会学術講演梗概集(北海道), pp.821-824, 1956.7

(Tada H et al. The research study of Aseismic Isolation System by the Enforcement Construction, Part. 12, 13. Proceedings of Architectural Institute of Japan (AIJ) Annual Conference 1956;821-824.)

[1-12] 高山峯夫，多田英之，瓜生 満，鈴木政美，北村春幸，吉江慶祐，鉛ダンパーのエネルギー吸収能力に関する実大実験，日本建築学会大会学術講演梗概集(北海道), pp.605-606, 1995.8

(Takayama M et al. Experimental Study on Energy Dissipation Capacity of Lead Damper for Base Isolation System. Proceedings of Architectural Institute of Japan (AIJ) Annual Conference 1995;605-606.)

[1-13] 昭和電線ケーブルシステム株式会社，天然ゴム系積層ゴムアイソレータ Ver.7

https://www.swcc.co.jp/cs/products/catalog/pdf/seimic_isolator.pdf

2021/09

[1-14] Blandford E, Keldrauk E, Laufer M, Mieler M, Wei J, Stojadinovic B, and

Peterson P. Advanced seismic base isolation methods for modular reactors. Departments of Civil and Environmental Engineering and Nuclear Engineering University of California Berkeley, California. September 30, 2009.

[1-15] 日鉄エンジニアリング株式会社，日鉄エンジニアリング NS-SSB 免震デバイス
https://www.eng.nipponsteel.com/steelstructures/product/base_isolation/nsssb/
2022/07/07

[1-16] 株式会社ティーメック，制震用オイルダンパー
https://t-mec.co.jp/department/overseas/dep12_2/
2022/07/07

[1-17] 住友金属鉱山シポレックス株式会社，免震鉛ダンパー
https://www.sumitomo-siporex.co.jp/data/download/pdf/lead_damper.pdf
2022/01/20

[1-18] 日鉄エンジニアリング株式会社，免震 NSU ダンパー
https://www.eng.nipponsteel.com/business/building_and_infrastructure/response_control_and_seismic_isoloation_devices/nsu/
2022/07/07

[1-19] Echavarría A, Aguirre M, Maldonado J, López O. Dynamic behavior of two types of energy dissipation devices ‘Shear-Panel’ and ‘Oval-Shaped Steel Strips’. Proceedings, 11th World Conference on Earthquake Engineering, Acapulco, Mexico. June 1996.

[1-20] Kato S, Kim Y, Nakazawa S, Ohya T. Simulation of the cyclic behavior of J-

shaped steel hysteresis devices and study on the efficiency for reducing earthquake responses of space structures. Journal of constructional steel research, 2005; 61:1457–1473.

[1-21] Deng K, Pan P, Su Y, Xue Y. Shape optimization of U-shaped damper for improving its bi-directional performance under cyclic loading. Engineering Structures 2015;93:27–35.

[1-22] Khatibinia M, Jalaipour M, Gharehbaghi S. Shape optimization of U-shaped steel dampers subjected to cyclic loading using an efficient hybrid approach. International Journal of Steel Structures 197 (2018): 108874.

[1-23] Atasever K, Celik O, Yuksel E. Development and cyclic behavior of U-shaped steel dampers with perforated and nonparallel arm configurations. International Journal of Steel Structures 2018;18(5):1741–1753.

[1-24] Jiao Y, Kishiki S, Yamada S, Ene D, Konishi Y, Hoashi Y, Terashima M. Low cyclic fatigue and hysteretic behavior of U-shaped steel dampers for seismically isolated buildings under dynamic cyclic loadings. Earthquake Engineering & Structural Dynamics, 2015;44:1523–38.

[1-25] 吉敷祥一，山田 哲，露出柱脚の基礎コンクリート周辺ひび割れに基づく損傷評価，“見える損傷”の定量化に基づく鋼構造骨組の即時損傷評価法，その 1，日本建築学会構造系論文集 第 79 巻 第 704 号, pp.1547-1557, 2014.10 (Kishiki S et al. Damage evaluation based on crack pattern and its width on the concrete foundation of exposed column base. Quick inspection method for steel structures based on the visible damage Part 1. Journal of Structural and Construction Engineering (Transactions of AIJ) 2014;79(704):1547–1557.)

[1-26] 吉敷　祥一, 巽　信彦, 単一山形鋼ブレースの残留たわみと両脚の開きに基づく損傷評価, “見える損傷”の定量化に基づく鋼構造骨組の即時損傷評価法, その 2, 日本建築学会構造系論文集 第 81 巻 第 719 号, 143-153, 2016.1
(Kishiki S et al. Damage evaluation based on the residual out-of-plane deformation and the leg opening of single angle brace. Quick inspection method for steel structures based on the visible damage Part 2. Journal of Structural and Construction Engineering (Transactions of AIJ) 2016;81(719):143–153.)

[1-27] 吉敷祥一, 岩崎祐介, 局部座屈変形に基づく鋼柱の残存耐力評価, “見える損傷”の定量化に基づく鋼構造骨組の即時損傷評価法, その 3, 日本建築学会構造系論文集 第 82 巻 第 735 号, 735-743, 2017.5
(Kishiki S et al. Evaluation of residual strength based on local buckling deformation of steel column. Quick inspection method for steel structures based on the visible damage Part 3. Journal of Structural and Construction Engineering (Transactions of AIJ) 2017;82(735):735–743.)

[1-28] Ufuk Y. The use of post-earthquake residual displacements as a performance indicator in seismic assessment. Doctoral Thesis, Middle East Technical University (METU). Ankara, Turkey. 2009

[1-29] Raghunandan M, Liel A, Luco N. Aftershock collapse vulnerability assessment of reinforced concrete frame structures. Earthquake Engineering & structural dynamics 2015; 44:419–439.

[1-30] 吉敷祥一, 大河原勇太, 山田　哲, 和田　章, 免震構造用 U 字形鋼材ダ

ンパーの繰り返し変形性能に関する研究，日本建築学会構造系論文集，第 73 巻，第 624 号, pp.333-340, 2008.2

(Kishiki S et al. Experimental evaluation of cyclic deformation capacity of U-shaped steel damagers for base-isolated structures. Journal of Structural and Construction Engineering (Transactions of AIJ) 2008;73(624):333–340.)

[1-31] 吉敷祥一，高山　大，山田　哲，エネ　デイアナ 小西克尚，川村典久，村嶋正雄，水平 2 方向載荷下における繰り返し変形性能に関する実験，免震構造用 U 字形鋼材ダンパーの水平 2 方向特性，その 1，日本建築学会構造系論文集，第 77 巻，第 680 号, pp.1579-1588, 2012.12

(Kishiki S et al. Experimental evaluation of cyclic deformation capacity of U-shaped damagers subjected to bi-directional loadings. Bi-directional characteristics of U-shaped steel dampers for base-isolated structures Part 1. Journal of Structural and Construction Engineering (Transactions of AIJ) 2012;77(680):1579–1588.)

[1-32] Ene D, Kishiki S, Yamada S, Jiao Y, Konishi Y, Terashima M, Kawamura N. Experimental study on the bidirectional inelastic deformation capacity of U-shaped steel dampers for seismic isolated buildings. Earthquake Engineering & Structural Dynamics 2016;45(2):173–192.

[1-33] Ene D, Yamada S, Jiao Y, Kishiki S, Konishi Y. Reliability of U-shaped steel dampers used in base-isolated structures subjected to biaxial excitation. Earthquake Engineering & Structural Dynamics 2017;46:621–

Chapter 2

Deformation behavior of U-shaped steel damper under cyclic loading with constant deformation amplitude

2. Deformation behavior of U-shaped steel damper under cyclic loading with constant deformation amplitude

2.1. Introduction

Indicating the relationship between the deformation behavior and the cumulative damage of U-damper is the top priority of the present study. Chapter 2 focuses on quantitatively evaluating the dampers' deformation behavior and mathematically describing the correlation between the shape change and cumulative damage of the dampers loaded under constant deformation. This is fundamental for investigating the effect of earthquake-induced excitations.

The fatigue behavior of U-damper is firstly systematically formulated by Ohkawara et al. in 2007 [2-1]. They composed a cyclic deformation capacity prediction method for single U-shaped elements loaded under in-plane constant deformation amplitude based on Manson-coffin law (APPENDIX A). Whereas, the fatigue life of differently sized dampers can only be described through the corresponding deformation amplitude (δ_t, Figure. 2-1)-number of loading cycles to fracture (N_f) relationship.

Kishiki et al. (2008) [2-2] presented that the fatigue life of differently sized U-damper can be precisely evaluated using a dimensionless indicator—peak-to-peak horizontal shear angle γ_t (%) (Eq (2-1)(a)). h_0 is the original height of the dampers (Figure. 1-9).

$$\gamma_t = \frac{\delta_t}{h_0} \qquad \text{(a)} \quad \text{Eq (2-1)}$$

Correspondingly, the peak deformation amplitudes on the positive and negative sides were converted to γ_+ (%) (Eq (2-1)(b)) and γ_- (%) (Eq (2-1)(c)), respectively.

$$\gamma_+ = \frac{\delta_+}{h_0} \qquad \text{(b)} \quad \text{Eq (2-1)}$$

$$\gamma_- = \frac{\delta_-}{h_0} \qquad \text{(c)}$$

Additionally, in the process loading test, the dampers' deformation δ can be expressed as γ(%) (Eq (2-1)(d)).

$$\gamma = \frac{\delta}{h_0} \qquad \text{(d)} \quad \text{Eq (2-1)}$$

And optimized the evaluation method composed by Ohkawara et al. (Eq (2-2)). N_f indicates the number of loading cycles to fracture. γ_t, γ_e, and γ_p denote the peak-to-peak, elastic, and plastic deformation amplitude. The fatigue life of U-damper is precisely but slightly underestimated by this curve.

$$\gamma_e = 35 \cdot N_f^{-0.15} \qquad \text{(a)} \quad \text{Eq (2-2)}$$

$$\gamma_p = 3620 \cdot N_f^{-0.80} \qquad \text{(b)}$$

$$\gamma_t = 35 \cdot N_f^{-0.15} + 3620 \cdot N_f^{-0.80} \qquad \text{(c)}$$

However, the value of N_f corresponding to a certain deformation amplitude γ_t cannot be calculated directly using this equation. To resolve this problem, Kishiki et al. dropped the way to separately evaluate the fatigue behavior of U-damper loaded under plastic and elastic deformation amplitude and composed a simplified but more accessible equation in 2012 (Eq (2-3)) [2-3].

$$_{0^\circ}\gamma_t = 2370 \cdot N_f^{-0.66} \quad 20\% \le {}_{0^\circ}\gamma_t \le 500\% \qquad \text{Eq (2-3)}$$

Meanwhile, a set of equations for fatigue behavior evaluation under out-of-plane excitation (Eq (2-4)) is composed [2-3].

$$_{90^\circ}\gamma_t = 2535 \cdot N_f^{-0.55} \quad 20\% \le {}_{90^\circ}\gamma_t \le 253.5\% \qquad \text{(a)} \quad \text{Eq (2-4)}$$

$$_{90^\circ}\gamma_t = 644 \cdot N_f^{-0.23} \quad 253.5\% \le {}_{90^\circ}\gamma_t \le 500\% \qquad \text{(b)}$$

Based on the previous discussion about the fatigue life of U-damper, Ene et al. (2016) developed a cumulative damage evaluation method for U-dampers under bidirectional excitation (Figure. 2-2) based on Miner's law (APPENDIX A). The damage in the in-plane (Eq (2-5)(a)) and out-of-plane directions (Eq (2-5)(b)) was assumed to accumulate simultaneously. Consequently, the cumulative damage to the dampers was evaluated by calculating the sum of the damage in both directions (Eq (2-5)(c)) [2-4] [2-5].

$$_{0^\circ}D = \sum_{i=1}^{n}\left(\frac{n_i}{{}_{0^\circ}N_{f,i}}\right) \qquad \text{(a)} \quad \text{Eq (2-5)}$$

$$_{90^\circ}D = \sum_{j=1}^{m}\left(\frac{n_j}{{}_{90^\circ}N_{f,j}}\right) \qquad \text{(b)}$$

$$D = \sum_{i=1}^{n}\left(\frac{n_i}{{}_{0^\circ}N_{f,i}}\right) + \sum_{j=1}^{m}\left(\frac{n_j}{{}_{90^\circ}N_{f,j}}\right) \qquad \text{(c)}$$

Where n_i and n_j are the frequency of the cycles having deformation amplitude $\gamma_{t,i}$ for 0-degree direction and $\gamma_{t,j}$ for 90-degree direction. $N_{f,i}$, and $N_{f,j}$ are the corresponding number of cycles to the fracture. The value of $N_{f,i}$, and $N_{f,j}$ are defined by Eq. (2-3) and Eq. (2-4), respectively. n and m are the total numbers of cycles in 0-degree and 90-degree directions.

Meanwhile, it is indicated that ignoring the effect of the torsion deformation of the dampers leads to unsafe estimated values of cumulative damage. After checking the cumulative damage of the dampers loaded with circular and elliptical patterns, in her own words, Diana Ene explained: "*The cyclic deformation capacity under bidirectional loading is reduced by the presence of torsion induced by the swaying motion of the upper structure*". Thus, an empirical index—sway-motion index J_f—is introduced in Ene et al. (2016) [2-4] to quantify the complexity of the displacement orbit experienced by the base-isolated layer, and index J_f is employed further to estimate the effect of the torsion deformation on the reduction of cyclic deformation capacity of U-dampers. Consequently, the upper limit to the reduction of the cyclic deformation capacity caused by the dampers'

torsion deformation was founded. The cyclic deformation capacity of a U-damper loaded under a pattern with a relatively large J_f (over 30 rad) might decrease to 0.4 times that loaded under unidirectional loading (APPENDIX C).

Additionally, Kishiki et al. (2008) indicated that, although U-dampers always operate under bidirectional excitations, the damage is primarily caused by in-plane excitations. When loaded with identical deformation amplitudes, the number of loading cycles to fracture under in-plane excitation is substantially less than that under out-of-plane excitation. Moreover, because an observable change in the shape of the U-damper initiates only under in-plane excitations, this study focused on the deformation behavior of a U-damper under in-plane excitation The effect of bidirectional loading and the torsion deformation of U-damper on the cumulative damage evaluation based on deformation behavior remains to be further studied.

Eq (2-2) (c) is adopted to evaluate the dampers' cyclic loading capacity (Eq (2-6)). Based on Miner's rule (Miner 1945), the estimated value of the number of cycles until fracture ($N_{f,i}$) under a constant deformation amplitude can also be applied to evaluate the cumulative damage (D) of the U-damper loaded under seismic excitation. The present study focuses on the deformation behavior of U-damper induced by in-plane cyclic loading, Thus, Eq (2-3)(a) is adopted to describe the dampers' cumulative damage D (Eq (2-7)).

$$\gamma_{t,i} = 35 \cdot N_{f,i}^{-0.15} + 3620 \cdot N_{f,i}^{-0.80} \qquad \text{Eq (2-6)}$$

$$D = \sum_{i=1}^{n} \left(\frac{n_i}{N_{f,i}} \right) \qquad \text{Eq (2-7)}$$

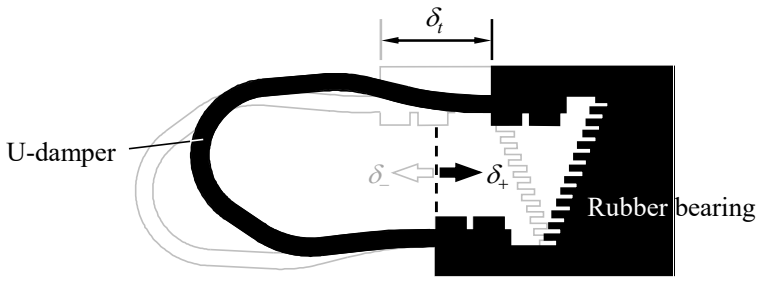

Figure. 2-1 Deformation amplitude (δ_t)

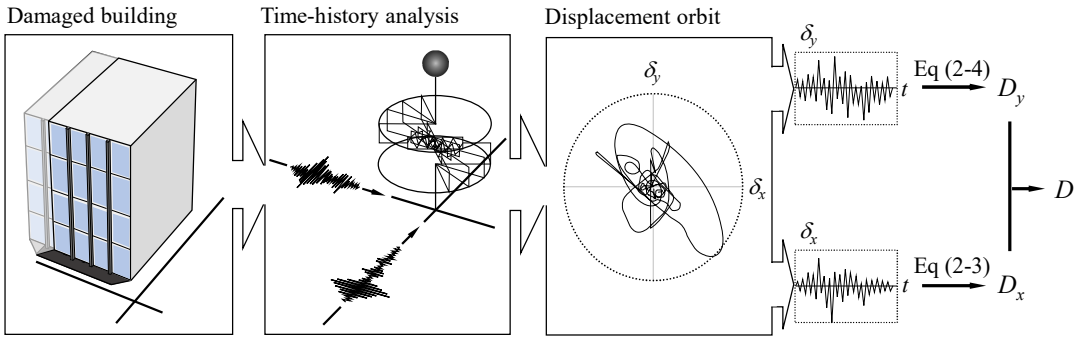

Figure. 2-2 Cumulative damage evaluation method of U-damper loaded under bidirectional loading (Ene et al. 2016)

2.2. Residual plastic deformation caused by cyclic loading

Residual plastic deformation initiates on the parallel arms of U-dampers due to cyclic loading. The cause of this phenomenon is investigated in this section using Finite Element Method (FEM modeling).

2.2.1. Creation of the FEM model

Before the cyclic loading tests, problems, such as residual plastic deformation of the

parallel arms' which area is most obvious that can be used as an indicator to evaluate the dampers' deformation behavior, should be determined in advance. For this purpose, a FEM model has been composed in the present study to indicate the deformation behavior of such a single U-shaped element loaded under cyclic loading.

The creation of the FEM model obeys the following rules:

1). The Model is a three-dimensional FEM single U-shaped element created by ABAQUS/CAE 2020. The element type is set to be general purpose linear brick element C3D8R (8-node linear brick, reduced integration with hourglass control). The size of the FEM model remains the same as that of U-damper UD.40 [Table 1-1].

2). Material properties. Taking the results of coupon tests of U-damper from the previous study as a reference [2-6], the analytical model's material property is simplified to a bilinear constitutive model. Young's Modulus and Poisson's ratio are respectively assumed to be 205GPa and 0.3 according to AIJ Standard for Allowable Stress Design of Steel Structure [2-7]. Yield and tensile strength remain the same as that of coupon test results [2-6] and are set to be 380GPa and 540GPa, respectively. Additionally, the material's hardening behavior is described as the kinematic hardening rule. The material property (true strain (ε_t)-true stress (σ_t) relationship) used in the input file is illustrated in Figure. 2-3.

3). Mesh refinement (Figure. 2-4(a)). The deformation behavior of the parallel arms is the main investigation objective. Therefore, the element size of parallel arms is purposely assigned to be smaller than that of the curved part and connection part in the process of mesh refinement to ensure that the strain distribution on the parallel arms can be more accurately resolved.

4). Boundary conditions (Figure. 2-4(b)). The lower connection part of de damper is

fixed. In-plane excitations are applied on nodes at the top surface of the upper connection part to simulate the parallel horizontal movement applied in the dampers through experiment equipment such as an actuator. The vertical displacement of the upper connection part is not allowed.

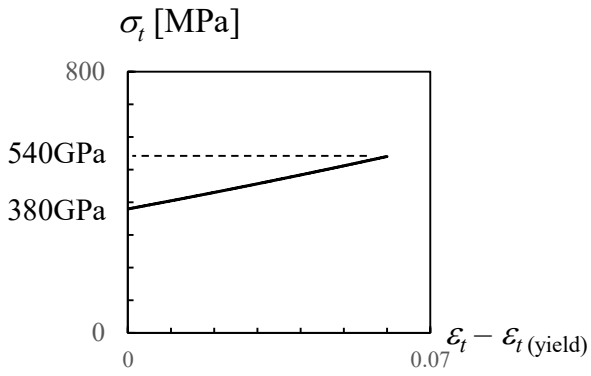

Figure. 2-3 Material properties of FEM modeling

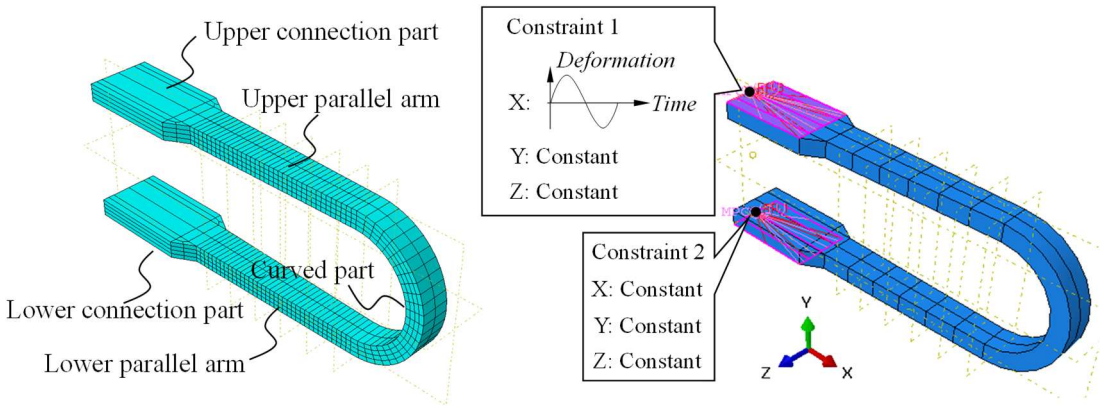

(a) Mesh refinement (b) Boundary condition

Figure. 2-4 Analytical model

2.2.2. Analytical results

Figure. 2-5 illustrates both experimental and FEM modeling results. experimental

result of the specimen's force-deformation (Q-γ) [2-2] is precisely reproduced by FEM modeling. The deformation behavior under monotonic loading is illustrated in Figure. 2-6. Measurement points P_1 to P_{17} (Figure. 2-7) are assigned on the parallel arms and curved part to facilitate the description of the damper's deformation behavior. The part around section P_6 starts to yield. Subsequently, the plastic area tends to distribute along the parallel arm. The bending-rolling motion of parallel arms is considered to be the main cause of outward protrusion.

Figure. 2-8 indicates curvature change of section P_4 in the first loading cycle with γ_t = 110%. The sum of ϕ_{max} and ϕ_{min} is used to evaluate the cyclic loading induced residual plastic deformation. The residual plastic deformation of the parallel arm's other sections can be evaluated in the same way (Figure. 2-9). The bending-rolling motion makes the area from section P_2 to P_5 severely deformed and protrude outwards. The analytical result is highly consistent with the image of the deformed damper's upper arm (Figure. 2-9).

Moreover, the residual plastic deformation caused by the first loading cycle with other deformation amplitudes (γ_t = 55, 90, and 110%) is illustrated in Figure. 2-10. It is worth noting that section P_4 normally has the most obvious deformation. Thus, using the shape change between sections P_4 and P_{14} as an indicator to describe the deformation behavior of U-damper seems reasonable.

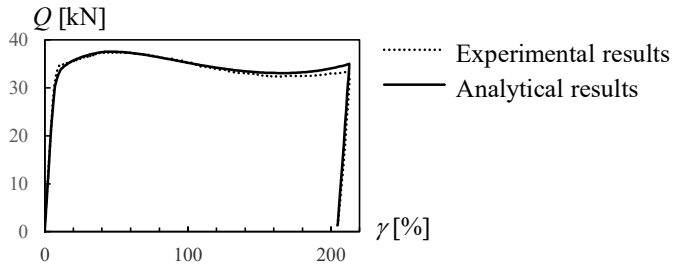

Figure. 2-5 force-deformation (Q-γ) relation

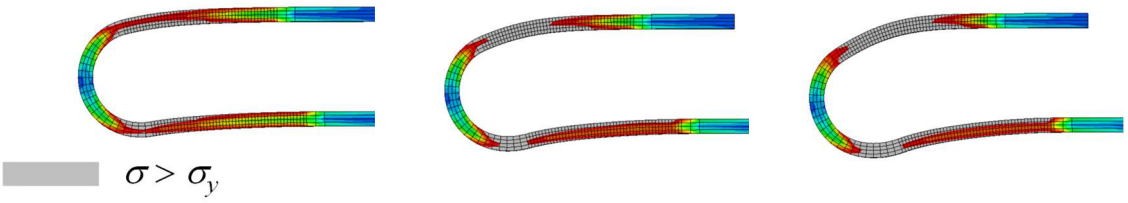

(a) δ= 30mm (b) δ= 45mm (c) δ= 65mm

(d) δ= 105mm (e) δ= 130mm (f) δ= 175mm

Figure. 2-6 Deformation behavior of U-damper under monotonic loading

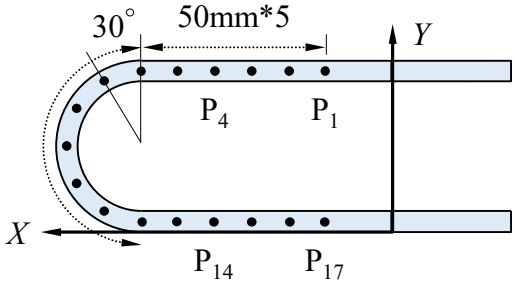

Figure. 2-7 Measurement point

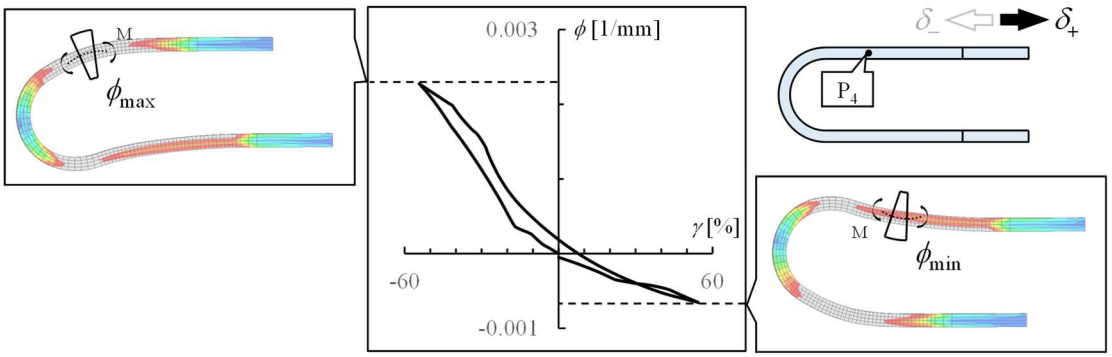

Figure. 2-8 Curvature change of section P_4

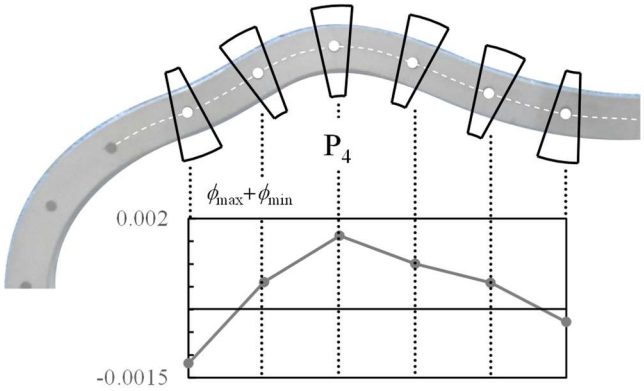

Figure. 2-9 Residual plastic deformation of U-damper's parallel arm (1 cycle; γ_t = 110%).

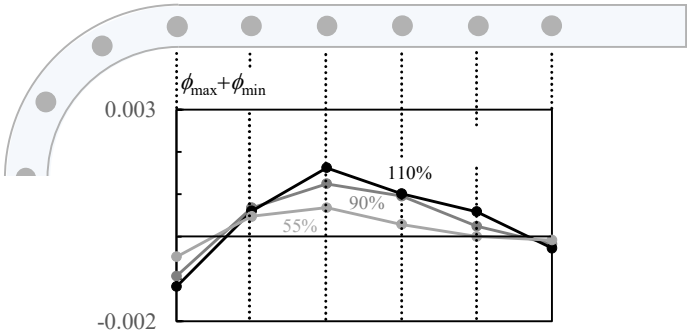

Figure. 2-10 Residual plastic deformation of U-damper's parallel arm (1 cycle; γ_t = 55, 90, and 110%).

2.3. In-plane cyclic loading tests under constant deformation amplitude

In this section, the results of unidirectional constant amplitude cyclic loading tests of single U-damper elements are presented. All of the specimens were loaded until fracture. The objective is to have a clear idea of the relation between the cumulative damage, residual plastic deformation, and deformation amplitude of the dampers. Meanwhile, the scale effect, hysteretic behavior, and low-cycle fatigue characteristics of the dampers were

confirmed. Subsequently, a mathematical model was established to evaluate the residual plastic deformation–cumulative damage relation of U-dampers with regards to any constant deformation amplitude.

2.3.1. Specimen

In the present study, full-scale single U-damper elements (UD40) were tested. Meanwhile, previous experimental results [2-8] (UD50) were compiled to indicate the scale effect of U-dampers; the dimensions of single U-shaped element UD40 and UD50 are listed in Table 1-1. The material characteristics, manufacturing process, and proportions of the geometric characteristics of the specimens of our study and previous research [2-8] remain the same.

2.3.2. Loading equipment

The test equipment is illustrated in Figure. 2-11 (APPENDIX D). The specimens were tested under horizontal loading in the in-plane direction with respect to the symmetry axis of the U-damper. The lower arms of the U-dampers were connected to a reaction jig fixed on a reaction beam through base plates; the reaction jig at the bottom is to obtain the reaction force. The upper arms were connected to the loading unit through base plates and a loading jig. The loading unit was installed on a horizontal roller of the reaction beam and connected to a dynamic actuator (±250 mm, ±2000 kN, ±50 cm/s (max)). Therefore, the parallel horizontal movement during cyclic loading could be applied in the dampers through an actuator until the fracture of the specimens. The U-dampers are typically

integrated with rubber bearings or placed under elements that do not transmit vertical force; thus, no vertical loads were applied in this experiment.

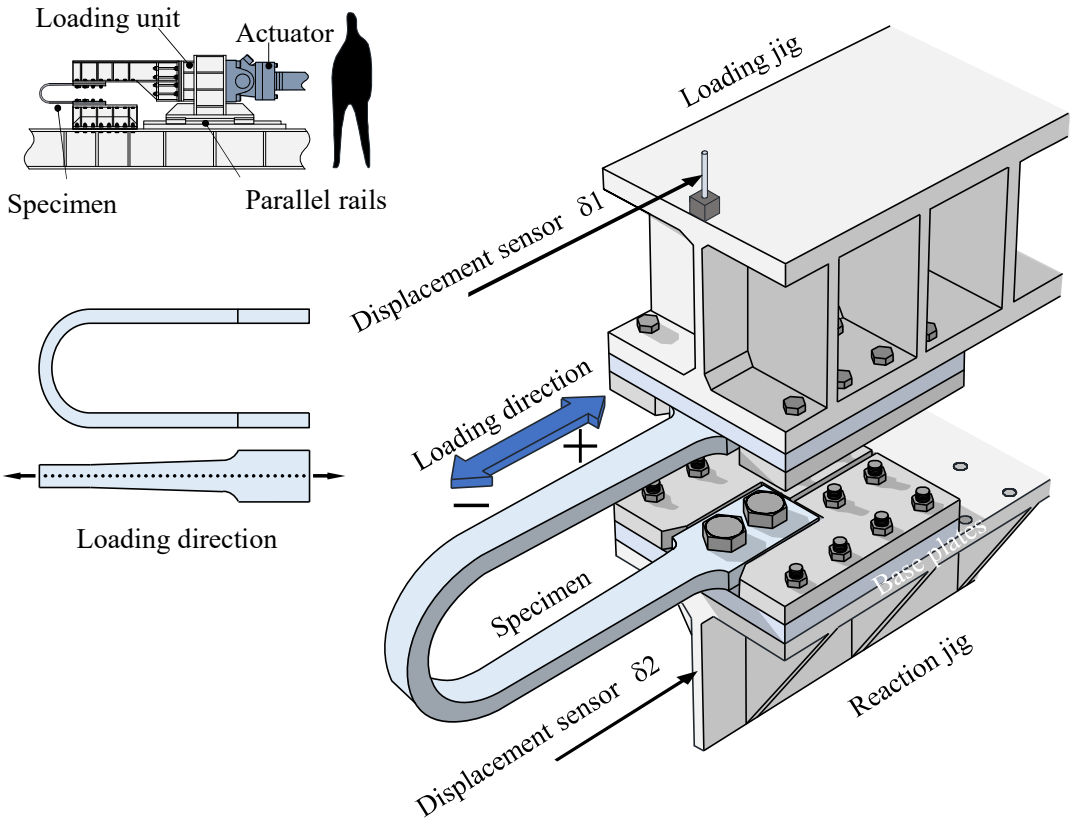

Figure. 2-11 Experimental Equipment

2.3.3. Measurement plan

The force-deformation relations of the specimens were recorded during the loading tests. A built-in load cell in the actuator measured the force Q in the system. The horizontal deformation of the system was obtained through wire displacement transducers $\delta 1$ and $\delta 2$, as shown in Figure. 2-11. The real-time deformation behavior during loading was recorded by digital cameras, which were set at fixed locations. Then, image analysis

[2-9] [2-10] was used to reproduce the deformation behavior of the dampers through the measurement points distributed along the damper (shown in Figure. 2-7).

As mentioned in Section 2.2 the residual plastic deformation tends to concentrate in the middle part (between measurement points P_4 and P_{14}) of the parallel arms. Residual plastic deformation h_t (Figure. 2-12)—the sum of the distance between P_4 and P_{14} (horizontal deformation equals 0 mm) and the thickness of the dampers—is used to reflect the magnitude of shape change. Meanwhile, the measurement of h_t was performed through a metal scale as well to verify the precision of image analysis. h_t was converted to the residual plastic deformation ratio ξ using Eq (2-8) for quantitatively evaluating the deformation behavior of different sized U-damper. h_0 is the original height of the dampers (Figure. 1-8).

$$\xi = \frac{h_t}{h_0} \qquad \text{Eq (2-8)}$$

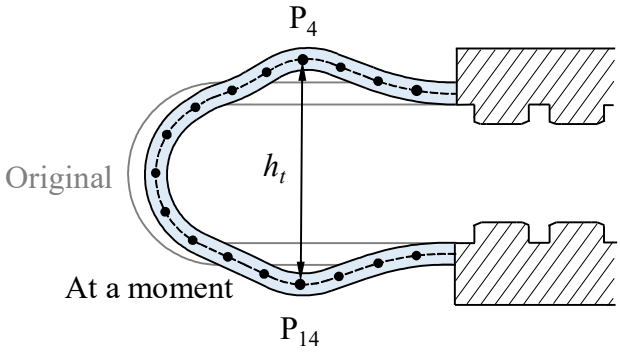

Figure. 2-12 Residual plastic deformation h_t

2.3.4. Test program

The loading information and fatigue life of single U-damper specimens are listed in Table 2-1. The loading history and the size of the dampers were the test parameters. The peak-to-peak horizontal shear angle γ_t was selected from the range of 25% to 110%. Unlike the specimens loaded with positive/negative symmetry amplitude, specimen I-4 was loaded with an offset deformation amplitude, of which γ_+ was 55%, while γ_- was 0 (Figure. 2-13). Previous experimental data [2-8] are listed in Table 2-1 as series III. Notably, although the U-dampers were all fabricated using structural steel SN490B, the steel material lot of series I actually differed from that of series II, which is presented in Chapter 3. The difference in the steel material lot caused a slight difference in the material characteristics, i.e., yield strength, tensile strength, and elongation. However, the material of I-6 was the same as that of series II, rather than the other specimens of series I. Test I-6 was conducted as a supplement to the cyclic loading test with constant deformation amplitude, hence it is listed in series I rather than series II.

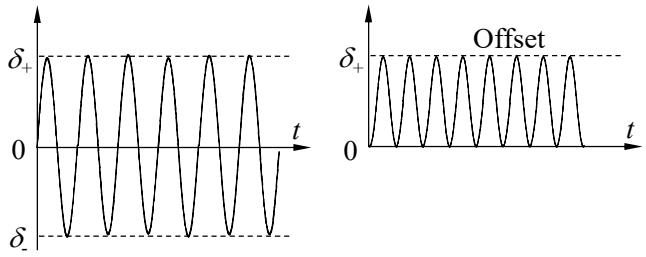

Figure. 2-13 Offset deformation amplitude

Table 2-1 Specimen list and experimental results

	Damper size	Series	No.	γ_t	Amplitude (mm)	Amplitude deviation	Frequency (Hz)	Fatigue life (cycle)
Present research	UD40	I	I-1	110%	±127.6	Symmetry	0.008	128
			I-2	70%	±81.2	Symmetry	0.012	312
			I-3	55%	±62.4	Symmetry	0.016	418
			I-4	55%	127.6	offset	0.016	302
			I-5	25%	±29	Symmetry	0.035	1381
			I-6	90%	±103.5	Symmetry	0.01	179
Previous research	UD50	III	III-1	40%	±67	Symmetry		617
			III-2	70%	±118	Symmetry		267
			III-3	150%	±251	Symmetry		64
			III-4	300%	±502	Symmetry		25

2.4. Experimental results

This section focuses on the experimental results of in-plane dynamic cyclic loading test under constant deformation amplitude. Hysteretic behavior, fatigue characteristics, plastic deformation, and energy dissipation capacity are confirmed. The correlation between the residual plastic deformation ratio ξ and cumulative damage D is discussed and an evaluation method of ξ-D relationship under constant deformation amplitude is established.

2.4.1. Force–deformation (Q–γ) relations

The ultimate state of specimens I-5, I-2, and I-1 are illustrated in Figure. 2-14. Specimen I-5 loaded with γ_t = 25% fractured near the damper's curved part (P_6). Dampers tended to fracture in the area around the middle part of the parallel arms as the increment

of deformation amplitude. The force–deformation (Q-γ) relations of U-dampers loaded with constant deformation amplitude are indicated in Figure. 2-15 and Figure. 2-16; the Y-axis is the force in system Q, while the X-axis is the horizontal shear angle γ. The hysteresis loops of specimens I-2, I-3, I-5, and I-6 are shown in comparison with that of I-1. The full hysteresis loops indicate the excellent energy dissipation capability of U-dampers; moreover, the energy dissipated in each loading cycle increases proportionally with the deformation amplitude. Although the increment of loading cycles induces strength deterioration, stiffness deterioration occurs only in the last few loading cycles. U-dampers maintain pretty good energy dissipation until their ultimate state. The steel material lot of specimen I-6 actually differed from that of the others in series I, and the maximum force of these two specimens are slightly different. However, their initial stiffness and the unloading stiffness are similar; this proves that the hysteresis loop of a U-damper is not strongly affected by slight differences in material characteristics within tolerance limits.

As illustrated in Figure. 2-16, the force–deformation relation of I-4 is compared with that of I-3. Their similar outline of hysteresis loops suggests that as long as γ_t remains the same, the energy dissipated in each loading cycle is mostly unchanging, and almost not related to whether the deformation amplitude has positive or negative symmetry.

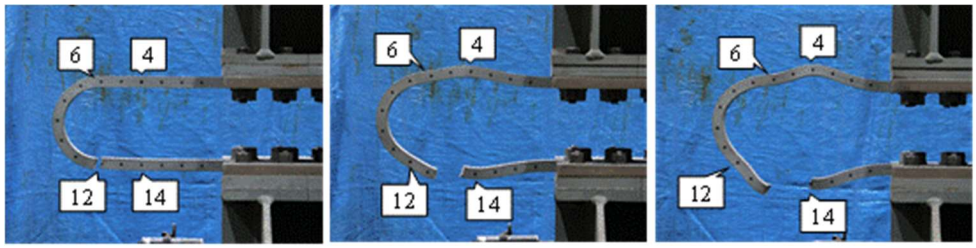

(a) γ_t = 25% I-5 (b) γ_t = 70% I-2 (c) γ_t = 110% I-1

Figure. 2-14 Fracture of single U-shaped element

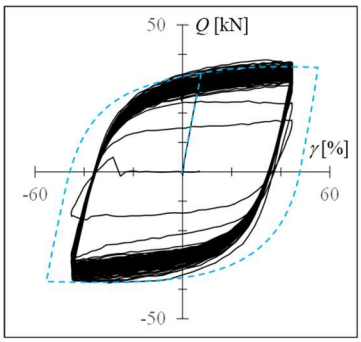

I-6, $\gamma_t = 90\%$
I-1, $\gamma_t = 110\%$

(a) I-6 $\gamma_t = 90\%$

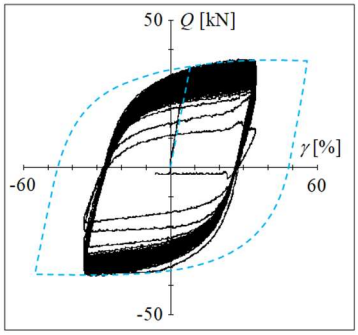

I-2, $\gamma_t = 70\%$
I-1, $\gamma_t = 110\%$

(b) I-2 $\gamma_t = 70\%$

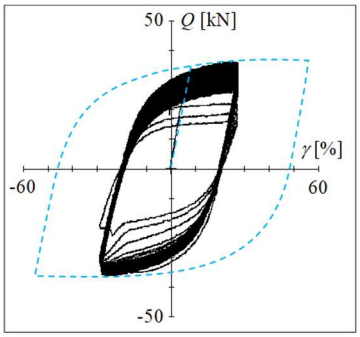

I-3, $\gamma_t = 55\%$
I-1, $\gamma_t = 110\%$

(c) I-3 $\gamma_t = 55\%$

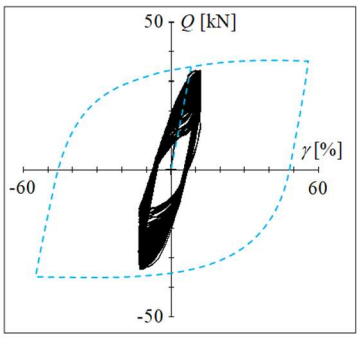

I-5, $\gamma_t = 25\%$
I-1, $\gamma_t = 110\%$

(d) I-5 $\gamma_t = 25\%$

Figure. 2-15 Force–deformation (Q-γ) relation (positive/negative symmetry)

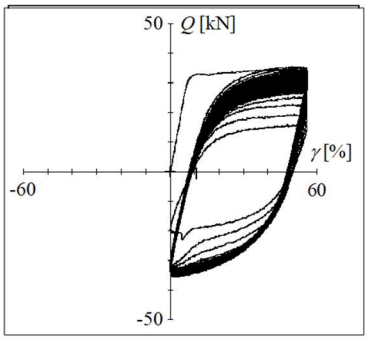

I-4, γ_t = Offset 55%

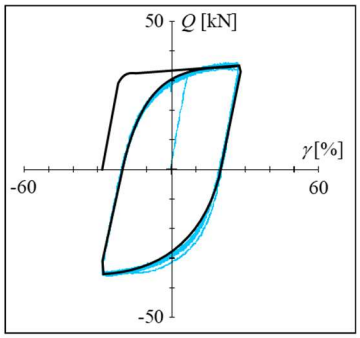

I-4, γ_t = Offset 55%
I-3, $\gamma_t = 55\%$

Figure. 2-16 Force–deformation (Q-γ) relation (offset deformation amplitude)

2.4.2. Fatigue characteristics

The experimental results of single U-shape elements' number of loading cycles until fracture N_f are illustrated in Figure. 2-17 and compared with Eq (2-6). The damper's fatigue life is conservatively estimated when the damper is loaded under γ_t within 100%, erring on the side of safety is beneficial to the design practice of seismic isolated structures with U-dampers.

Although the deformation amplitude of I-4 is asymmetrical, and the specimens of series I and series III differ in size, their fatigue behaviors are all precisely evaluated by Eq (2-6); this indicates that the symmetry of the deformation amplitude is negligible in fatigue evaluation, and the fatigue behavior of the dampers that differ in size can be evaluated through γ_t.

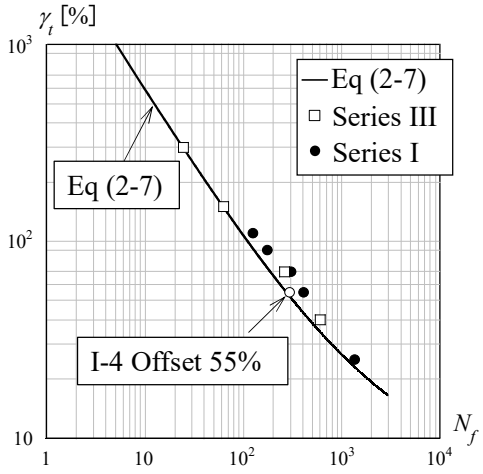

Figure. 2-17 Experimental results of U-dampers' fatigue behavior

2.4.3. Deformation behavior

The image analysis results of specimen I-6 (deformation amplitude: ±103.5 mm) are shown in Figure. 2-18, as an example of the deformation behavior of dampers in the cyclic loading test. The growths of the residual plastic deformation (horizontal deformation: 0 mm) of specimens I-1 (γ_t = 110%), I-6 (γ_t = 90%), and I-5 (γ_t = 25%), in the whole process of the cyclic loading test, are shown in Figure. 2-19. As mentioned above, the residual plastic deformation caused by cyclic loading tends to concentrate in the middle part of the parallel arms, and increases with the growth of cumulative damage *D*.

Contrastingly, for specimen I-5 (γ_t = 25%), no obvious residual plastic deformation was observed until fracture. Evaluating cumulative damage through residual plastic deformation has proven to be ineffective with γ_t smaller than 25%.

Additionally, for specimen I-4 (γ_t = Offset 55%), although the residual plastic deformation accumulates in the lower parallel arm because of the offset deformation amplitude in the positive side only, the growth of the shape change between points P_4 and P_{14} keeps in almost the same level as that of the damper loaded under positive/negative symmetry deformation amplitude with the same γ_t (specimen I-3, γ_t = 55%). The detail of offset amplitude's effect on the deformation behavior of U-damper will then be discussed.

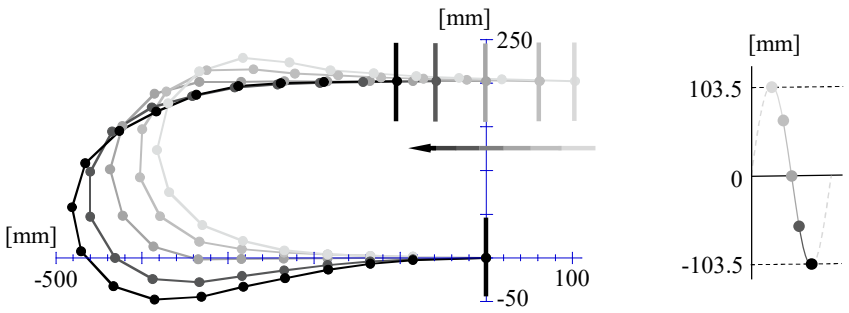

Figure. 2-18 Deformation behavior (first loading cycle of I-6)

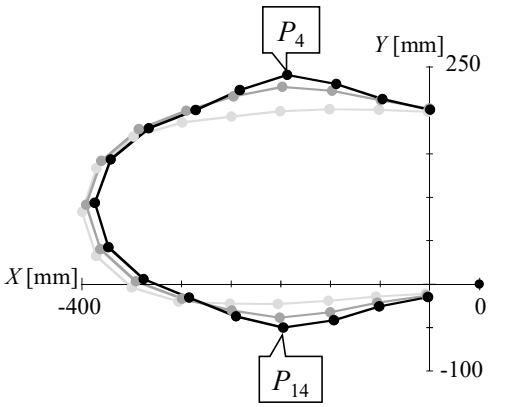

(a) I-1 γ_t = 110%

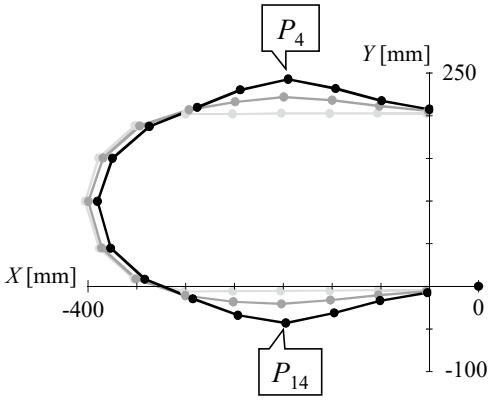

(b) I-6 γ_t = 90%

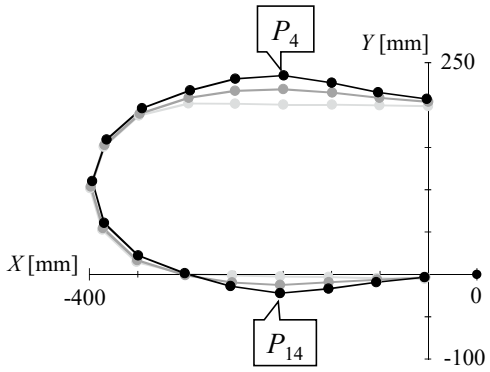

(c) I-2 γ_t = 70%

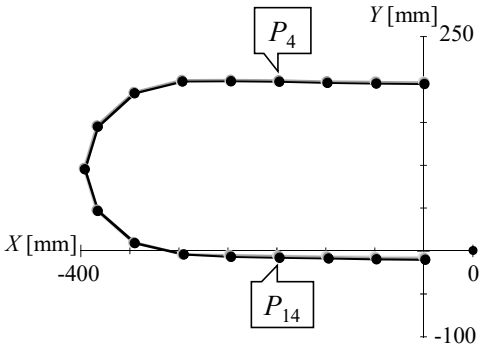

(d) I-5 γ_t = 25%

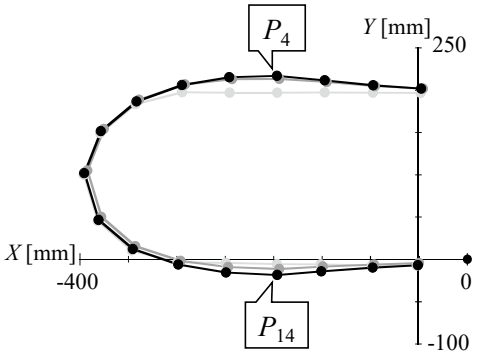

(e) I-3 γ_t = 55%

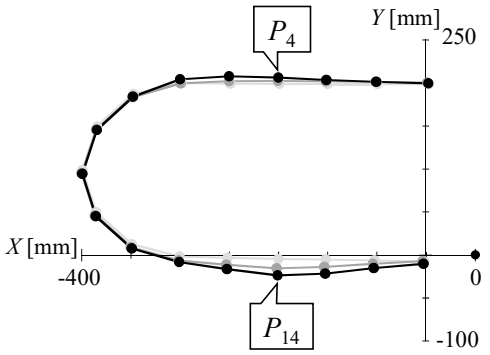

(f) I-4 γ_t = Offset 55%

Figure. 2-19 Growth of residual plastic deformation.

2.4.4. Residual plastic deformation–cumulative damage (ξ-D) relation

The residual plastic deformation ratio–cumulative damage (ξ-D) relation is plotted in Figure. 2-20(a); the measurement results, which are shown as marks using a metal scale, are consistent with the results of image analysis (solid line). Image analysis is an effective method for real-time tracing of U-damper deformation behavior.

As indicated in Section 2.7, the residual plastic deformation increases with the growth of cumulative damage. The ξ of specimens, which is loaded with relatively large γ_t, tends to be higher than that of the specimens loaded with relatively small γ_t for the same value of D. Note that almost the same ξ-D relationships were obtained in loading tests I-4 and I-3; this suggests that the ξ-D relationship of U-dampers loaded with the same γ_t is not strongly affected by the symmetry of deformation amplitude.

In Figure. 2-20(b), the test results of series III are shown with a dashed line and compared with that of series I. Although the specimens of series III and I differ in size, the ξ-D relationships of the specimens with the same γ_t (I-2 and III-3; γ_t = 70%) are congruent with each other. Meanwhile, the ξ-D relation of III-1 (γ_t = 40%) fills the vacancy during that of I-3 (γ_t = 55%) and I-5 (γ_t = 25%). The experimental results of U-dampers that differ in size are found to be complementary to each other. It is highly likely that similarity principles are still applicable to the evaluation of the dampers' deformation behavior, as in the previous discussion [2-6]. The effect of size can be eliminated through the index γ_t as well as in the ξ-D relation evaluation of U-dampers.

Overall, it is confirmed that there is a corresponding ξ-D relation of any particular γ_t of a loading test. The D of the dampers, which is subjected to γ_t within the range from 25% to 110%, can be evaluated through the corresponding ξ-D relationship.

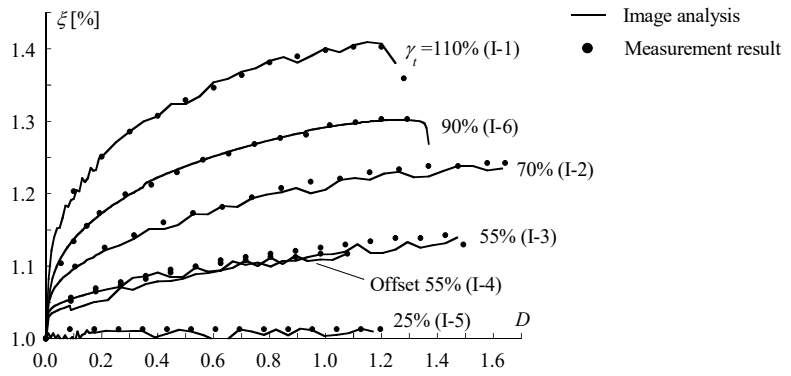

(a) image analysis and measurement results

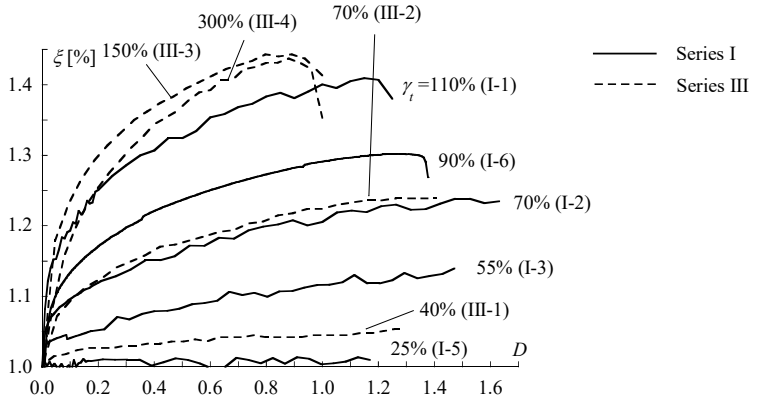

(b) experimental results of the present study and previous research

Figure. 2-20 Residual deformation ratio–cumulative damage (*ξ-D*) relation

2.4.5. Numerical model of *ξ-D* relationship

ξ-D relations under constant deformation amplitudes that are far beyond the types of γ_t tested in cyclic loading test series I and III are necessary for investigating the effect of random waves, such as earthquake-induced vibrations. As indicated in Figure. 2-20, U-dampers' residual plastic deformation normally grows rapidly at the very beginning of the cyclic loading test, whereas the increment of *ξ* gradually slows down when *D* exceeds a certain value. The *ξ-D* relation was approximated by a series of natural logarithm functions in the present study (Figure. 2-21, Eq (2-9)):

$$\xi = k(D,\beta) = \frac{\ln\left(1+D/\alpha\right)}{\beta} + 1 \qquad \text{Eq (2-9)}$$

Where α is 0.013, and β is related to the peak-to-peak horizontal shear angle γ_t.

$$\beta = g(\gamma_t) = 7.846 \cdot \gamma_t^{-2.672} \quad 0 \le \gamma_t < 73\% \qquad \text{Eq (2-10)}$$

$$\beta = g(\gamma_t) = -20 \cdot \gamma_t + 33.167 \quad 73\% \le \gamma_t$$

The *Y*-axis of the lower part of Figure. 2-21 presents the experimental results of the residual plastic deformation ratio (ξ_{exp}) normalized by the evaluated values of the residual plastic deformation ratio (ξ_{cal}), while the *X*-axis presents the cumulative damage *D*. The results are overestimated until *D* reaches 0.6; subsequently, the value of ξ_{exp}/ξ_{cal} gradually converges to one. Overall, ξ is estimated precisely by the composed numerical model within the range from 0.96 to 1.04.

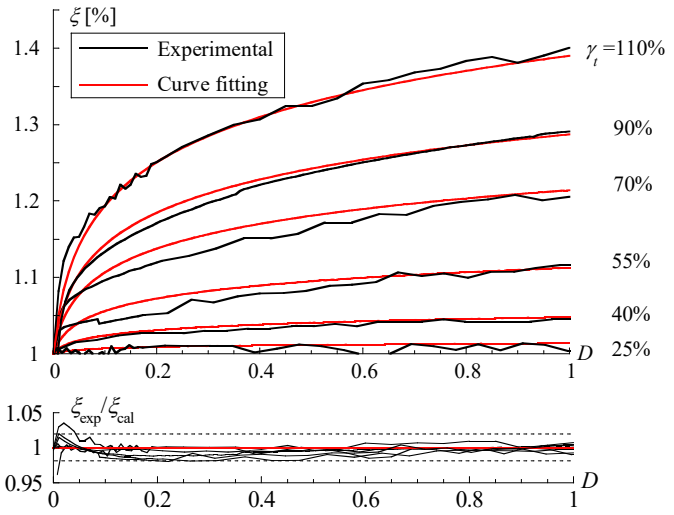

Figure. 2-21 Numerical model of ξ-*D* relationship and precision analysis

2.5. Conclusion

In this chapter, the deformation behavior of U-damper loaded under constant deformation amplitude is indicated through a series of in-plane dynamic cyclic loading tests. The main conclusions are listed below.

1). Cumulative damage of U-shaped damper is proven to be tightly correlated to the residual plastic deformation caused by cyclic loading.

2). Residual plastic deformation tends to accumulate around the middle part of the parallel arms. residual plastic deformation ratio ξ is adopted in the present study as an indicator to quantitatively evaluate the deformation behavior of U-damper.

3). The effect of the U-shaped steel dampers' size is proved to be negligible in the deformation behavior evaluation based on the residual plastic deformation ratio ξ under the condition that deformation amplitude γ_t remains smaller than 110%.

4). No obvious residual plastic deformation was observed when γ_t equals 25%. The residual plastic deformation ratio was proven to be an ineffective index of cumulative damage evaluation when γ_t was smaller than 25%. Thus, another evaluation method is required for this case.

5). Independent of whether the amplitude deformation has positive or negative symmetry, the ξ-D relationships of U-shaped steel dampers loaded with constant deformation amplitude, which are the same in γ_t (in the range from 25% to 110%), are congruent.

6). There is a corresponding ξ-D relation of any particular γ_t within the range from 25% to 110%. An evaluation method of U-shaped steel dampers' ξ-D relationship. Is composed in this chapter.

2.6. Reference

[2-1] 植草雅浩, 大河原勇太, 吉敷祥一, 山田 哲, 和田 章, 免震Uダンパーの実大動的実験, その 1, 2, 日本建築学会大会学術講演梗概集(九州), pp.1051-1054, 2007.8

(Uekusa M et al. Dynamic loading Test of U-shaped Steel Damper for Seismic Isolation, Part 1, 2. Proceedings of Architectural Institute of Japan (AIJ) Annual Conference 2007;1051-1054.)

[2-2] 吉敷祥一, 大河原勇太, 山田 哲, 和田 章, 免震構造用 U 字形鋼材ダンパーの繰り返し変形性能に関する研究, 日本建築学会構造系論文集, 第 73 巻, 第 624 号, pp.333-340, 2008.2

(Kishiki S et al. Experimental evaluation of cyclic deformation capacity of U-shaped steel damagers for base-isolated structures. Journal of Structural and Construction Engineering (Transactions of AIJ) 2008;73(624):333–340.)

[2-3] 吉敷祥一, 高山 大, 山田 哲, エネ デイアナ 小西克尚, 川村典久, 村嶋正雄, 水平 2 方向載荷下における繰り返し変形性能に関する実験, 免震構造用 U 字形鋼材ダンパーの水平 2 方向特性, その 1, 日本建築学会構造系論文集, 第 77 巻, 第 680 号, pp.1579-1588, 2012.12

(Kishiki S et al. Experimental evaluation of cyclic deformation capacity of U-shaped damagers subjected to bi-directional loadings. Bi-directional characteristics of U-shaped steel dampers for base-isolated structures Part 1. Journal of Structural and

Construction Engineering (Transactions of AIJ) 2012;77(680):1579–1588.)

[2-4] Ene D, Kishiki S, Yamada S, Jiao Y, Konishi Y, Terashima M, Kawamura K. Experimental study on the bidirectional inelastic deformation capacity of U-shaped steel dampers for seismic isolated buildings. Earthquake Engineering & Structural Dynamics 2016;45(2):173–192.

[2-5] Ene D, Yamada S, Jiao Y, Kishiki S, Konishi Y. Reliability of U-shaped steel dampers used in base-isolated structures subjected to biaxial excitation. Earthquake Engineering & Structural Dynamics 2017;46:621–639.

[2-6] Jiao Y, Kishiki S, Yamada S, Ene D, Konishi Y, Hoashi Y, Terashima M. Low cyclic fatigue and hysteretic behavior of U-shaped steel dampers for seismically isolated buildings under dynamic cyclic loadings. Earthquake Engineering & Structural Dynamics, 2015;44:1523–38.

[2-7] 日本建築学会, 鋼構造許容応力度設計規準, 2019

(Architectural Institute of Japan, AIJ Standard for Allowable Stress Design of Steel Structures, 2019)

[2-8] Response Control Building Research Committee, Seismic Isolation Structural Design Subcommittee. Damper WG Report (In Japanese) 2014;2:1–5.

[2-9] 2D/3D motion analysis software DIPP-MotionV.

https://www.ditect.co.jp/en/software/dipp_motionv.html

[2-10] OptiTrack Documentation Wiki - NaturalPoint Product Documentation (Ver 2.2)

https://v22.wiki.optitrack.com/index.php?title=Motive_Documentation

Chapter 3

Effect of complicated loading history on U-shaped steel dampers' residual plastic deformation-cumulative damage relation of U-shaped steel damper and precision verification of the exciting cumulative damage evaluation method

3. Effect of complicated loading history on U-shaped steel dampers' residual plastic deformation-cumulative damage relation of U-shaped steel damper and precision verification of the exciting cumulative damage evaluation method

3.1. Introduction

As mentioned in Section 2.1, Kishiki et al. (2008) [2-1] conducted numerous cyclic loading tests under unidirectional excitation and developed a fatigue behavior evaluation method of U-dampers. Based on this, Ene et al. (2016, 2017) [2-2] [3-3] developed a cumulative damage evaluation method for U-dampers under biaxial excitation using the seismic response of the structure obtained from a time-history analysis.

However, excessive reliance on numerical analysis makes it difficult to certify the estimated value of cumulative damage. Ground motion recorded by the sites (K-NET or KiK-net in Japan (NIED, 2019) [3-4] around the target building has been used to reproduce the structural response during earthquakes. However, selecting a reliable ground motion record remains a sensitive task because the earthquake-induced excitation acting on structures is significantly influenced by different soil types (rock, closed, and soft) and geological structures (more-or-less hemmed in valleys, sedimentary basins, and synclinal and anticlinal basins) of the locations of the target buildings and sites (JASO, 1997) [3-5]. Konishi et al. (2012) [3-6] proposed a precision verification approach for the existing cumulative damage evaluation method of U-dampers (Ene et al. 2016) [2-2] by evaluating the residual plastic deformation capacity of dampers that are dismantled from damaged structures using cyclic loading tests until fracture. However, this approach is uneconomical, ineffective, and unfeasible in most cases. Therefore, the previously

reported cumulative damage evaluation method should be complemented with a simple and feasible precision verification approach (Figure. 3-1). A precision verification approach is composed in this chapter based on the investigation of the relationship between U-dampers' residual plastic deformation and cumulative damage. Although U-dampers' ξ-D relationship has been quantitatively evaluated in Chapter 2, the effect of more complicated loading history, such as incremental and decremental deformation amplitude, is still unknown. For this purpose, a series of in-plane dynamic loading tests under constant deformation amplitude is conducted.

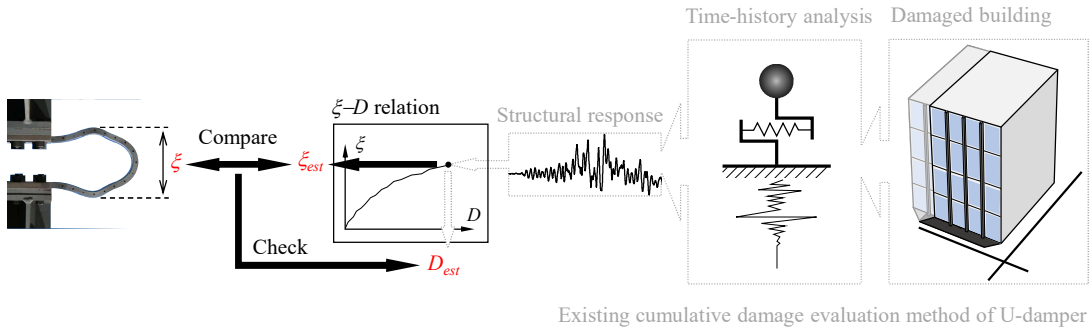

Figure. 3-1 Precision verification of exciting cumulative damage method of U-damper.

3.2. Unidirectional cyclic loading test under complicated loading history

This section presents the experimental results of U-dampers loaded with complicated loading histories. A ξ-D relationship evaluation method was proposed based on the above-mentioned numerical model (Figure. 2-21) and the investigation of experimental results. To simplify the following representation, cyclic loading with constant and positive/negative symmetry deformation amplitude was defined as standard loading. The

U-damper elements loaded under standard loading (series I and III) are referred to here as standard specimens.

3.2.1. Specimen and experimental equipment

The size of the specimens (Single U-shaped element UD40) and experimental equipment used in cyclic loading tests under complicated loading history remains the same as that of loading test series I.

3.2.2. Overview of loading histories

Several loading patterns (series II, Table 3-1) were considered to investigate the ξ-D relation of U-dampers with regard to more complicated loading histories. The material characteristics and manufacturing process of the specimens of series II remained the same as that of series I and III. The loading tests were conducted under the same conditions as described in Chapter 2, and the U-damper elements were loaded until fracture as well.

The loading information of test series II is listed in Table 3-1. Deformation amplitude was changed on the timing marked by triangles. The U-damper elements were loaded with a sine wave and corresponding loading speed shown in Table 2-1. The γ_t was set to be smaller than 110% ($\gamma_t \leq 55\%$) except for test II-4. To investigate the deformation behavior of the dampers loaded with γ over 55%, the γ of test II-4 was set to be higher than 55%. It is important to note that the dampers are considered to be reaching their ultimate state when D reaches one in the evaluation of the ξ-D relation; hence, the deformation behavior until D reaches one is regarded as the main object of observation

in this study. Specimens II-1 and II-4 were tested under the condition that γ_t only increased; by contrast, specimens II-2 and II-3 were loaded with decreasing γ_t, until D reached one. The loading history of II-5 was composed of both increasing and decreasing γ_t. Additionally, as mentioned above, it is indicated that the ξ-D relationship is not strongly affected by the symmetry of deformation amplitude through tests I-3 (γ_t = 55%) and I-4 (offset 55%). Therefore, to check whether this is still valid to the dampers loaded under relatively complicated loading history, the deformation amplitude of II-5 was set to have positive/negative asymmetry deformation amplitude and change gradually. Therefore, to check whether this is still valid for the dampers loaded under relatively complicated loading histories, the deformation amplitude of II-5 was set to have positive/negative asymmetry deformation amplitude and change gradually.

Loading history II-7 was obtained by simplifying a structural response to investigate the effect of a relatively complicated loading history which is approximated to the earthquake-induced verification. The steps of simplifying the wave are shown as follows (Figure. 3-2):

Step 1. Filtered out the loading cycles with deformation amplitude smaller than 25%. Counted the number of loading cycles and deformation amplitude of each loading cycle.

Step 2. Adjusted the deformation amplitude of each loading cycle, and the deformation amplitude was selected from γ_t equals 25%, 40%, 55%, 70%, 90%, and 110% (the γ_t used in the dynamic loading test under constant deformation amplitude). For instance, γ_t = 61% approximately equals 55%, thus, the deformation amplitude of this loading cycle was replaced by γ_t = 55% in the simplified wave.

The deformation amplitude of each loading cycle was adjusted to be consistent with that used in the dynamic loading test under constant deformation amplitude. Therefore,

the trend change of the residual plastic deformation-cumulative damage (ξ-D) relationship caused by complicated loading history caould be checked through the experimental results of ξ-D relationship under constant deformation amplitude.

Wave II-6 was made by rearranging the loading cycles of five times of wave II-7 in ascending order of γ_t (Figure. 3-3). A triangular wave (constant loading speed: 8 mm/s) was used in tests II-6 and II-7 to simplify the experimental procedure.

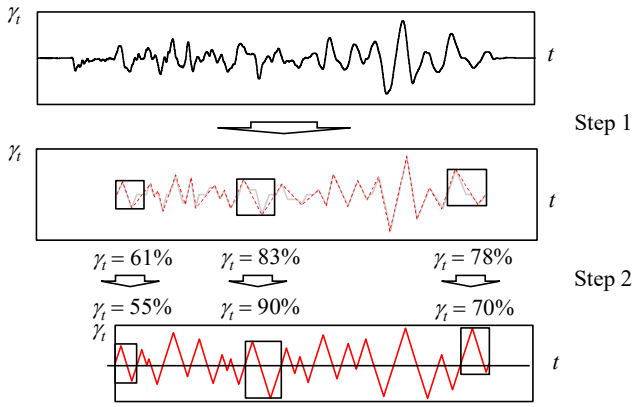

Figure. 3-2 Creation of loading history II-7

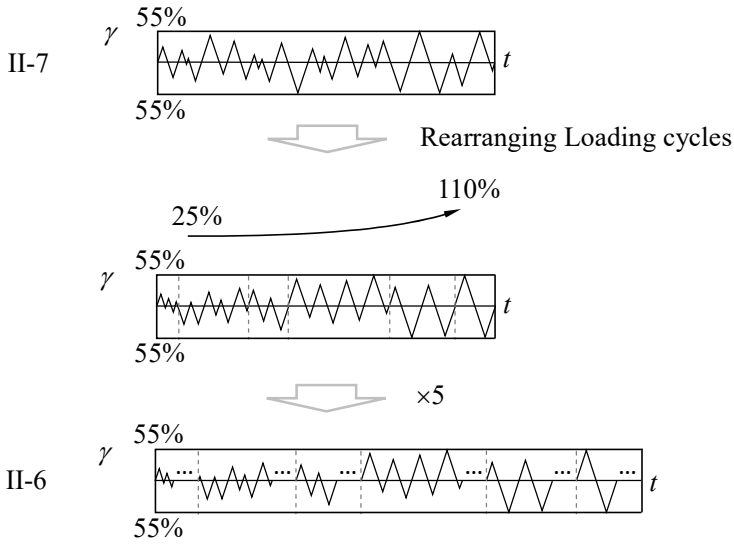

Figure. 3-3 Creation of loading history II-6.

Table 3-1 List of loading histories

Damper size	Series	No.	Loading History	*D*
UD40	II	II-1	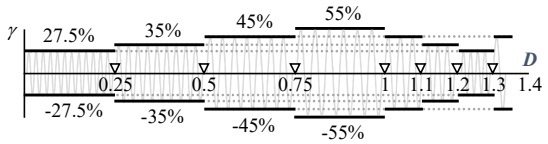	1.3
		II-2	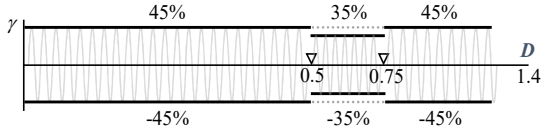	1.32
		II-3	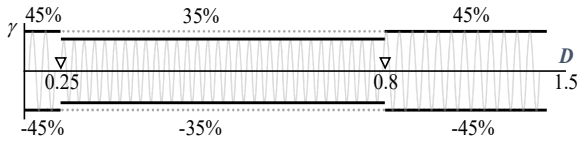	1.45
		II-4	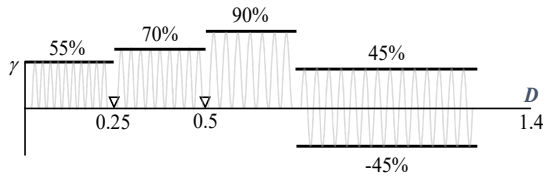	1.26
		II-5	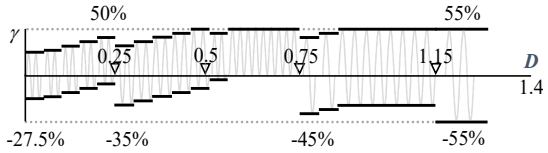	1.29
		II-6	Refer to Figure. 3-2.	1.5
		II-7	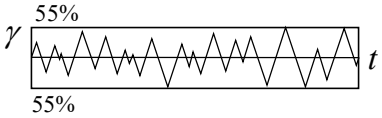	1.25

3.3. Residual plastic deformation ratio–cumulative damage (ξ-D) relationship

The ξ-D relationships of loading test series II (solid) are presented in comparison with that of the standard specimens (dashed) in Figure. 3-4. The loading histories are shown with graphs to indicate the trend changes of ξ-D relationships caused by the changes of deformation amplitude. These relationships of standard specimens I-3 (γ_t = 55%), I-4 (γ_t = 70%), I-6 (γ_t = 90%), and I-1 (γ_t = 110%) are shown in blue, black, green, and red, respectively. The ξ-D relationships of series II are colored with the same colors over the interval of D, where the dampers are loaded with the corresponding γ_t. However, because of the almost random loading histories, the ξ-D relationships of II-6 and II-7 would be difficult to discern if shown in color; thus, their ξ-D relations are compared and shown only in black (Figure. 3-4(f)). Furthermore, for demonstrating the links between the ξ-D relationships of series II and standard specimens, parts of these relationships are horizontally translated (parallel to the X-axis) to the vicinity of that of the standard specimens with the corresponding γ_t.

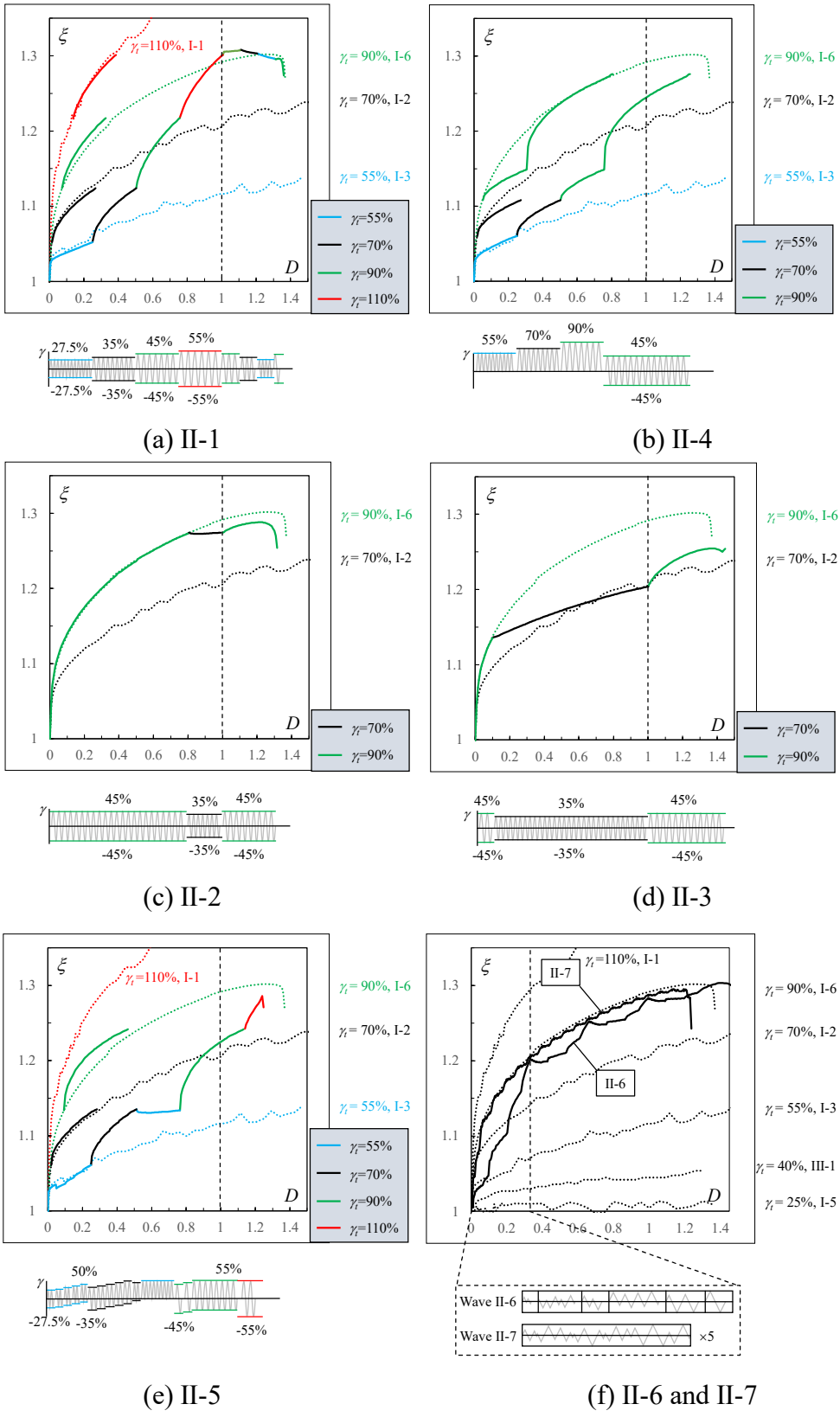

Figure. 3-4 *ξ-D* relationships (series II).

3.3.1. Increase in deformation amplitude

For II-1 (Figure. 3-4(a)), it is apparent that ξ grows sharply after every increment of the deformation amplitude. The horizontal translation of the ξ-D relationship over the interval for D ranging from 0.25 to 0.5 is almost coincident with the ξ-D relationship of the standard specimen with the corresponding γ_t (I-2, γ_t = 70%); a similar phenomenon is observed over the interval for D ranging from 0.5 to 0.75 as well as 0.75 to 1. This similarity indicates that the trend change of ξ-D, which is caused by the increase of γ_t, can be estimated by the ξ-D relationship of the damper loaded under standard loading with the target γ_t.

For II-4 (Figure. 3-4(b)), the offset deformation amplitude was applied over the interval from D = 0 to 0.75. Similar to II-1, the ξ-D relationship of II-4 is consistent with that of I-3 over the interval from D = 0 to 0.25; further, the rapid growth of ξ caused by the increase of γ_t is observed. However, the growth of ξ over the interval from D = 0.25 to 0.5 (γ_t = 70%) and 0.5 to 0.75 (γ_t = 90%) is much slower than that of I-2 and I-6, respectively. The growth of ξ caused by the peak deformation amplitude over 55% is approximately half of that caused by standard loading with the corresponding γ_t. This suggests that when γ exceeds 55%, the growth of ξ would be overestimated if the ξ-D relation of the standard specimen with the corresponding γ_t is applied in the ξ-D relation evaluation. Moreover, after the rapid growth of ξ at the first step since the deformation amplitude changed to ±45% from 90% offset (+90%, 0) when D equals 0.75, the horizontal translation of the ξ-D relation of II-4 and I-6 finally converges as cumulative damage D increases. It is likely that the growth trend of ξ can still be estimated precisely by the ξ-D relationship of the dampers, which are loaded under standard loading with the

corresponding γ_t, even though the γ exceeds 55% temporarily.

3.3.2. Deformation amplitude decrease

For tests II-2 (Figure. 3-4(c)) and II-3 (Figure. 3-4(d)), γ_t was decremented at different times. The γ_t of II-2 decreased from 90% to 70% (D = 0.8), when ξ had already exceeded the ξ_{max} of I-2 (1.2); ξ_{max} is defined as the residual plastic deformation ratio when D equals one. By contrast, for test II-3, γ_t was decremented at a moment (D = 0.1) that ξ was still smaller than the ξ_{max} of I-2. The ξ of II-2 remains stable after the decrement of the deformation amplitude. By contrast, the ξ of II-3 still grows slowly after decreasing the deformation amplitude; subsequently, the growth rate remains at almost the same level as that of I-2 as D reaches 0.7.

3.3.3. Complicated loading history

The ξ-D relation of II-5 is almost consistent with that of II-1 over the interval from D = 0 to 0.5. Meanwhile, similar to II-2, the stable ξ-D relation appears owing to the decrement of γ_t, which was applied when ξ had already exceeded ξ_{max} of the standard specimen with target γ_t; ξ_{max} of I-3 is 1.12. These similarities indicate that as long as the maximum value of γ remains smaller than 55%, the ξ-D relation of the U-damper that is loaded with relatively complicated loading history is not as strongly affected by the symmetry of the deformation amplitude.

The only difference between loading histories II-6 and II-7 is the arrangement of the loading cycles; therefore, their ξ-D relations are compared and illustrated in the same

figure (Figure. 3-4(f)). Note that the ξ of the U-damper after every 5 times loading with II-7 is nearly the same as that of the U-damper after every loading with II-6. Finally, ξ tends to be the same, even though rearranging loading cycles in ascending order of γ_t results in different ξ-D relationships.

3.4. Evaluation of ξ-D relationship under complicated loading history

Based on the experimental results of cyclic loading test series II, an evaluation method of residual plastic deformation-cumulative damage relationship of U-damper is composed in this section.

3.4.1. Evaluation of ξ-D relationship of U-dampers loaded with increasing deformation amplitude

The numerical model (Figure. 2-21) was used as a tool to evaluate the ξ-D relation of U-dampers. Based on the investigation of II-1 and II-4, an evaluation method for the ξ-D relation of U-dampers loaded with increasing deformation amplitude only was formulated (Figure. 3-5).

The ξ-D relation of U-dampers loaded with increasing deformation amplitude is expressed by Eq. (7). Under the condition that the peak deformation amplitude γ remains smaller than 55%, the trend change of the ξ-D relation that is caused by the increment of γ_t can be evaluated by the ξ-D relation of the standard specimen with target γ_t (where μ of Eq. (7) equals 1); the target γ_t denotes $\gamma_{t,2}$ in Figure. 3-5. D_c and ξ_c denote the cumulative damage index D and the residual plastic deformation ratio ξ at the time of changing

deformation amplitude, respectively. D_k denotes the D of the standard specimen with target γ_t when ξ equals ξ_c. Furthermore, as mentioned in Section 3.2, the growth of ξ caused by γ over 55% is approximately half of that caused by standard loading with the corresponding γ_t. Eq (3-1) can also reflect the low growth of ξ caused by γ over 55% when the value of μ is 0.5.

$$\xi_{c,i} = \mu \cdot \left(k\left(D_{k,i-1} + \Delta D, \beta\left(\gamma_{t,i}\right)\right) - \xi_{c,i-1} \right) + \xi_{c,i-1} \qquad \text{Eq (3-1)}$$

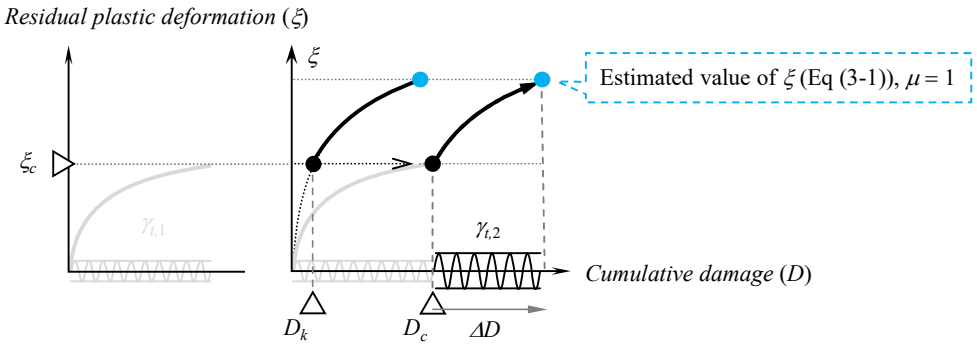

(a) $\pm\ \gamma_2 \leq 55\%$

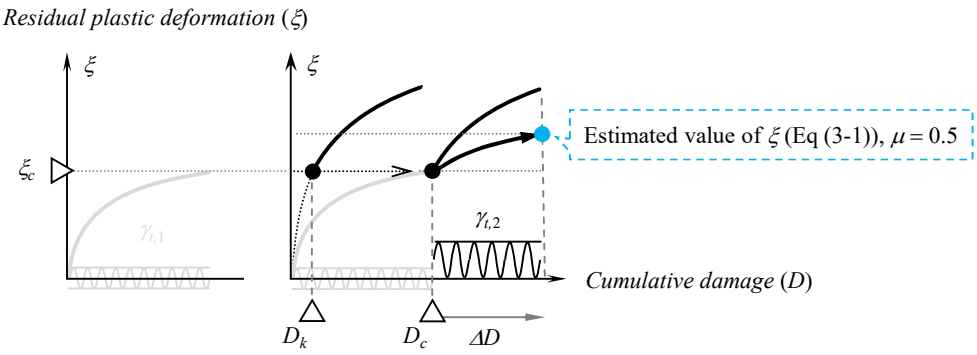

(b) $+\ \gamma_2 > 55\%$

Figure. 3-5 ξ-D relationship evaluation

(deformation amplitude increasing, $\gamma_{t,2} > \gamma_{t,1}$)

3.4.2. Evaluation of ξ-D relationship of U-dampers loaded with other loading histories

The final ξ of U-dampers, which are loaded with loading histories that only differ in the arrangement of loading cycles, have proven to be similar to each other based on the investigation of II-6 and II-7. Applying this characteristic, as illustrated in Figure. 3-6, the ξ-D relationship evaluation of a single U-damper element loaded with any random excitations is achieved in three steps:

(i) converting the wave into a simple loading history of which the deformation amplitude only increases.

(ii) calculating the residual plastic deformation ratio ξ at any particular value of cumulative damage D by applying Eq (2-3).

(iii) repeating the previous steps after the accomplishment of each loading cycle.

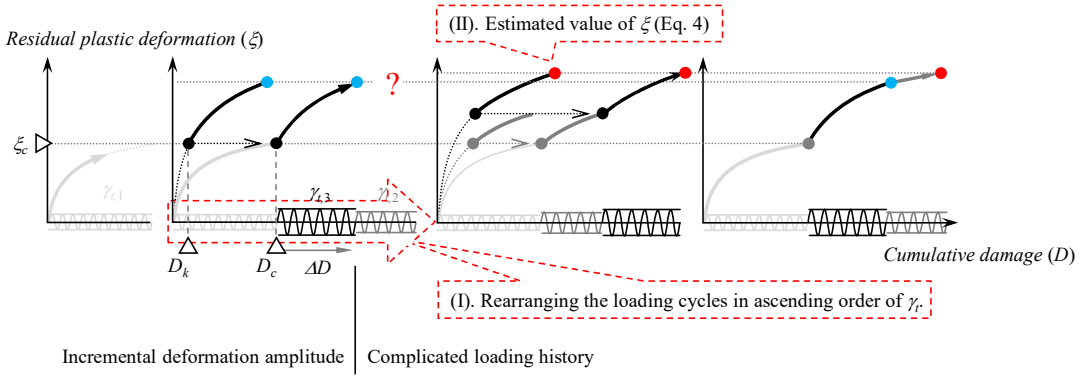

Figure. 3-6 ξ-D relationship evaluation

(Complicated loading history)

3.5. Comparison of evaluated values and experimental results

The evaluated values of ξ (red) compared with experimental results (black) are shown in Figure. 3-7 and Figure. 3-8.

For the ξ-D relation of II-1, II-4, and II-5 (from D = 0 to 0.5) that are shown in Figure. 3-7 (a), (d), and (e), although the experimental results are slightly overestimated, the increase in the growth rate of the ξ-D relation caused by the increment of γ_t is reproduced precisely by Eq (2-3). Meanwhile, when coefficient μ equals 0.5, Eq (3-1) can describe the low growth of ξ due to γ being over 55%, which occurred in test II-4 over the interval from D = 0.25 to 0.75.

As illustrated in Figure. 3-7(b) (II-2), γ_t was decreased on the timing that ξ had already exceeded the ξ_{max} of the standard specimen with target γ_t (I-2). The slow growth of the evaluated values of ξ was observed since γ_t decreases to 70% from 90%; this is slightly different from the stable residual plastic deformation ratio shown in the experimental results. There is a similar occurrence in Figure. 3-7(e) (II-5) over the interval from D = 0.5 to 0.75. The stable ξ-D relations due to the decrement of γ_t cannot be reflected correctly by the evaluation method described in Figure. 3-6. Meanwhile, for II-3 (Figure. 3-7(c)), γ_t was decreased on the timing that ξ had not yet exceeded the ξ_{max} of I-2. After observing the experimental results, it is obvious that the growth rate of the ξ-D relation decreases significantly after the decrement of γ_t when D equals 0.1. Subsequently, ξ slowly increases at a relatively stable growth rate. However, the significant reduction in the growth rate is not precisely reproduced by the evaluation method (Figure. 3-6), which is considered to be the main reason why ξ is overestimated after the decrement of γ_t in Figure. 3-7(c).

The sufficient applicability of the evaluation method (Figure. 3-6) is demonstrated in Figure. 3-7(d) and Figure. 3-8, when U-dampers are loaded with almost random excitations. Although the experimental results are slightly underestimated at the very beginning of the loading test (until D reaches 0.2; refer to Figure. 3-8(a)), the evaluated values tend to be almost consistent with the experimental results subsequently. It is worth mentioning that the numerical model of the ξ-D relationship was proposed on the principle that the experimental results are precisely reproduced over the whole process of the loading test; this can cause the experimental results to be overestimated sometimes and underestimated at other times. Therefore, positive and negative errors tend to cancel out each other when the dampers are loaded with a relatively complicated loading history. This is considered to be the reason why the experimental results of II-6 and II-7 are evaluated more precisely in comparison with other specimens. Overall, the deformation behavior of the dampers that are loaded under almost random excitation is precisely described by the combination of Eq (2-3) and the evaluation method defined in Figure. 3-7, even though there is still room for improvement in the numerical model.

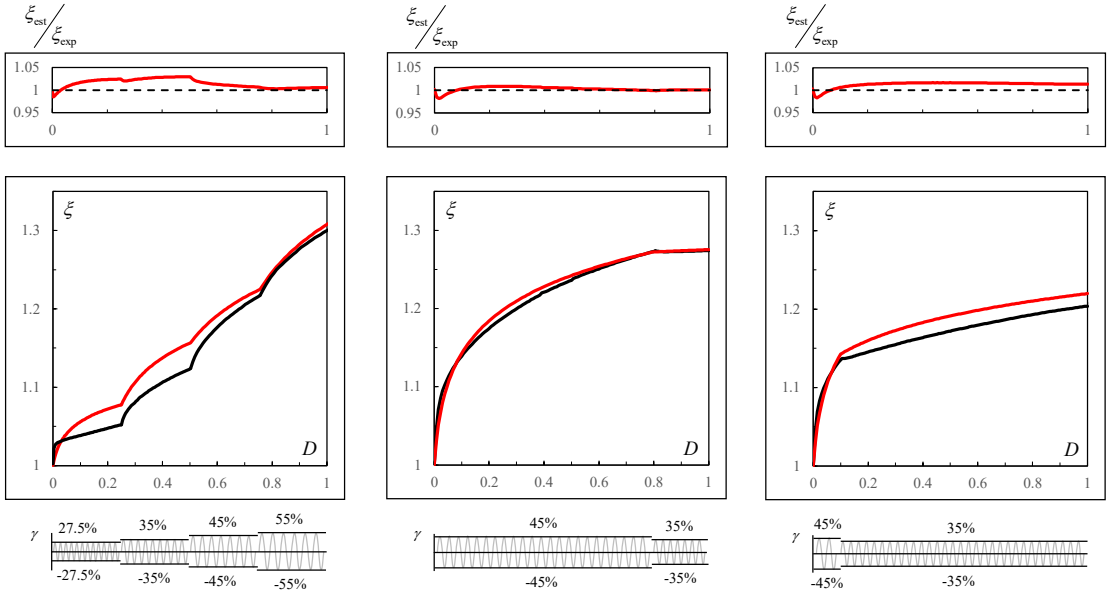

(a) II-1

(b) II-2

(c) II-3

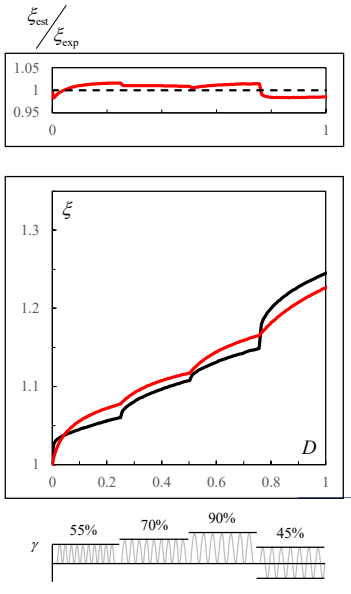

(d) II-4

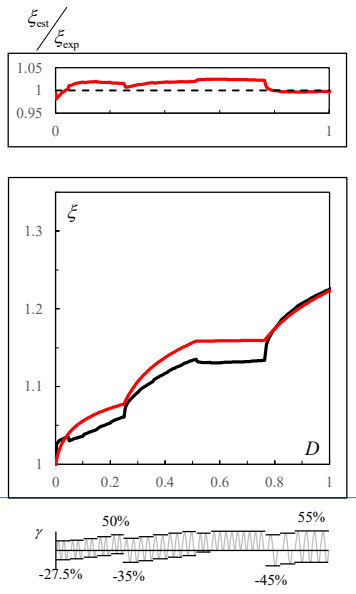

(e) II-5

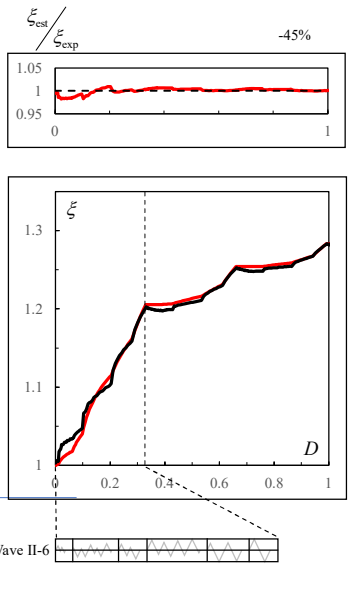

(f) II-6

Figure. 3-7 *ξ-D* relationship evaluation

(deformation amplitude increasing, $\gamma_{t,2}>\gamma_{t,1}$)

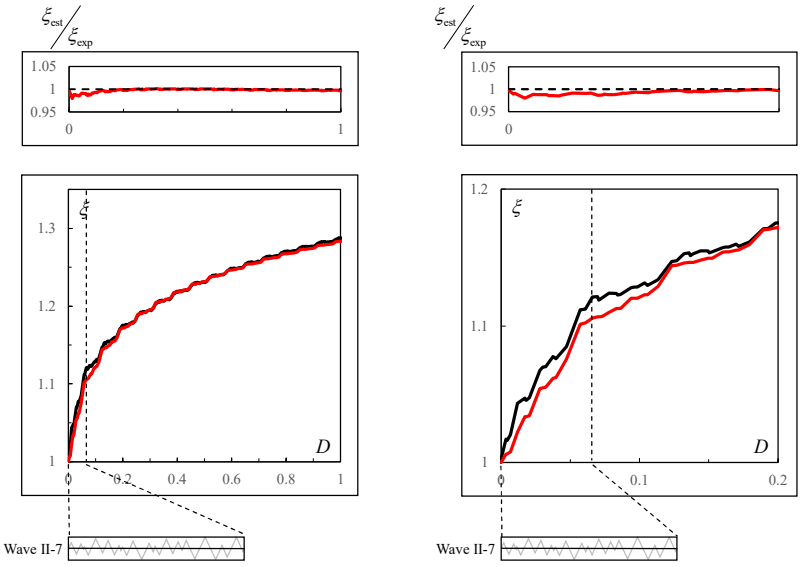

(a) D = 0 ~ 1.0 (b) D = 0 ~ 0.2

Figure. 3-8 Experimental results and evaluated values (II-7)

3.6. Precision verification of the exciting cumulative damage evaluation method

When the previously reported evaluation method (Ene et al. 2016) [3-2] is applied to evaluate the dampers' cumulative damage after an earthquake, ground motions recorded by the observation stations around the damaged building can be used to reproduce the seismic response of the structure. Additionally, the value of ξ corresponding to the selected ground motion records can be conveniently estimated using the ξ–D relation evaluation method depicted in Figure. 3-6. Consequently, the most appropriate ground motion record that can precisely reflect the excitations experienced by the target building can be identified by comparing the estimated and measured values of ξ.

3.7. Conclusion

Significant conclusions were obtained through loading tests with complicated loading histories:

1). The trend change of ξ-D relations, which was caused by the increase of γ_t, could be evaluated through the ξ-D relations of a U-shaped steel damper loaded under standard loading with target γ_t.

2). The final residual plastic deformation ratio ξ of the U-shaped steel dampers, suffered from loading histories that only differ in the arrangement of the loading cycles, tend to be similar to each other. After applying these properties, a method for the ξ-D relation evaluation of the U-shaped steel dampers loaded with any excitations, such as ground motion, was developed in the present study.

3). Applying this ξ-D relation evaluation method, a precision verification approach for the exciting cumulative damage evaluation method (Ene et al. 2016) [2-2] is proposed by comparing the estimated and measured value of residual plastic deformation ratio ξ corresponding to the ground motion records used in cumulative damage evaluation.

Furthermore, this mechanical and simple deformation behavior estimation method facilitates the determination of deformation behavior statistics of U-dampers loaded under various ground motions.

3.8. Reference

[3-1] 吉敷祥一，大河原勇太，山田　哲，和田　章，免震構造用 U 字形鋼材ダンパーの繰り返し変形性能に関する研究，日本建築学会構造系論文集，第 73 巻，第 624 号, pp.333-340, 2008.2

(Kishiki S et al. Experimental evaluation of cyclic deformation capacity of U-shaped steel damagers for base-isolated structures. Journal of Structural and Construction Engineering (Transactions of AIJ) 2008;73(624):333–340.)

[3-2] Ene D, Kishiki S, Yamada S, Jiao Y, Konishi Y, Terashima M, Kawamura M. Experimental study on the bidirectional inelastic deformation capacity of U-shaped steel dampers for seismic isolated buildings. Earthquake Engineering & Structural Dynamics 2016;45(2):173–192.

[3-3] Ene D, Yamada S, Jiao Y, Kishiki S, Konishi Y. Reliability of U-shaped steel dampers used in base-isolated structures subjected to biaxial excitation. Earthquake Engineering & Structural Dynamics 2017;46:621–639.

[3-4] National Research Institute for Earth Science and Disaster Resilience (NIED), Strong-motion seismograph networks K-NET, KiK-net, https://www.kyoshin.bosai.go.jp/

[3-5] Japan Institute of Architects and Japan Aseismic Safety Organization (JASO). Earthquake-resistant Building Design for Architects, revised edition. 28–41. 1997. Shokokusha. https://www.jaso.jp/pdf/earthquake_resistant.pdf

[3-6] Konishi Y, Kawamura N, Terashima M, Kishiki S, Yamada S, Aiken I, Black C, Murakami K, Someya T. Evaluation of the fatigue life and behavior characteristics of

U-shaped steel dampers after extreme earthquake loading. In 15th World Conference on Earthquake Engineering, Lisboa, Portugal 2012.

Chapter 4

Quick inspection of U-damper based on shape change

4. Quick inspection of U-shaped steel damper based on shape change.

4.1. Introduction

The cumulative damage evaluation method composed by Ene et al. [4-1] [4-2] is theoretically valid only when insufficient information, such as reliable ground motion records and dynamic properties of the structure, is available. As a time-consuming information-gathering process is detrimental to the functional recovery of damaged buildings, establishing a more convenient and intuitive damage evaluation method (quick inspection) for U-dampers is essential.

Researchers have made great efforts to simplify the cumulative damage evaluation of U-dampers. Jiao et al. (2014) [4-3] determined that the cumulative damage of U-dampers is very likely related to the area of the circumscribed rectangle corresponding to the displacement orbit (Figure. 4-2). Kawamura et al. (2014) [4-4] presented a cumulative damage evaluation approach that relies on the comparison between the seismic input energy (dissipated by the damper) and its ultimate energy dissipation capacity. These methods can simplify the process of cumulative damage evaluation to a degree. However, similar to that composed by Ene et al. (2016) [4-1], the lack of precision verification approaches seriously constrains the implementation of these methods as well. ξ-D relationship evaluation method established in Chapter 2 and Chapter 3 makes it possible to estimate the dampers' cumulative damage through the shape change that initiates on its parallel arms.

However, as shown in Figure. 4-1, the residual plastic deformation of U-dampers loaded under relatively large deformation might be the same as that of the ones loaded

under relatively small deformation amplitude, even though they differ in cumulative damage. Seems that cumulative damage evaluation cannot rely solely on residual plastic deformation. A set of strong ground motion records from Japan was applied in the time-history analysis to find indicators that might be helpful to achieving the quick inspection of U-dampers. Section 4.3. presents the details of the time-history analysis and analytical results. In section 4.4, the equivalent deformation amplitude (γ_{eq} in Figure. 4-3) is introduced in the evaluation of the cumulative damage of U-dampers. Herein, the damper subjected to seismic excitation is assumed to be loaded under a constant deformation amplitude with an equivalent deformation amplitude. Easily obtainable indicators, such as the maximum value of the deformation experienced by the dampers recorded using the scratch plates (Figure. 4-2) installed in isolation layers (γ_{max} (γ_{peak}) in Figure. 4-3) and the significant deration of the earthquake record are found to be tightly correlated to the value of equivalent deformation amplitude.

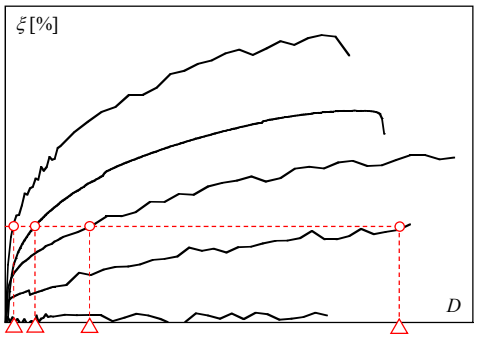

Figure. 4-1 Different cumulative damage of dampers with the same ξ

Figure. 4-2 Scratch plate and record of displacement orbit [4-3]

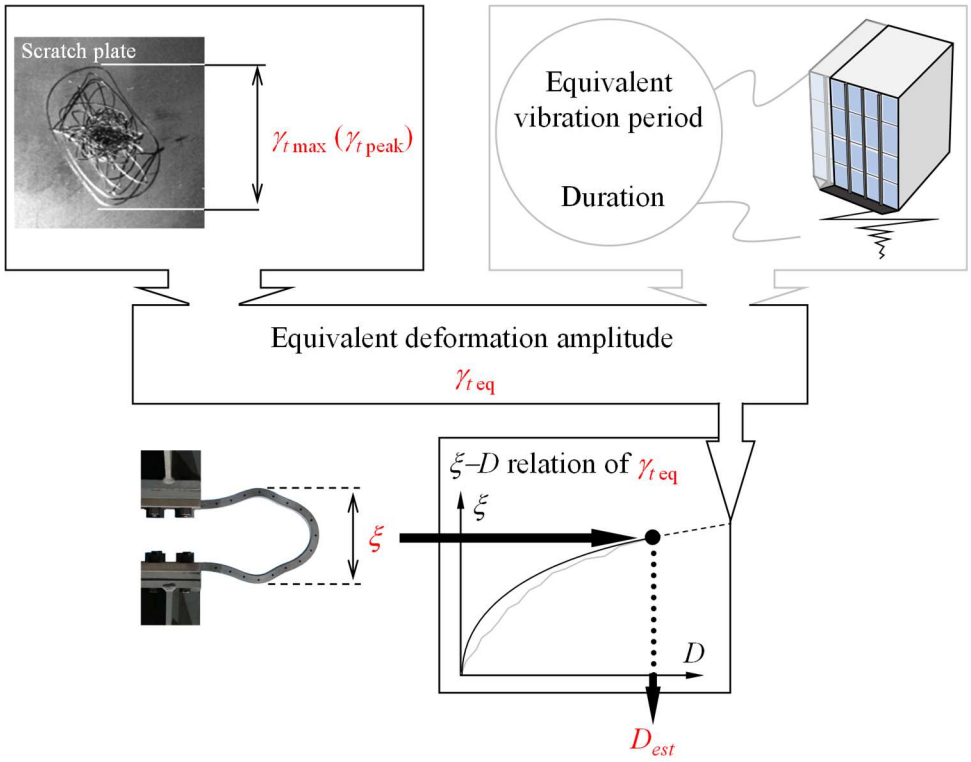

Figure. 4-3 Quick inspection of U-damper

4.2. Fatigue behavior evaluation equation of U-damper applied in the time-history analysis

As aforementioned, Kishiki et al. (2012) [4-5] simplified the fatigue life prediction equation in 2012 because the value of N_f corresponding to a certain deformation amplitude γ_t cannot be calculated directly using Eq (2-2)(c). The simplified one is more accessible to estimate the value of N_f corresponding to a set of various deformation amplitudes from a random wave such as earthquake-induced excitations. Only 6 types of deformation amplitudes (γ_t = 25, 40, 55, 70, 90, and 110%) are applied in cyclic loading tests, so the value of N_f can still be obtained easily through the functional image of the fatigue curve Eq (2-2)(c). However, it is necessary to count the number of loading

cycles to fracture corresponding to far more than 6 types of γ_t in time-history analysis. The simplified fatigue curve Eq (2-3) has become a more desirable choice here. Therefore, replacing Eq (2-7) (the same as Eq (2-2)(c)), Eq (2-3) is applied as the low-cycle fatigue behavior evaluation equation of U-damper in this chapter (Eq (4-1)).

$$\gamma_{t,i} = 2370 \cdot N_{f,i}^{-0.66} \quad 20\% \le \gamma_t \le 500\% \qquad \text{Eq (4-1)}$$

As illustrated in Figure. 2-17, the experimental results (Series I) of the number of loading cycles to fracture are precisely but slightly overestimated by Eq (4-1), which is similar to Eq (2-7). Eq (4-1) is considered to be reliable in the fatigue behavior evaluation of the single U-shaped element specimens of the present study as well. Detailed discussion about the applicability of Eq (4-1) refers to APPENDIX F.

It is worth mentioning that, the scope of application of Eq (4-1) is $20\% \le \gamma_t \le 500\%$. Only the cumulative damage and residual plastic deformation caused by loading cycles with γ_t over 20% are considered in time-history analysis.

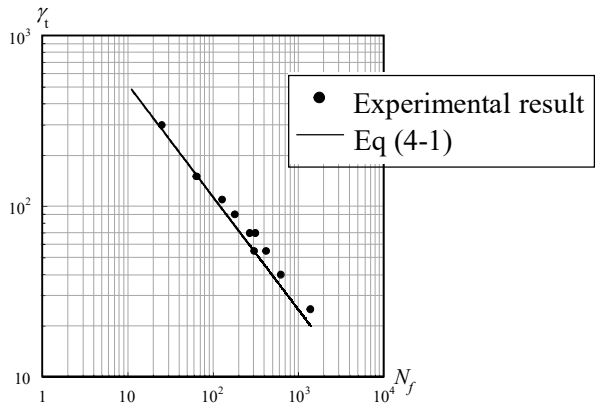

Figure. 4-4 Fatigue behavior evaluation of U-damper

4.3. Scope of application of deformation amplitude in evaluating the ξ–D relation of the U-damper

Single U-shaped elements (UD40) are known to yield when the deformation reaches 18 mm in the monotonic loading test (Jiao et al. 2015 [4-6]) at approximately γ_t = 16%. The damper remains in an elastic state when loaded under γ_t of approximately 16% and does not begin exercising its function of energy dissipation under this negligible deformation amplitude. The results of the cyclic loading tests indicate that no apparent residual plastic deformation was initiated when γ_t was less than 25%. This provides a more precise reference value of the lower limit of γ_t in evaluating the ξ–D relation of the U-damper. Figure. 2-10 indicates the analytical results obtained from FEM modeling. Residual plastic deformation caused by a single loading cycle when the damper is loaded with γ_t = 25, 55, 90, 110, and 150% are compared and shown together. It is found that almost no residual plastic deformation is caused by a single loading cycle with γ_t = 25%. It neatly explains the reason why the shape of the damper's parallel arms did not obviously change when loaded with γ_t = 25% in test I-3.

For dampers loaded under γ_t > 110%, residual plastic deformation tends to accumulate around the part connected to the structure rather than concentrating on the middle part of the parallel arms. This phenomenon is observed in the deformation behavior of the damper loaded under an offset increasing deformation amplitude with γ > 55% or γ_t > 110% (Figure. 3-4(b), II-4). The residual plastic deformation of this specimen accumulated on the lower parallel arms because it was loaded only in the positive direction. However, the upper parallel arm would exhibit a similar deformation behavior

if the loading direction was converted to negative. This test result provides a significant reference for identifying the deformation behavior of dampers loaded with $\gamma_t > 110\%$.

Residual plastic deformation accumulates in the middle part of the parallel arms before D reached 0.25 under a constant deformation amplitude $\gamma = 55\%$. However, it remained at nearly the same level as γ was increased to 70 and 90%, as indicated in Figure. 4-6(b) and Figure. 4-6(c), respectively. Conversely, the residual plastic deformation that accumulated around the connection to the structure (right side of the middle part in Figure. 4-6) increased considerably. Therefore, ξ grows more slowly than expected when γ exceeds 55%. Moreover, it is observed that the ξ of III-4 is always lower than that of III-3 for the same value of cumulative damage D (Figure. 2-20(b)), despite the deformation amplitude of III-4 (γ_t = 300%) being larger than that of III-3 (γ_t = 150%). This phenomenon indicates that ξ can no longer correctly describe the development of the residual plastic deformation when the U-damper is loaded with $\gamma > 55\%$ ($\gamma_t > 110\%$) even though the deformation behavior is also precisely evaluated by Eq (3-1) (μ = 0.5). Additionally, the analytical results of FEM modeling (Figure. 2-10) indicated that the most obvious residual plastic deformation caused by a single loading cycle initiates around P_3 rather than P_4. The analytical result matches well with the description of the experimental results.

In summary, the cumulative damage can be correctly reflected using ξ only when loaded with γ_t ranging from 25 to 110%. This principle is applied to the time-history analysis presented in the next section. The values of D and ξ were considered only when the maximum deformation caused by the ground motion occurred in this range of γ_t. The relation between residual plastic deformation and cumulative damage of U-damper can be evaluated using Eq (4-2) in time-history analysis.

$$\xi_{c,i} = k(D_{k,i-1} + \Delta D_i, \beta_{c,i}) \qquad \text{Eq (4-2)}$$

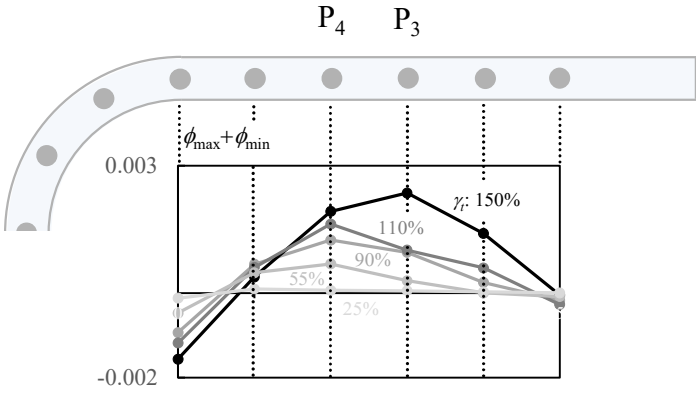

Figure. 4-5 Residual plastic deformation initiates on the parallel arm of U-dampers (1 cycle; γ_t = 25, 55, 90, 110, and 150%).

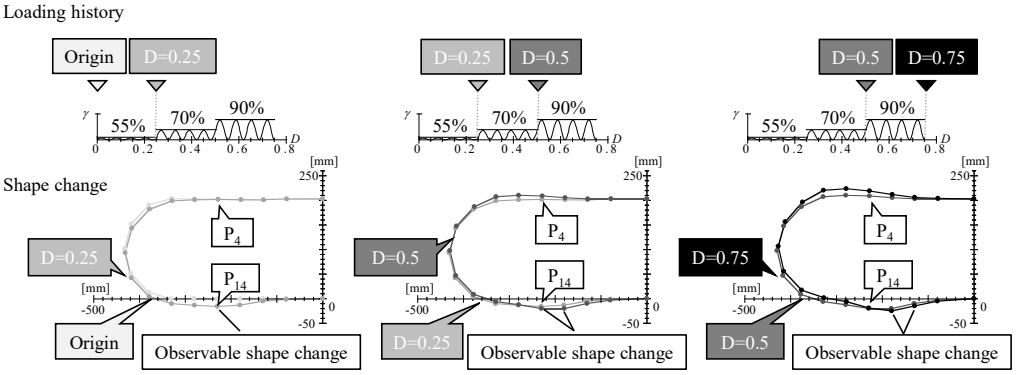

(a) D = 0 ~ 0.25 (b) D = 0.25 ~ 0.5 (c) D = 0.5 ~ 0.75

Figure. 4-6 Deformation behavior of specimen II-4

4.4. Nonlinear time-history analysis

The effects of seismic excitations on the residual plastic deformation (ξ) and cumulative damage (D) are investigated in this section. As this requires a set of realistic

unidirectional displacement histories, a set of strong ground motions and a series of analytical models were established. The deformation behavior evaluation method (Chapter 3) was applied to estimate the values of the residual plastic deformation of the U-damper that corresponds to the ground motion records. Additionally, the equivalent deformation amplitude (equivalent peak-to-peak horizontal shear angle (γ_{eq})) was induced to simplify the approach of investigating the effect of ground motions and dynamic properties of structures.

4.4.1. Ground motion set

U-dampers are widely used in Japan for designing isolated structures. A subset of ground motions from K-NET and KiK-net (NIED, 2019 [4-7]) in Japan was used for the time-history analysis. Over 900 strong ground motion records from 190 different seismic events with magnitudes greater than five ($5 \leq M \leq 9$) were selected (APPENDIX H). Both horizontal components of each ground motion were considered. Although selecting appropriate ground motions to perform a reliability analysis for nonlinear systems is a sensitive task and has been extensively studied, it is beyond the scope of this study. Rather than selecting a certain set of ground motions based on a specific seismological parameter, the ground motions in this study were selected as widely as possible to obtain more universal and representative analytical results. Furthermore, the selected ground motion records were not scaled to ensure that the analytical results reflect the actual use of dampers with high precision.

4.4.2. Analytical model

For a base-isolated structure, the response of the entire system is always designed to concentrate on the level of the isolation layer to protect the superstructure. Therefore, the superstructure was modeled as a rigid body and reduced to a single mass (m = 750t) with one degree of freedom in the analytical model (Figure. 4-7).

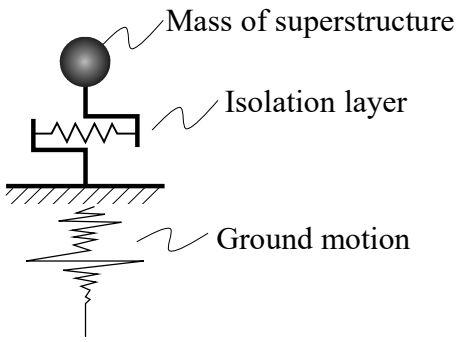

Figure. 4-7 Analytical model.

The isolation layer is assumed to comprise natural rubber bearings and hysteretic dampers. Figure. 4-8 depicts the restoring-force characteristics of the isolation layer. The assumed hysteretic behavior for the dampers is a linear elastic-perfect plastic behavior, whereas the isolator (rubber bearing) is modeled as linear elastic. The yield deformation of the isolation layer was identical to that of the damper element (18 mm).

The isolation period (T_i) is defined as the period of the structure with only isolators and can be evaluated using Eq (4-3); here, m represents the mass of the superstructure, and k_i denotes the stiffness of the isolator. Based on the design practice followed in Japan (Pan et al. 2005 [4-8]), T_i is commonly higher than 3.5 s. In this study, T_i was set to 4, 5, and

6 s to rebuild the seismic response of base-isolated structures with different dynamic properties.

$$T_i = 2\pi\sqrt{\frac{m}{k_i}} \qquad \text{Eq (4-3)}$$

The damper strength ratio (α_s) defined as the ratio of the total yield strength of the hysteretic dampers (Q_y^d) to the weight of the superstructure (m) is another significant parameter involved in the establishment of analytical models. In this study, the values of α_s were set to 0.02, 0.04, and 0.06 (Pan et al. 2005 [4-8]; Qu et al. 2013 [4-9]). Correspondingly, the initial stiffness of the hysteretic damper was modified using the same scale to demonstrate that the increase in α_s is caused by an increase in the number of dampers installed in the system. By integrating the aforementioned parameters, namely T_i and α_s, nine analytical models were adopted for the time-history analysis.

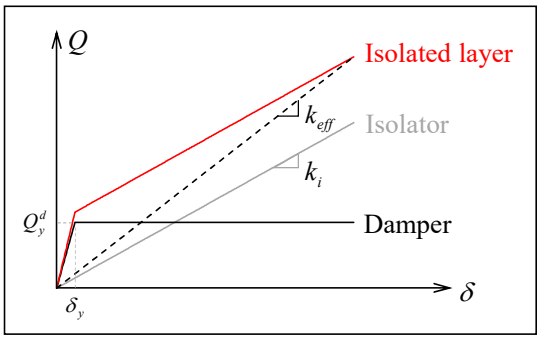

Figure. 4-8 Analytical model.

4.4.3. Equivalent deformation amplitude $\gamma_{t\,eq}$

The cumulative damage (D) caused by strong vibratory motion (with $\gamma_t > 20\%$) and the

corresponding value of the residual plastic deformation ratio (ξ) are calculated using Eq (2-7) and Eq (4-2), respectively. Figure. 4-9 illustrates the obtained analytical results, D_{ana} and ξ_{ana}. Where the rainflow counting method was adopted to count the number of loading cycles (Amzallag et al. 1994 [4-10]). Subsequently, (D_{ana}, ξ_{ana}) was plotted in a coordinate system with D as the X-axis and ξ as Y-axis. Although the damper is not loaded under a constant deformation amplitude, one corresponding value of γ_t exists when the values of D and ξ are known. Eq (4-4) is obtained by rewriting Eq (2-9) to convert (D_{ana}, ξ_{ana}) to an equivalent peak-to-peak horizontal deformation angle ($\gamma_{t\,\mathrm{eq}}$).

$$\gamma_{t\mathrm{eq}} = g^{-1}(\beta_{\mathrm{eq}}) \qquad \text{(a)} \quad \text{Eq (4-4)}$$

Where

$$\beta_{\mathrm{eq}} = b(D_{ana}, \xi_{ana}) = \frac{\ln(1+\dfrac{D_{ana}}{\alpha})}{\xi_{ana} - 1} \qquad \text{(b)} \quad \text{Eq (4-4)}$$

Consequently, the cumulative damage of the dampers caused by seismic excitations can be estimated conveniently using the measured values of ξ and ξ–D relation under constant deformation amplitude with the corresponding $\gamma_{t\ \mathrm{eq}}$. Additionally, the introduction of $\gamma_{t\,\mathrm{eq}}$ significantly simplifies the approach by avoiding the investigation of the effect of the dynamic properties of the structure and seismic excitation on the values of ξ and D. The results of the time-history analysis are explained in terms of $\gamma_{t\,\mathrm{eq}}$ in next the section.

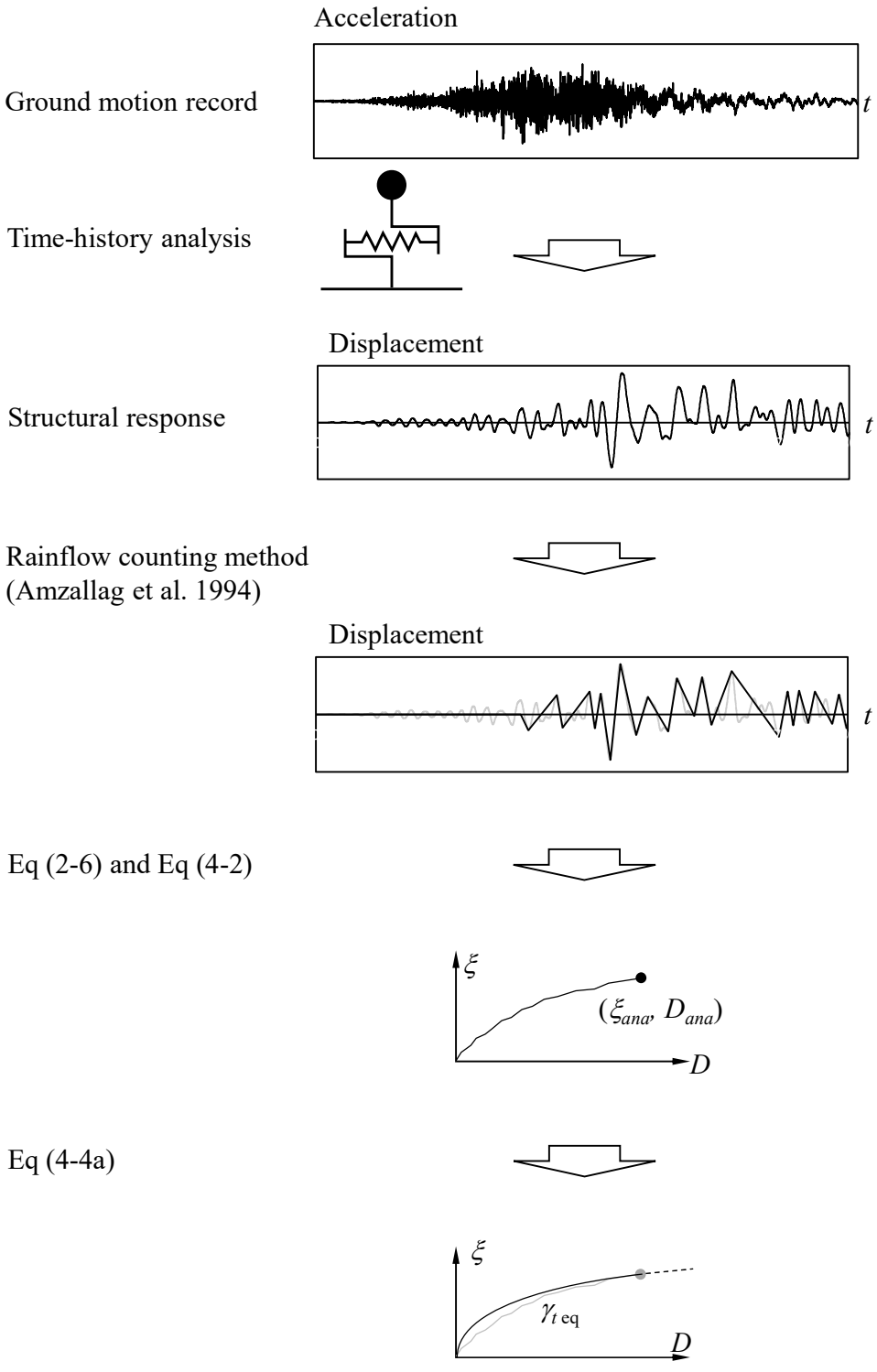

Figure. 4-9 Calculation of $\gamma_{t\,\mathrm{eq}}$.

4.4.4. Results pf the nonlinear time-history analysis

As depicted in Figure. 4-10, although the maximum value of the damper deformation in both the positive and negative directions can be easily obtained using the displacement orbit recorded by the scratch plate installed at the isolation layer, the sum of the absolute values of the maximum deformation in both directions ($\gamma_{t\,peak}$) does not always equal the maximum deformation amplitude ($\gamma_{t\,max}$). Moreover, $\gamma_{t\,peak}$ is a more significant reference indicator in the quick inspection of the U-damper because $\gamma_{t\,max}$ cannot be obtained without time-history analysis. Therefore, $\gamma_{t\,eq}$ is plotted in Figure. 4-11, Figure. 4-12, and Figure. 4-13 with $\gamma_{t\,max}$ ($\gamma_{t\,peak}$) as the *X*-axis. As explained in Section 2.4, cumulative damage can be reflected correctly only using ξ when the damper is loaded with γ_t ranging from 25 to 110%. Therefore, the analytical results with $\gamma_{t\,peak}$ only within this interval are discussed in this study.

For simplification, the analytical models are referred to as (T_f, α_s). In the case of model (5, 0.02) (black in Figure. 4-11, and Figure. 4-12), $\gamma_{t\,eq}$ increases with the increase in $\gamma_{t\,max}$ and $\gamma_{t\,peak}$. The linear relationship between $\gamma_{t\,eq}$ and $\gamma_{t\,max}$ is more significant than that between $\gamma_{t\,eq}$ and $\gamma_{t\,peak}$. As all models are derived from model (5, 0.02), the analytical results of these models (red in Figure. 4-11, and Figure. 4-12) are illustrated as representatives in comparison with those of model (5, 0.02). The value of $\gamma_{t\,eq}$ is not significantly affected by the dynamic properties of the analytical models.

Figure. 4-13 depicts the analytical results of the ground motion records from earthquakes that differ in intensities against the background of all analytical results. Typically, $\gamma_{t\,eq}$–$\gamma_{t\,max}$ ($\gamma_{t\,peak}$) relationships are not significantly affected by the intensities of earthquakes. However, when $\gamma_{t\,max}$ or $\gamma_{t\,peak}$ remains the same, $\gamma_{t\,eq}$ of high-magnitude

earthquakes (M = 9) tends to be lower than that of relatively low-magnitude earthquakes (M ≤ 7). Particularly, this behavior is prominent when $\gamma_{t\,peak}$ or $\gamma_{t\,max}$ is greater than 0.5.

The correlation between the duration of strong ground motion and destruction experienced by structures during earthquakes has been widely discussed in the literature (Trifunac 1971 [4-11]; Bommer et al. 2004 [4-12]). Bommer and Martinez-Pereira (1999) [4-13] reported that for ground motion records with similar amplitudes of accelerograms, those with longer durations tend to be more destructive; whereas, for records with the same energy content, the ones with shorter durations are capable of causing more destruction. Additionally, $\gamma_{t\,eq}$ equals $\gamma_{t\,max}$ ($\gamma_{t\,peak}$) under extreme conditions, wherein only one full loading cycle is completed owing to the short duration of the ground motion. Subsequently, an increased duration leads to more loading cycles, whereas the value of $\gamma_{t\,eq}$ would never be as large as $\gamma_{t\,max}$ ($\gamma_{t\,peak}$). In other words, $\gamma_{t\,eq}$ is highly likely to be negatively correlated with the duration of ground motion under constant $\gamma_{t\,max}$ ($\gamma_{t\,peak}$). To verify this conjecture, this study adopted "significant duration," which indicates the time interval required for the Arias Intensity (I_A) (Arias 1970 [4-14]) of an earthquake to reach two relative thresholds to quantitatively evaluate the duration of strong vibratory motions (APPENDIX G). Two commonly used measures of significant duration are the time intervals between 5–75% and 5–95% of the final value of I_A, denoted as $SD_{5\text{-}75}$ and $SD_{5\text{-}95}$, respectively (Somerville et al. 1997 [4-15]; Bradley 2011 [4-16]). As the cumulative damage caused by a single loading cycle with γ_t < 20% cannot be evaluated using Eq (4-1), loading cycles with γ_t < 20% were excluded from the evaluation of the cumulative damage to the dampers. In this study, strong vibration is defined as vibration with a deformation amplitude (γ_t) greater than 20%. This causes the duration of the strong vibratory motion to be grossly overestimated by $SD_{5\text{-}95}$. Therefore, Figure. 4-14 illustrates

$\gamma_{t\,eq}$ of ground motion records with similar $\gamma_{t\,max}$ ($\gamma_{t\,peak}$) with $SD_{5\text{-}75}$ as X-axis, and any reference to "duration" represents $SD_{5\text{-}75}$.

Similar to model (5, 0.02) (Figure. 4-14), the analytical results are depicted in different colors to indicate the effect of the intensities of earthquakes. Earthquakes with high magnitude (M = 9) are indicated in red, whereas black spots denote the $\gamma_{t\,eq}$ of the ground motion records from the earthquakes with relatively lower magnitude (M < 7). When $\gamma_{t\,max}$ ($\gamma_{t\,peak}$) remains the same, the corresponding value of γ_t to ground motion with a relatively longer duration tends to be smaller. The negative correlation between $\gamma_{t\,eq}$ and the duration of strong motion with a similar $\gamma_{t\,max}$ ($\gamma_{t\,peak}$) was confirmed. Additionally, the duration of ground motion records from high-magnitude earthquakes is always longer than that obtained from low-magnitude earthquakes. Previous studies (Kempton and Stewart 2006 [4-17]; Bahrampouri, Rodriguez-Marek, and Green 2021 [4-18]) have reported that the duration of strong motion with a similar source-to-site distance exhibits a positive correlation with the intensity of events. A similar trend change is observed in Figure. 4-14 when $\gamma_{t\,max}$ ($\gamma_{t\,peak}$) remains nearly the same.

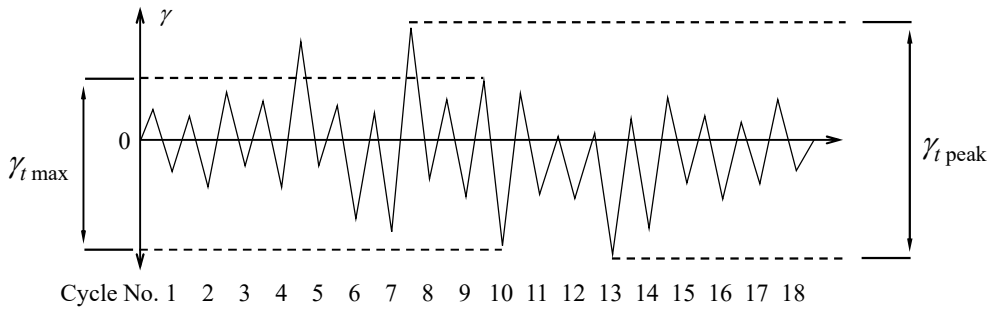

Figure. 4-10 Definitions of $\gamma_{t\,peak}$ and $\gamma_{t\,max}$.

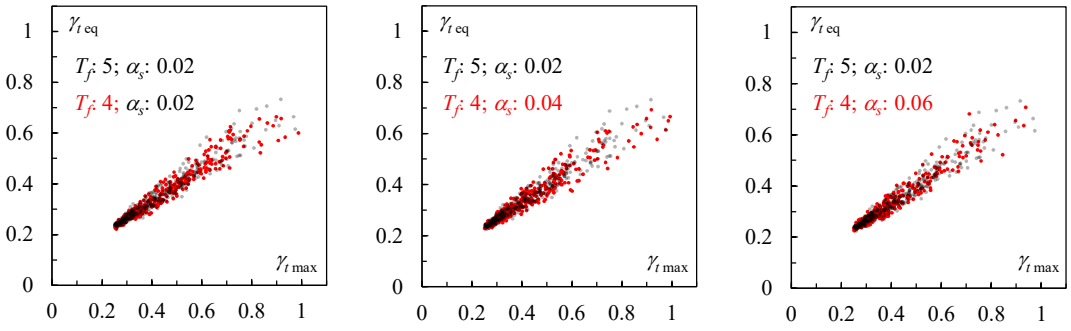

(a) T_f = 4s; α_s = 0.02

(b) T_f = 4s; α_s = 0.04

(c) T_f = 4s; α_s = 0.06

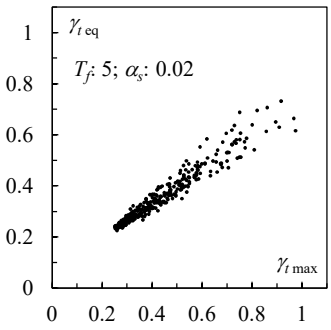

(d) T_f = 5s; α_s = 0.02

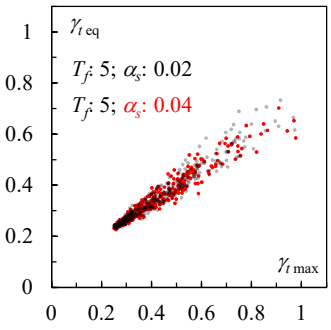

(e) T_f = 5s; α_s = 0.04

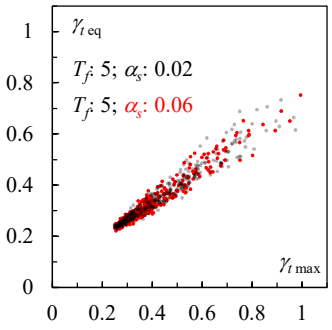

(f) T_f = 5s; α_s = 0.06

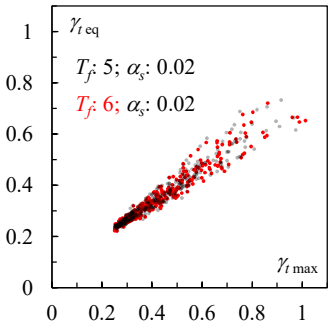

(g) T_f = 6s; α_s = 0.02

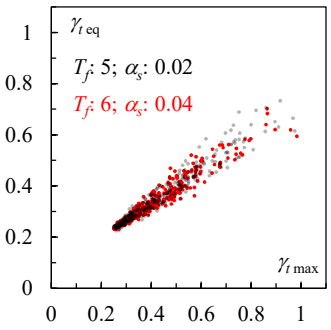

(h) T_f = 6s; α_s = 0.04

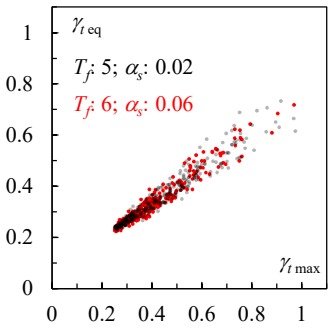

(i) T_f = 6s; α_s = 0.06

Figure. 4-11 Analytical results ($\gamma_{t\,eq}$) in terms of $\gamma_{t\,eq}$–$\gamma_{t\,max}$ relationships.

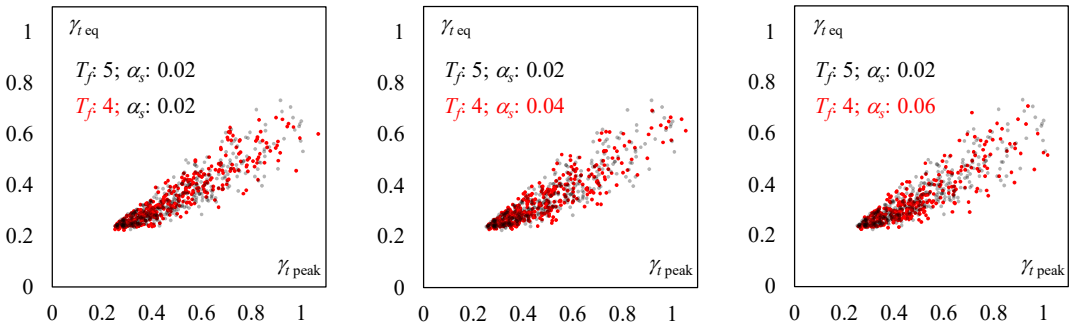

(a) T_f = 4s; α_s = 0.02

(b) T_f = 4s; α_s = 0.04

(c) T_f = 4s; α_s = 0.06

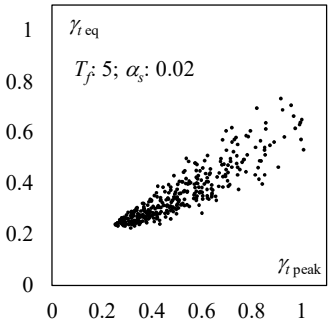

(d) T_f = 5s; α_s = 0.02

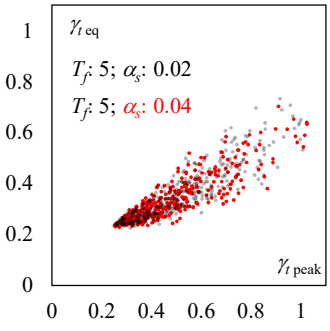

(e) T_f = 5s; α_s = 0.04

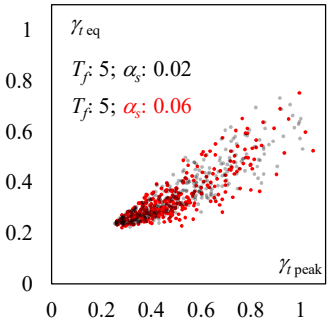

(f) T_f = 5s; α_s = 0.06

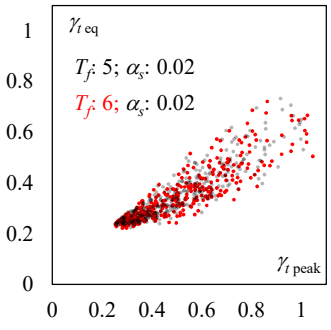

(g) T_f = 6s; α_s = 0.02

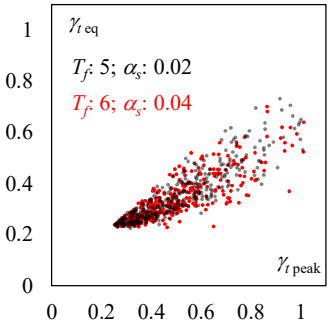

(h) T_f = 6s; α_s = 0.04

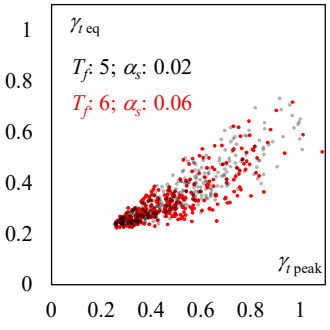

(i) T_f = 6s; α_s = 0.06

Figure. 4-12 Analytical results ($\gamma_{t\,eq}$) in terms of $\gamma_{t\,eq}$–$\gamma_{t\,peak}$ relationships.

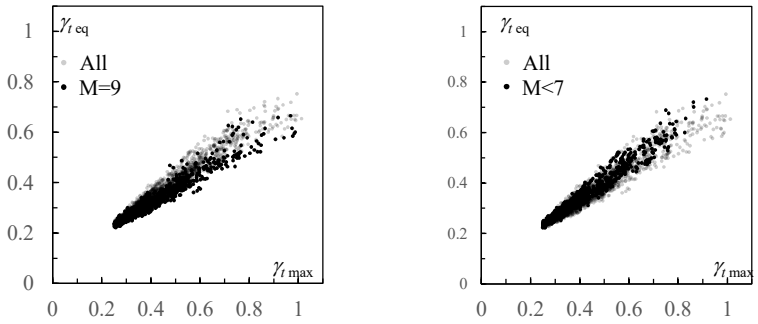

(a) $\gamma_{t\,eq}$–$\gamma_{t\,max}$ relationships.

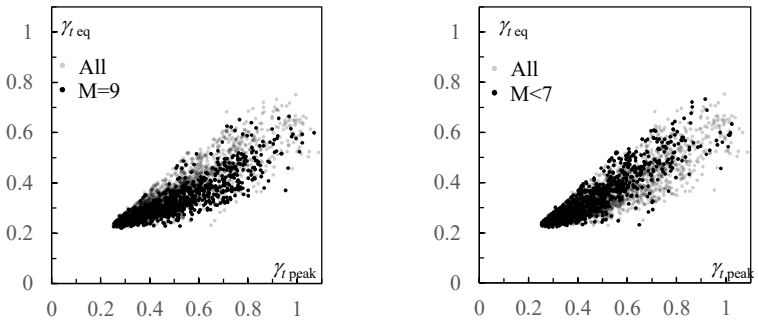

(b) $\gamma_{t\,eq}$–$\gamma_{t\,peak}$ relationships.

Figure. 4-13 Effect of the intensities of earthquakes

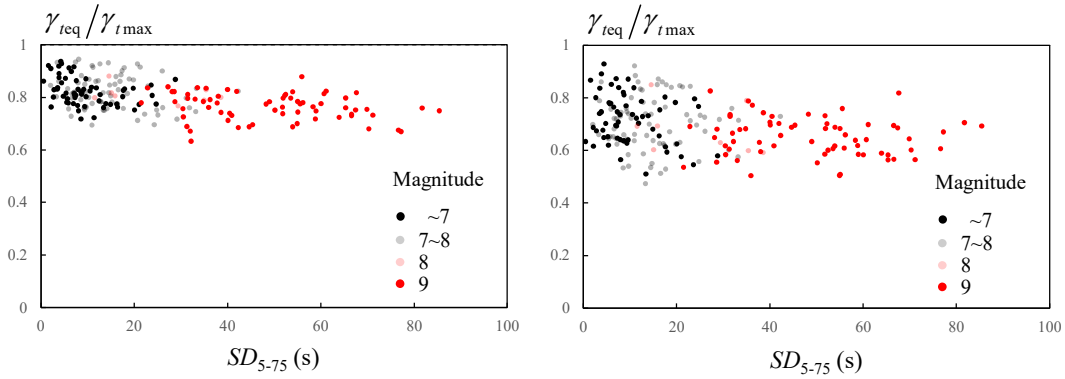

(a) $\gamma_{t\,eq}$–$SD_{5\text{-}75}$ relation (identical to $\gamma_{t\,max}$).

(b) $\gamma_{t\,eq}$–$SD_{5\text{-}75}$ relation (identical to $\gamma_{t\,peak}$).

Figure. 4-14 $\gamma_{t\,eq}$-$SD_{5\text{-}75}$ relationship based on the analytical model

4.5. Cumulative damage evaluation method of U-dampers

As mentioned earlier, the cumulative damage of the U-damper caused by seismic excitations can be easily estimated using ξ and ξ–D relation under a constant deformation amplitude with $\gamma_{t\,\mathrm{eq}}$. Additionally, consolidating multiple research objects (ξ and D caused by a certain ground motion record) into one ($\gamma_{t\,\mathrm{eq}}$) simplifies the investigation of the effect of dynamic properties of structures and seismic excitations. The residual plastic deformation ξ can be easily obtained by determining the actual measurements after an earthquake. This section discusses the estimation approaches of $\gamma_{t\,\mathrm{eq}}$ based on easily available information, such as $\gamma_{t\,\mathrm{max}}$ ($\gamma_{t\,\mathrm{peak}}$) or duration of strong vibratory motion.

4.5.1. Estimation approach of $\gamma_{t\,\mathrm{eq}}$ based on the duration of earthquakes

The $\gamma_{t\,\mathrm{eq}}$ estimation approach is presented in this section based on the analysis of the relation between the duration of strong vibratory motion and $\gamma_{t\,\mathrm{eq}}$. The number of loading cycles experienced by dampers during an earthquake was estimated using Eq (4-5).

$$Num\_cycle = \frac{SD_{5-75}}{T_{eq}} \qquad \text{Eq (4-5)}$$

where T_{eq} denotes the equivalent vibration period of the analytical models under maximum displacement $\delta_{\max} = 400$ mm.

In most instances, the deformation amplitude of the other loading cycles remains unknown along with the value of $\gamma_{t\,\mathrm{max}}$ ($\gamma_{t\,\mathrm{peak}}$) despite estimating the number of loading

cycles. Therefore, the time history of the structure's response is simplified, as illustrated in Figure. 4-15, to identify a viable $\gamma_{t\,eq}$ estimation approach. A simplified wave comprises two primary components; only one loading cycle with γ_t equals $\gamma_{t\,max}$ ($\gamma_{t\,peak}$), whereas the others are reduced into loading cycles with γ_t = 25%. Figure. 4-11 and Figure. 4-12 validates that $\gamma_{t\,max}$ ($\gamma_{t\,peak}$) is closely associated with the value of $\gamma_{t\,eq}$, which indicates that $\gamma_{t\,max}$ ($\gamma_{t\,peak}$) cannot be omitted in the simplification of the time history. For ground motion records with similar $\gamma_{t\,max}$ ($\gamma_{t\,peak}$), a longer duration implies more loading cycles with γ_t = 25%. This decreases the value of $\gamma_{t\,eq}$ and precisely reflects the effect of duration (Figure. 4-14) using the simplified wave. Furthermore, as discussed in Section 2.3, the residual plastic deformation caused by loading cycles with γ_t < 25% is insufficient for observation. Therefore, for ground motions with $\gamma_{t\,eq}$ < 25%, $\gamma_{t\,eq}$ is considered to be 25% in this study as they result in almost non-observable residual plastic deformation. Reducing the loading cycles, except for the one with $\gamma_{t\,max}$ ($\gamma_{t\,peak}$) to γ_t = 25%, can ensure that the estimated value of γ_t does not reduce below 25%. D* and ξ* indicate the cumulative damage and residual plastic deformation of the simplified wave, respectively. The estimated value of $\gamma_{t\,eq}$ can be obtained by substituting D* and ξ* in Eq. 6.

As the estimated results of all analytical models were similar, only those of the analytical model (5, 0.02) are illustrated in Figure. 4-16. The estimated values of $\gamma_{t\,eq}$ were compared with the analytical results and plotted in Figure. 4-16(a) and (c). Eq (4-6) is obtained by rewriting Eq (2-9) to estimate the cumulative damage of the dampers using the measured value of ξ (substituted by the analytical value of ξ) and the ξ–D relation under a constant deformation amplitude with $\gamma_{t\,eq}$.

$$D_{est} = d(\xi, \beta_{eq}) = \alpha \cdot (e^{(\xi-1)\cdot\beta_{eq}} - 1) \qquad \text{(a)} \quad \text{Eq (4-6)}$$

Where

$$\beta_{eq} = g(\gamma_{teq}) \qquad \text{(b)}$$

Figure. 4-16(b) and (d) depict the estimated values of D. Although $\gamma_{t\,eq}$ is precisely estimated using $\gamma_{t\,max}$, $\gamma_{t\,eq}$ is overestimated by replacing $\gamma_{t\,max}$ with $\gamma_{t\,peak}$. Consequently, the cumulative damage D is precisely estimated by $\gamma_{t\,max}$ and slightly underestimated by $\gamma_{t\,peak}$. However, over 80% of the estimated results (D_{est}) are distributed in the interval from $\mu-\sigma$ to $\mu+\sigma$ of the analytical value (D_{ana}) for both $\gamma_{t\,max}$ and $\gamma_{t\,peak}$.

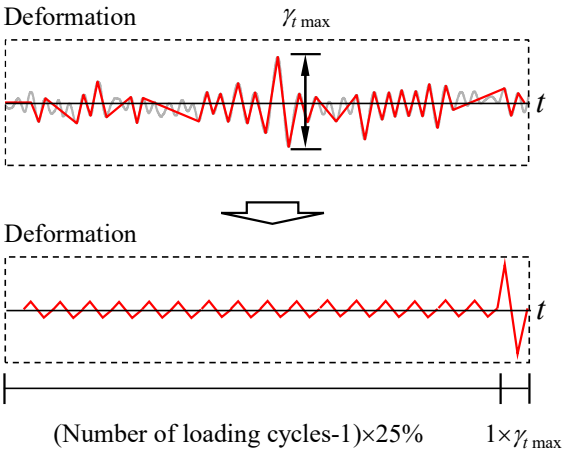

Figure. 4-15 Simplification of the response analysis results.

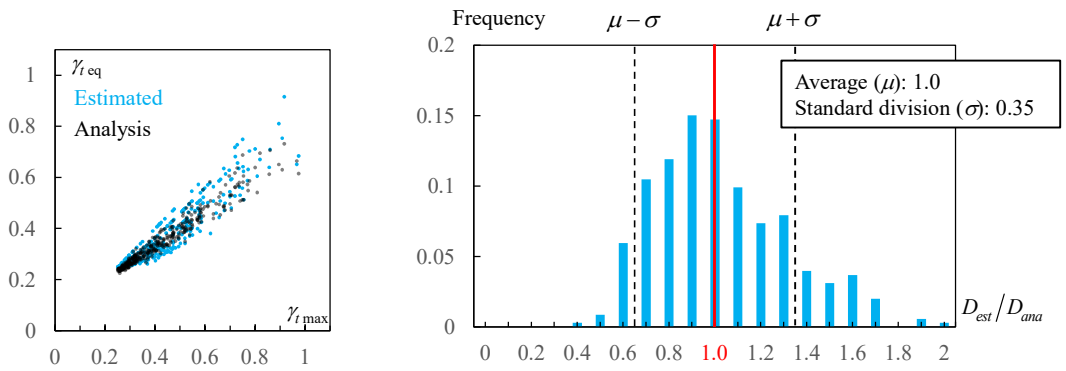

(a) Estimated value of $\gamma_{t\,eq}$ ($\gamma_{t\,max}$). (b) Estimated value of D ($\gamma_{t\,max}$).

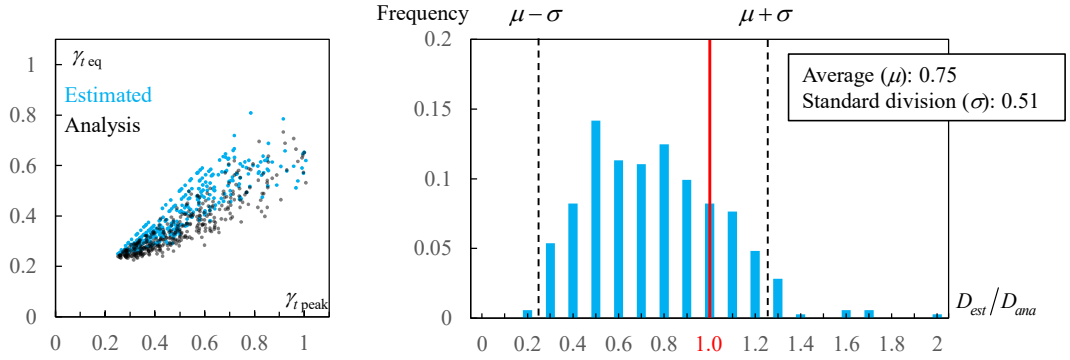

(c) Estimated value of $\gamma_{t\,eq}$ ($\gamma_{t\,peak}$). (d) Estimated value of D ($\gamma_{t\,peak}$).

Figure. 4-16 Estimated value of cumulative damage (D) and equivalent deformation amplitude ($\gamma_{t\,eq}$) with T_f = 5 s and α_s = 0.02.

4.5.2. Estimation approach of $\gamma_{t\,eq}$ based on $\gamma_{t\,max}$ or $\gamma_{t\,peak}$

As depicted in Figure. 4-11 and Figure. 4-12, $\gamma_{t\,eq}$ is almost linearly correlated with $\gamma_{t\,max}$ ($\gamma_{t\,peak}$). This correlation is not significantly affected by the dynamic properties of analytical models and the intensities of earthquakes. Eq (4-7) provides a reference value of the lower limit of $\gamma_{t\,eq}$ ($\gamma_{t\,eq(L)}$) for over 80% of the sample size; the estimated value of $\gamma_{t\,eq(L)}$ was lower than the analytical value of $\gamma_{t\,eq}$. Estimating $\gamma_{t\,eq}$ conservatively overestimates the cumulative damage of the dampers in most cases.

$$\gamma_{t\,eq(L)} = 0.54 \times (\gamma_{t\,max} - 0.2) + 0.2 \quad 0.25 \le \gamma_{t\,max} \le 1.1 \qquad \text{Eq (4-7)}$$

Additionally, $\gamma_{t\,eq}$ would not be greater than $\gamma_{t\,max}$ ($\gamma_{t\,peak}$) in any circumstance. Therefore, the upper limit of $\gamma_{t\,eq}$ ($\gamma_{t\,eq(U)}$) can be expressed using Eq (4-8) as

$$\gamma_{t\,eq(U)} = \gamma_{t\,max}, \text{ or } \gamma_{t\,eq(U)} = \gamma_{t\,peak} \qquad \text{Eq (4-8)}$$

To estimate the value of $\gamma_{t\,\mathrm{eq}}$ more precisely, Eq (4-9) was derived from Eq (4-7) and Eq (4-8) to ensure that the average ratio between the analytical and estimated values of $\gamma_{t\,\mathrm{eq}}$ is approximately 1.

$$\gamma_{t\,\mathrm{eq}} = \frac{3 \cdot \gamma_{t\,\mathrm{eq(L)}} + \gamma_{t\,\mathrm{eq(U)}}}{4} \qquad \text{Eq (4-9)}$$

By statistically analyzing the values of $\gamma_{t\,\mathrm{peak}}$ and $\gamma_{t\,\mathrm{max}}$, the average value of the ratio between ($\gamma_{t\,\mathrm{peak}}$−0.2) and ($\gamma_{t\,\mathrm{max}}$−0.2) was determined to approach 1.5. Therefore, $\gamma_{t\,\mathrm{eq}}$ can be estimated conservatively using $\gamma_{t\,\mathrm{peak}}$, as follows:

$$\gamma_{t\,\mathrm{eq(L)}} = 0.54 \times \frac{(\gamma_{t\,\mathrm{peak}} - 0.2)}{1.5} + 0.2 \quad 0.25 \le \gamma_{t\,\mathrm{peak}} \le 1.1 \qquad \text{Eq (4-11)}$$

Furthermore, $\gamma_{t\,\mathrm{eq}}$ can be precisely estimated using $\gamma_{t\,\mathrm{peak}}$ and Eq (4-9).

$$\gamma_{t\,\mathrm{eq}} = \frac{3 \cdot \gamma_{t\,\mathrm{eq(L)}} + \gamma_{t\,\mathrm{eq(U)}}}{4} \qquad \text{Eq (4-12)}$$

All analytical results ($\gamma_{t\,\mathrm{eq}}$) are plotted in Figure. 4-17(a) and Figure. 4-18(a) based on Eq (4-7) to Eq (4-12).

Figure. 4-17(b) and (c) depict the estimated results of cumulative damage, whereas Figure. 4-18(b) and (c) illustrate the results with the ratio between the analytical and estimated values of the cumulative damage (D_{ana}/D_{est}) as *X*-axis and frequency as *Y*-axis. As explained in Section 4.5.1, the lower limit of $\gamma_{t\,\mathrm{eq}}$ was set to 25% despite the estimated value of $\gamma_{t\,\mathrm{eq}}$ being lower than 25% in certain cases. As depicted in Figure. 4-17(b) and

Figure. 4-18(b), the cumulative damage can be precisely estimated using $\gamma_{t\,\max}$ and $\gamma_{t\,\text{peak}}$ (Eq (4-9) and Eq (4-12)). Over 80% of the estimated results were distributed within the interval $\mu \pm \sigma$. Conversely, Figure. 4-17(c) and Figure. 4-18(c) indicate that approximately 80% of the analytical results for the cumulative damage were overestimated using Eq (4-7) and Eq (4-11) ($D_{ana}/D_{est} > 1$), indicating that the equations satisfy the requirements completely. Although the cumulative damage of the U-damper was more precisely estimated by $\gamma_{t\,\max}$ and Eq (4-9), $\gamma_{t\,\text{peak}}$ is substantially easier to obtain from the displacement orbit recorded by the scratch plates or the displacement record of the superstructure. This indicates that the estimated value obtained using Eq (4-12) and $\gamma_{t\,\text{peak}}$ should be analyzed from an engineering point of view. Furthermore, the estimation approaches of $\gamma_{t\,\text{eq}}$ discussed in this and previous sections exhibit nearly the same level of estimation precision. The introduction of the strong-motion duration and dynamic properties of the structure failed to improve the precision of $\gamma_{t\,\text{eq}}$ estimation significantly. As the information required is less yet similar to the estimation precision, the $\gamma_{t\,\text{eq}}$ estimation approach based on $\gamma_{t\,\max}$ ($\gamma_{t\,\text{peak}}$) is considered more suitable for the quick inspection of U-dampers.

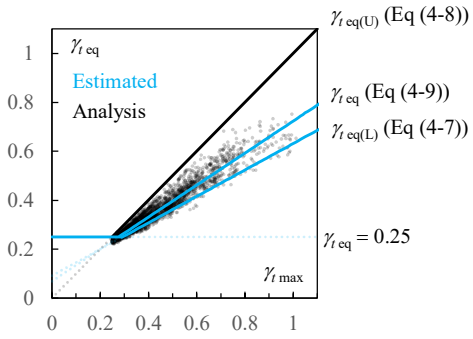

(a) Estimated and analytical values of $\gamma_{t\,eq}$

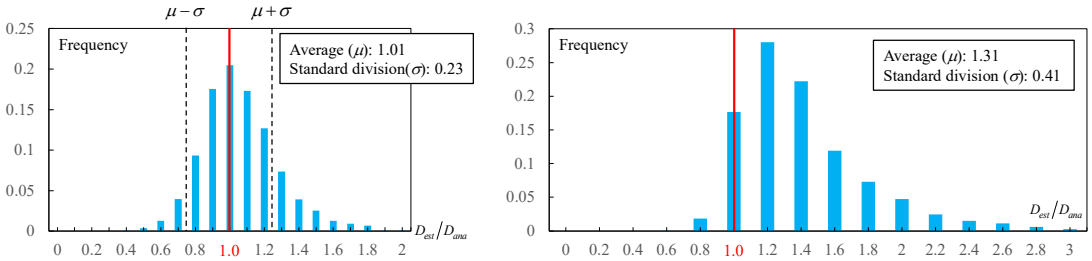

(b) Estimated value of D (Eq (4-9)) (c) Estimated value of D (Eq (4-7))

Figure. 4-17 Estimation of $\gamma_{t\,eq}$ and D using $\gamma_{t\,max}$

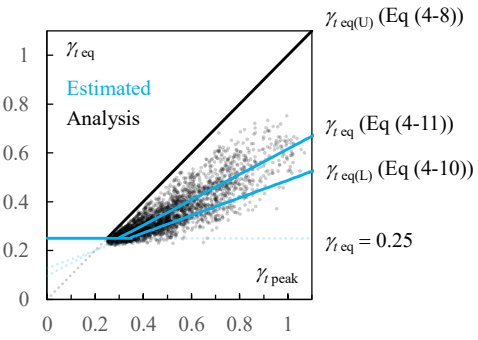

(a) Estimated and analytical values of $\gamma_{t\,eq}$

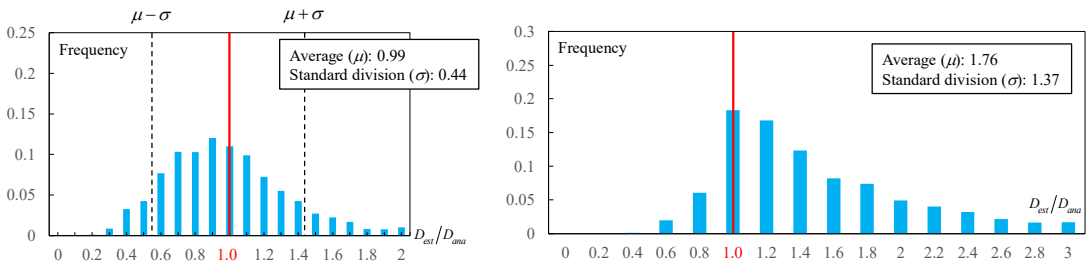

(b) Estimated value of D (Eq (4-12)) (c) Estimated value of D (Eq (4-11))

Figure. 4-18 Estimation of $\gamma_{t\,eq}$ and D using $\gamma_{t\,peak}$

4.6. Conclusion

U-shaped steel dampers are widely used in designing base-isolated structures in Japan. The observable shape changes caused by earthquake-induced excitations are closely associated with their cumulative damage. The major conclusions of Chapter 4 can be summarized as follows:

1). The process of investigating the effect of the dynamic properties of the structure and seismic excitations is significantly simplified by introducing the equivalent deformation amplitude $\gamma_{t\,\mathrm{eq}}$.

2). The time-history analysis confirms that the value of $\gamma_{t\,\mathrm{eq}}$ is positively correlated to the maximum deformation amplitude experienced by the dampers during an earthquake ($\gamma_{t\,\max}$ ($\gamma_{t\,\mathrm{peak}}$)), and the $\gamma_{t\,\mathrm{eq}} - \gamma_{t\,\max}$ ($\gamma_{t\,\mathrm{peak}}$) relation is not significantly affected by the dynamic properties of the structure and the intensities of earthquakes. Consequently, the cumulative damage of the dampers can be estimated conveniently by assuming that the damper is loaded under a constant deformation amplitude with $\gamma_{t\,\mathrm{eq}}$. The reduced calculation effort and adequate precision validate that the proposed method is highly effective for the quick inspection of U-shaped steel dampers.

4.7. Reference

[4-1] Ene D, Kishiki S, Yamada S, Jiao Y, Konishi Y, Terashima M, Kawamura N. Experimental study on the bidirectional inelastic deformation capacity of U-shaped steel dampers for seismic isolated buildings. Earthquake Engineering & Structural Dynamics 2016;45(2):173–192.

[4-2] Ene D, Yamada S, Jiao Y, Kishiki S, Konishi Y. Reliability of U-shaped steel dampers used in base-isolated structures subjected to biaxial excitation. Earthquake Engineering & Structural Dynamics 2017;46:621–639.

[4-3] 焦　瑜，山田　哲，エネ・ディアナ，小林良平，吉敷　祥一，小西克尚，寺嶋正雄，帆足勇磨，免震層の罫書き記録に基づく免震構造 U 型鋼材ダンパーの損傷評価法，日本建築学会技術報告集，第 21 巻，第 48 号，pp.649-654，2015.6

(Jiao Y et al. Damage evaluation method for U-shaped steel dampers based on the recorded orbits of based-isolated stories. AIJ Journal of Technology and Design 2015;21(48):649–654.)

[4-4] Kawamura N, Konishi Y, Terashima M, Jiao Y, Ene D, Kishiki S, Yamada S. Evaluation methods of residual fatigue life of U-shaped steel dampers after extreme earthquake excitation. Tenth U.S. National Conference on Earthquake Engineering Frontiers of Earthquake Engineering, July 21–25, 2014.

[4-5] 吉敷祥一，高山　大，山田　哲，エネ　デイアナ 小西克尚，川村典久，村嶋正雄，水平 2 方向載荷下における繰り返し変形性能に関する実験，免震

構造用 U 字形鋼材ダンパーの水平 2 方向特性，その 1，日本建築学会構造系論文集，第 77 巻，第 680 号, pp.1579-1588, 2012.12

(Kishiki S et al. Experimental evaluation of cyclic deformation capacity of U-shaped damagers subjected to bi-directional loadings. Bi-directional characteristics of U-shaped steel dampers for base-isolated structures Part 1. Journal of Structural and Construction Engineering (Transactions of AIJ) 2012;77(680):1579–1588.)

[4-6] Jiao Y, Kishiki S, Yamada S, Ene D, Konishi Y, Hoashi Y, Terashima M. Low cyclic fatigue and hysteretic behavior of U-shaped steel dampers for seismically isolated buildings under dynamic cyclic loadings. Earthquake Engineering & Structural Dynamics, 2015;44:1523–38.

[4-7] Disaster Prevention Research K-NEt, Kik-net. National Research Institute for Earth Science and Disaster Resilience, National Research Institute for Earth Science and Disaster Resilience (NIED) 2019.

[4-8] Pan P, Zamfirescu D, Nakashima M, Nakayasu N, Kashiwa H. Base-isolation design practice in Japan: Introduction to the post-Kobe approach. Journal of Earthquake Engineering 2005;9(1):147–171.

[4-9] Qu Z, Kishiki S, Nakazawa T. Influence of isolation gap size on collapse performance of seismically base-isolated buildings. Earthquake Spectra 2013;29(4):1477–1494.

[4-10] Amzallag C, Gerey J, Robert J, Bahuaudt J. Standardization of the rainflow counting method for fatigue analysis. 1994;16(4);287–293.

[4-11] Trifunac M. Response envelope spectrum and interpretation of strong earthquake ground motion. Bulletin of the Seismological Society of America 1971;61(2):343–356.

[4-12] Bommer J, Magenes G, Hancock J, Penazzo P. The influence of strong-motion duration on the seismic response of masonry structures. Bulletin of Earthquake Engineering 2004;2(1):1–26.

[4-13] Bommer J, Martinez-Pereira A. The effective duration of earthquake strong motion. Journal of Earthquake Engineering 1999;3(2):127–172.

[4-14] Arias A. A measure of earthquake intensity, In Seismic Design for Nuclear Power Plants, R. J. Hansen (ed.), Cambridge, MA, 1940, 438–483, The MIT Press.

[4-15] Somerville P, Smith N, Graves R, Abrahamson N. Modification of empirical strong ground motion attenuation relations to include the amplitude and duration effects of rupture directivity. Seismological Research Letters 1997;68(1):199–222.

[4-16] Bradley B. Correlation of significant duration with amplitude and cumulative intensity measures and its use in ground motion selection. Journal of Earthquake Engineering 2011;15(6):809–832.

[4-17] Kempton J, Stewart J. Prediction equations for significant duration of earthquake ground motions considering site and near-source effects. Earthquake spectra 2006;22(4):985–1013.

[4-18] Bahrampouri M, Rodriguez-Marek A, Green A. Ground motion prediction equations for significant duration using the KiK-net database. Earthquake spectra 2021;37(4):903–920.

Chapter 5

Conclusion

5.1. Conclusions

5.2. Future work

5. Conclusions

5.1. Conclusions

The deformation behavior of U-shaped steel dampers under in-plane excitation is systematically investigated in the present study. Cumulative damage of U-shaped dampers is proven to be tightly correlated to the residual plastic deformation caused by cyclic loading with constant deformation amplitude. As a tool to describe the cumulative damage of the dampers in the process of dynamic cyclic loading, low cycle fatigue behavior, and cumulative damage evaluation method of U-shaped steel dampers that is composed by Kishiki et al. (2008) and Ene et al. (2016) is applied in this research. The residual plastic deformation tends to grow with the increment of cumulative damage. The deformation residual plastic grows more obviously when the dampers are loaded under relatively larger constant deformation amplitudes (**Chapter 2**).

It is indicated in the dynamic cyclic loading tests under complicated loading histories (test Serious II) that, the residual plastic deformation-cumulative damage relationship of U-shaped steel dampers is severely affected by the dynamically changing deformation amplitudes. Whereas, the deformation behavior of the dampers can be simply predicted by rearranging the loading cycles in ascending order of deformation amplitudes. Based on this, the precision verification of the exciting cumulative damage evaluation method composed by Ene et al. (2016) can be achieved easily and effectively (**Chapter 3**).

The process of investigating the effect of the dynamic properties of the structure and seismic excitations is significantly simplified by introducing equivalent deformation amplitude. It is confirmed that the value of the equivalent deformation amplitude is tightly

correlated to the maximum displacement experienced by the seismic isolated layer and is not significantly affected by the magnitude of earthquakes and the dynamic properties of the structure (**Chapter 4**).

The main conclusion of the present study are:

1). Residual plastic deformation of U-shaped steel damper caused by cyclic loading tends to accumulate in the middle part of the parallel arms. Applying the shape change of the deformed parallel arms, residual plastic deformation ratio ξ is used as an indicator for describing the deformation behavior of U-shaped steel dampers.

2). No obvious residual plastic deformation was observed when γ_t equals 25%. The residual plastic deformation ratio is proven to be an ineffective index of cumulative damage evaluation when γ_t was smaller than 25%. $\gamma_{t\,max}$ = 25% is defined as the lower limit of cumulative damage evaluation of U-shaped steel dampers based on shape change.

3). It is indicated in cyclic loading under complicated loading history and FEM modeling that, the residual plastic deformation ratio is no longer an effective indicator for evaluating the deformation behavior of U-shaped steel dampers when deformation amplitude in positive or negative sides exceeds 55%. $\gamma_{t\,max}$ = 110% seems to be the upper limit of quick inspection of U-shaped steel dampers based on residual plastic deformation.

4). The effect of the U-shaped steel dampers' size is negligible in the dampers' residual plastic deformation-cumulative damage evaluation. Meanwhile, independent of whether the amplitude deformation has positive or negative symmetry, the ξ-D relationships of U-shaped steel dampers loaded with constant deformation amplitude, which are the same in γ_t (in the range from 25% to 110%), are congruent.

5). A residual plastic deformation-cumulative damage of U-shaped steel dampers is composed based on the experimental results of dynamic loading tests Series I to Series III. The deformation behavior of U-shaped steel dampers under random waves such as earthquake-induced excitations can be predicted precisely by rearranging the loading cycles in ascending order of deformation amplitudes.

6). Excessive reliance on numerical analysis makes it difficult to certify the estimated value of cumulative damage obtained from the existing cumulative damage method composed by Ene et al. (2016). The aforementioned finding provides the solution to the problem. Precision verification can be conducted effectively by comparing the estimated and measured values of the deformed parallel arms' residual plastic deformation corresponding to a certain ground motion record.

7). Equivalent deformation amplitude ($\gamma_{t\,\mathrm{eq}}$) is introduced in the quick inspection of U-shaped steel dampers. Estimating the cumulative damage of the dampers can be conducted easily through the residual plastic deformation-cumulative damage curve under constant deformation amplitude corresponding to $\gamma_{t\,\mathrm{eq}}$. it is indicated in the time-history analysis that, the value of $\gamma_{t\,\mathrm{eq}}$ seems not significantly influenced by the magnitude of the earthquake events and the dynamic properties of the structures and can be estimated through readily available information, such as the maximum deformation amplitude experience by the base-isolated layer and the structures' equivalent vibration period. This quick inspection method allows nonprofessionals such as users of the building to estimate the earthquake-induced damage and judge whether the building can be used continuously. This would undoubtedly contribute significantly to speeding up the urban function recovery after severe disasters.

5.2. Future works

The cumulative damage evaluation method composed in the present study provides valuable insight into the quick inspection of U-shaped steel dampers or even of other metallic energy dissipation devices. However, it is previously discussed that ignoring the effect of U-shaped steel dampers' torsional deformation and out-of-plane deformation results in unsafe evaluated results of cumulative damage. Indicating the effect of these factors on the quick inspection method proposed in the present study has been the focus of future work.

Appendix

APPENDIX

APPENDIX A. Effect of material properties on the deformation behavior of U-shape steel damper

Although the single U-shaped elements investigated in the present study are all fabricated from a type of high-quality rolled steel SN490B and the manufacturing process is mature and reliable, the effect of material on the deformation behavior of U-dampers is briefly discussed in APPENDIX A through the analytical results of FEM modeling. The outline of the FE model remains the same as that discussed in Section 2.2.

Single U-shaped elements that differ in material properties (stress-strain (σ-ε) relation) are tested. Two parameters (Figure. A-1) are considered: (1) yield strength σ_y (380 Mpa and 235Mpa for SN490B and SN400B); (2) tangent modulus E_t (0.01E and 0.03E, Young's Modulus E = 205Gpa).

Same as Section 2.2, the sum of ϕ_{max} and ϕ_{min} is used to estimate the residual plastic deformation caused by a single loading cycle. The residual plastic deformation initiates at the sections on the parallel arm is indicated in Figure. A-2.

Models with different stress-strain relations show a similar distribution of residual plastic deformation. Bending which occurs at sections from P_2 to P_5 makes the parallel arm of the damper protrudes outwardly. For the three models, section P_4 normally has the most obvious residual plastic deformation. Estimating the shape change of the dampers by the residual plastic deformation that initiates at the middle part (the area around section P_4) of the parallel arm is still the best selection for ξ-D relationship evaluation. Whereas, it is obvious that the value of residual plastic deformation for a single loading cycle is

different. The evaluation method of residual plastic deformation-cumulative damage (ξ-D) relationship under constant deformation amplitude should be adjusted to fit the variation of dampers' material. However, the ξ-D relationship evaluation equations for constant deformation amplitude can only be composed based on the experimental results of a series of dynamic loading tests of single U-shaped elements. Unfortunately, we are in no condition to experiment with U-shaped steel dampers that are fabricated from other metallic materials.

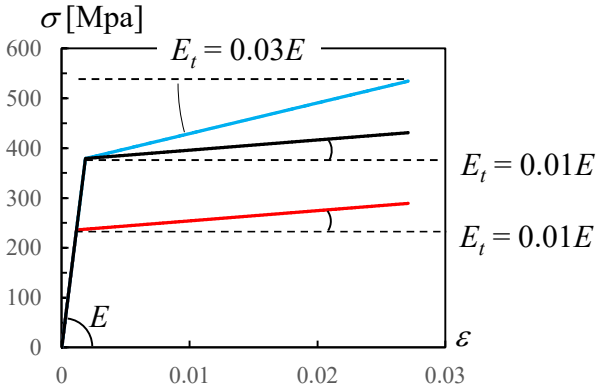

Figure. A-1 Stress-strain relation of FEM modeling

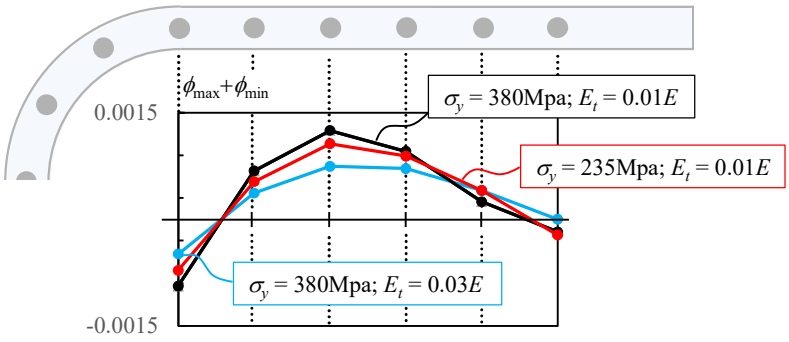

Figure. A-2 Residual plastic deformation initiates on the parallel arm of U-dampers (γ_t = 90%).

APPENDIX B. Fitness of the previously discussed cumulative damage evaluation method of U-shaped steel in the present study

The exciting cumulative damage evaluation method composed by Ene et al. (2016) is discussed in detail in Chapter 2. Miner's rule was applied to describe the fatigue behavior of U-damper loaded under complicated loading history such as earthquake-induced vibrations (Eq (A-1), same as Eq (2-7)).

$$D = \sum_{i=1}^{n} \frac{n_i}{N_{f,i}} \qquad \text{Eq (A-1)}$$

Where n_i is the frequency of the cycles having deformation amplitude $\gamma_{t,i}$, n is the total number of cycles, and $N_{f,i}$ is the corresponding number of cycles to the fracture. The value of $N_{f,i}$ is evaluated using a fatigue curve (Eq (A-2), same as Eq (2-6)) defined according to Manson-Coffin model (Kishiki et al. 2008 [A-1]).

$$\gamma_{t,i} = 35 \cdot N_{f,i}^{-0.15} + 3620 \cdot N_{f,i}^{-0.80} \qquad \text{(a)} \qquad \text{Eq (A-2)}$$

Or (Kishiki et al. 2012; same as Eq (4-1))

$$\gamma_t = 2370 \cdot N_f^{-0.66} \qquad \text{(b)}$$

Manson-Coffin and Miner's rules [A-2] [A-3] are prediction approaches for metallic materials' fractures caused by fatigue, which are widely applied in the cumulative damage

evaluation of steel components in fields such as civil engineering and architecture. The components are proposed to be fractured when the estimated value of cumulative damage D reaches 1.0. An indispensable condition for minimizing losses caused by structures' failure is establishing a prediction approach to the fracture of the structures' main components caused by fatigue. In order to exercise the function of "predicting the happening of fracture", engineers normally attempt to adjust the estimation equations and make the estimated value of D slightly exceed 1.0 when the fractures happen.

Experimental results of U-dampers' in-plane low cycle fatigue tests conducted in the present and previous studies (Kishiki et al. 2008 [A-1]) are indicated in Figure A-3 (a) and (c) in comparison with Eq (A-2) (a) and (b). Figure A-3 (b) and (d) illustrate the precision of both Eq (A-2) (a) and (b). Where the *X*-axis indicates the ratio of the estimated value and experimental results of the number of loading cycles to fracture ($N_{f\,(est)}$ and $N_{f\,(exp)}$). The experimental results are precisely but slightly underestimated by both equations which means the fracture of the damper has been conservatively predicted.

As defined in Eq (2-7), the estimated value of cumulative damage D is the sum of the damage caused by each loading cycle. Where, the damage caused by a loading cycle with a certain deformation amplitude $\gamma_{t,i}$ is the reciprocal of the estimated value of the number of cycles until fracture $N_{f,i}$ ($1/N_{f,i}$). Both Eq (A-2)(a) and (b) were proposed to underestimate the number of cycles until fracture in most cases because of the aforementioned reason. Therefore, the estimated value of cumulative damage D obtained from Eq (A-2)(a) and (b) normally exceeds 1.0 (Table 3-1).

Furthermore, the present study focuses on the relation between U-damper's cumulative damage and residual deformation. We are dedicated to establishing a cumulative damage evaluation method based on the damper's residual plastic deformation. Establishing an

effective approach for describing the deformation behavior of U-damper is the priority. The previously discussed cumulative damage evaluation method for U-damper is proven to be mature and reliable by both the experimental results of the previous and present studies, so it is adopted in the present study as a tool to describe the fatigue behavior of single U-shaped elements in the dynamic cyclic loading tests.

Certainly, improving the goodness of fit of Eq (A-2) is helpful to evaluate the cumulative damage of U-damper more precisely. Whereas, the purpose of predicting the failure of the dampers cannot be satisfied with an evaluated value of D less than 1 (it cannot be called a "prediction" for the fracture of the damper if an evaluated value of D less than 1 is obtained when the fracture happens). Additionally, it is worth mentioning that the optimization of the fatigue curve Eq (A-2) needs large samples. Only 6 specimens (γ_t = 25, 55, Offset 55, 70, 90, 110%) were tested in loading test series I (constant deformation amplitude) in the present study. Optimization of Eq (A-2) cannot be achieved with such a small sample size. Overall, U-dampers cumulative damage evaluation equations proposed by Jiao et al. (2015) and Ene et al. (2016) apply to the present study.

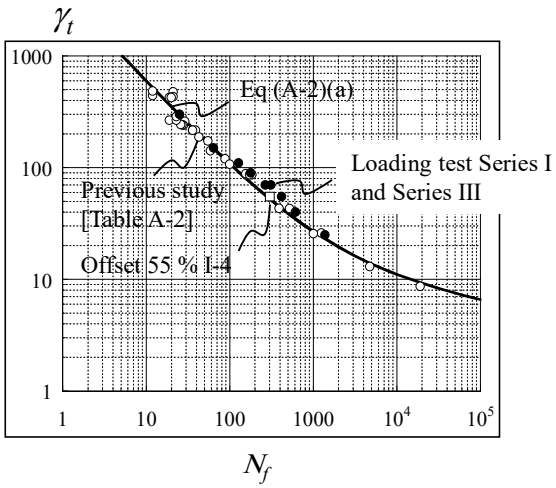

(a) Fatigue behavior evaluation

(Eq (A-2) (a))

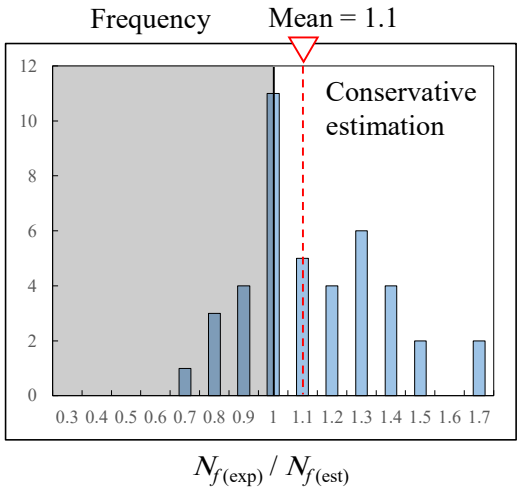

(b) Precision analysis

(Eq (A-2) (a))

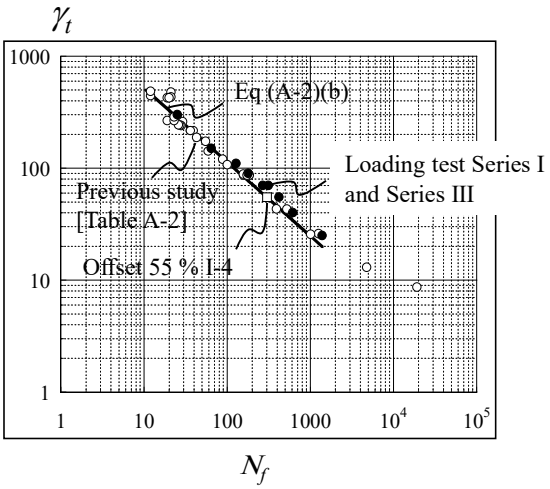

(c) Fatigue behavior evaluation

(Eq (A-2) (b))

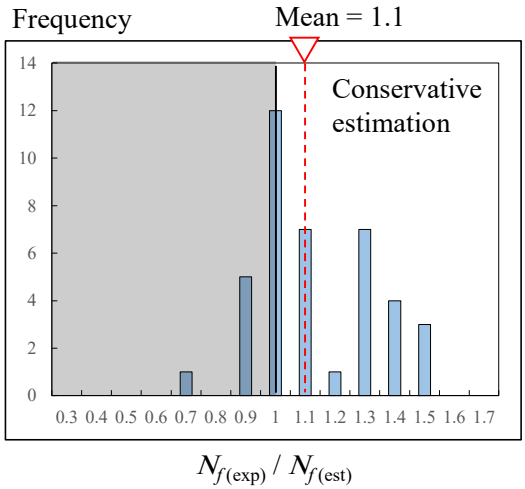

(d) Precision analysis

(Eq (A-2) (b))

Figure. A-3 Fatigue behavior evaluation equations

APPENDIX C. Effect of U-shaped steel damper's torsion and out-of-plane deformation on its inelastic deformation capacity

APPENDIX C is a brief introduction to the effects of U-damper's torsion and out-of-plane deformation on its inelastic deformation capacity.

1. Effect of U-dampers' torsion deformation

In Ene et al. (2016) [A-4], the cumulative damage of U-dampers loaded under unidirectional and bidirectional loading is defined by Eq (A-2) (a) and (b), respectively. Meanwhile, Ene et al. (2016) introduced an empirical index—sway-motion index J_f (defined in Eq (A-3))—to quantify the complexity of the displacement orbit experienced by the base-isolated layer, and index J_f is employed further to estimate the effect of the torsion deformation on the reduction of cyclic deformation capacity of U-dampers.

$$J_f = \sum_{i=1}^{n-1}\left(\gamma_i \cdot \gamma_{i+1}\frac{\gamma_i + \gamma_{i+1}}{2}\cdot\left|\Delta\varphi_i\right|\right) \qquad \text{Eq (A-3)}$$

where γ_i is the ratio of deformation amplitude (R_i in Eq (A-3)) to the original height of the damper.; $\Delta\varphi_i$ is the incremental in-plane rotation angle [rad] between two consecutive loading steps (Figure 1); and n is the total number of loading steps.

Figure. A-5 and Eq (A-5) indicate the way that J_f affects the ultimate inelastic deformation capacity (D^2_u) of U-damper loaded under bidirectional loading. In her own word, Diana ENE described that: "*On the one hand, for values of J_f smaller than 15 [rad], the loading history is approaching one-directional loading; therefore, the D_2 index will*

be limited to 1.0. On the other hand, for values of J_f larger than 30 [rad], D_2 is almost constant, resulting in the existence of an upper limit to the reduction of the cyclic deformation capacity." The dampers are proposed to be fractured when the estimated value of cumulative damage D_1 reaches 1.0 (Fracture limit for 1D, the left side of Figure. A-5) when loaded under unidirectional loading. While the ultimate inelastic deformation capacity of a U-damper loaded under bidirectional loading would decrease to about 0.4 (Fracture limit for 2D, the right side of Figure. A-5) when the value of J_f exceeds 30 [rad].

$$\begin{aligned} D_2^u &= 1.0 && J_f \le 15 \\ D_2^u &= 1.6 - 0.004 J_f && 15 < J_f \le 30 \\ D_2^u &= 0.4 && 30 < J_f \end{aligned} \qquad \text{Eq (A-4)}$$

However, the cumulative damage of U-dampers suffered from ground motion records (Figure. A-6) reveals that the damage produced by the original records is significantly small compared to the bidirectional interaction curve [A-5]. Sway motion induced by ground motion records seems much smaller than J_f =15 (inelastic deformation capacity of U-damper starts to decrease when J_f exceeds this value). It is highly likely that the effect of dampers' torsion deformation can be ignored when the dampers suffer from the original ground motion records.

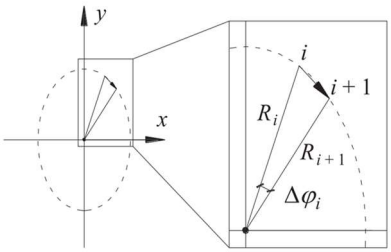

Figure. A-4 Computation of the shear deformation angle γ_i (elliptical loading history)

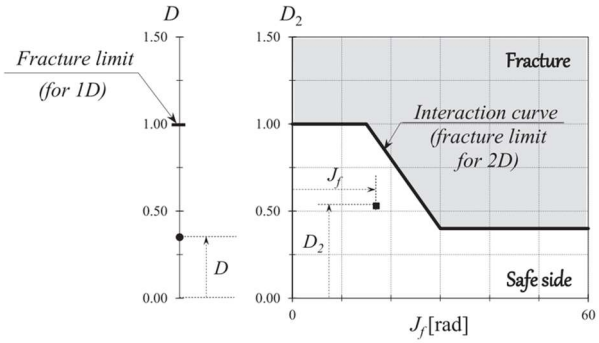

Figure. A-5 Fracture limits for one-directional (left) and bidirectional approaches (right). (Ene et al. 2016)

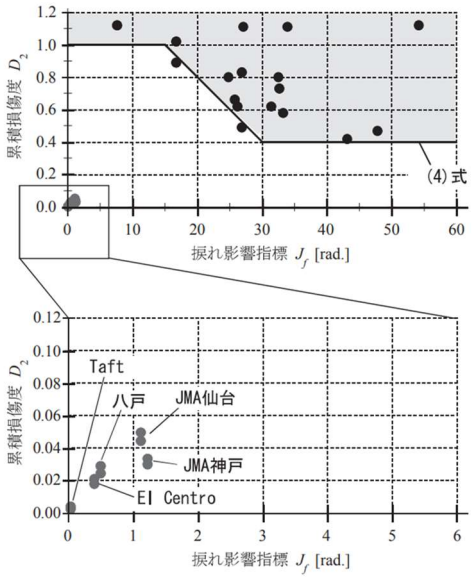

Figure. A-6 Cumulative damage of U-dampers caused by unscaled ground motion records (Kishiki et al. 2014)

2. Effect of out-of-plane deformation

The cumulative damage induced by a single loading cycle is compared in Figure. A-7. The *X*-axis is deformation amplitude γ_t. The *Y*-axis expresses the ratio of the cumulative damage induced by a loading cycle of a circular loading pattern (D_2) to that induced by a single in-plane loading cycle (D_1). The scope of application of deformation amplitude in ξ–D relation evaluation of the U-damper is γ_t = 25% to 110%. The effect of out-of-plane loading increases with the increment of deformation amplitude. D_2 reaches 1.35 times D_1 when γ_t equals 110%. That is also the reason why we proposed an underestimation approach of the equivalent deformation amplitude $\gamma_{t\ eq}$ to conservatively evaluate the cumulative damage in Chapter. 4 (Figure. 4-18). The mean value of D_{est}/D_{ana} reaches 1.7 using the underestimation equation of $\gamma_{t\ eq}$, which means the quick inspection method proposed in the present study is still reliable even if the damper is loaded under bidirectional loading.

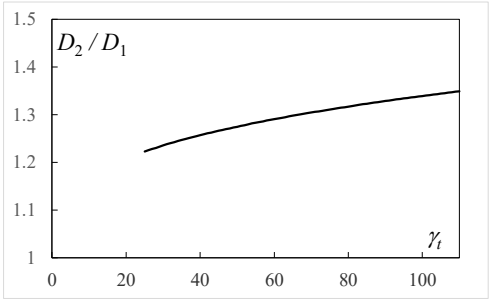

Figure. A-7 Effect of out-of-plane deformation on U-dampers' cumulative damage evaluation

APPENDIX D. The dimension of the loading equipment

The dimension of the loading equipment is marked in the following figure.

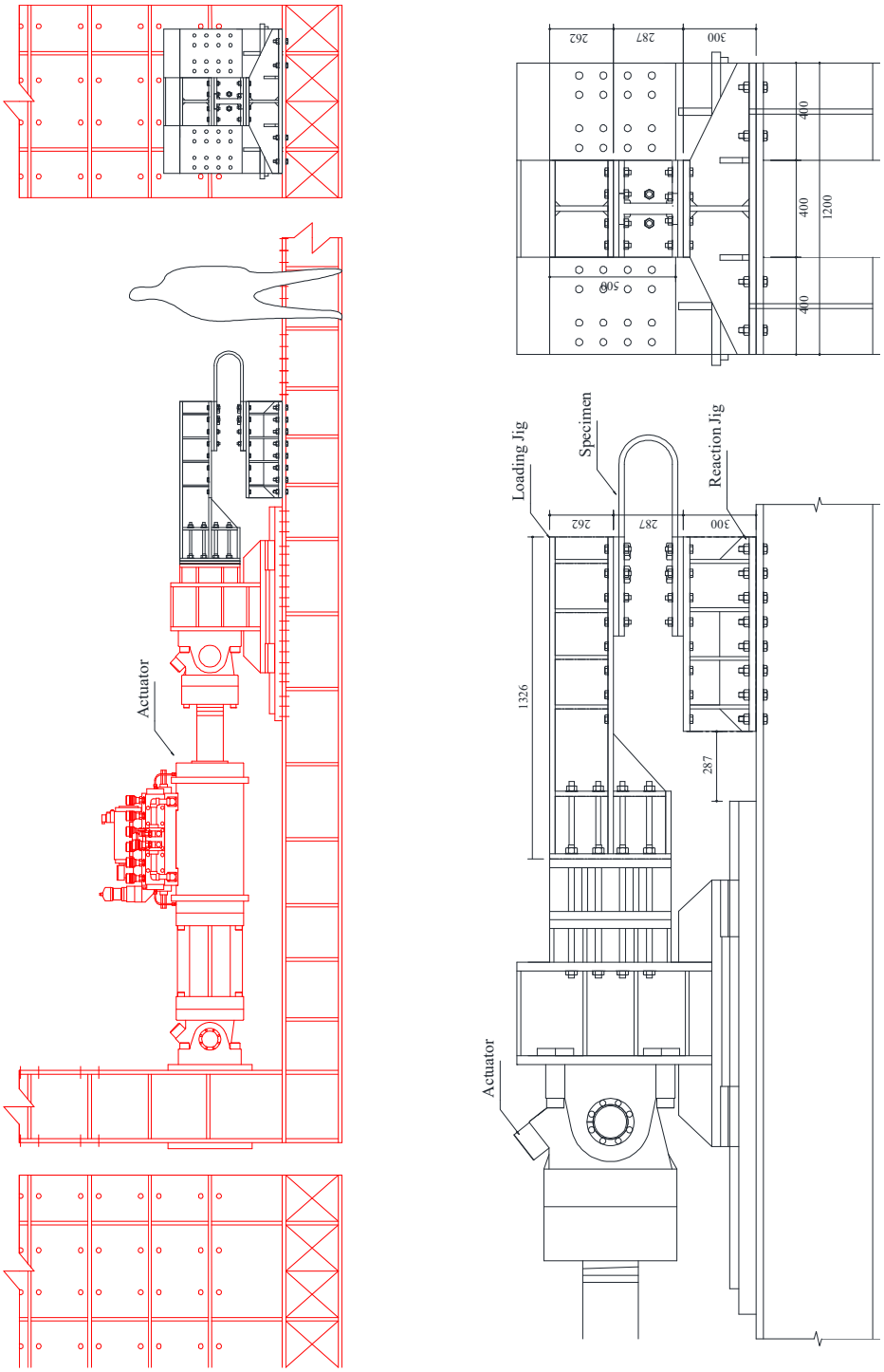

Figure. A-8 Loading equipment (unit: mm) damage evaluation

APPENDIX E. The most severely deformed part of parallel arms

Figure. 2-7 shows the measurement points attached to the single U-shaped element. The shape change of the specimen was traced through the displacement of these measurement points in dynamic loading tests. Test results are used to describe how the dampers' shape change developed along with deformation δ (Figure. A-9).

Figure. A-10 and Figure. A-11 indicate the experimental results of the damper loaded under complicated loading history II-7, and the loading history is demonstrated as a background image. Only the damper's deformation behavior under the first set of loading history II-7 is illustrated in both Figure. A-10 and Figure. A-11 because a similar phenomenon is observed in the whole process of the loading test. Residual plastic deformation ratio ξ is defined as the ratio of residual plastic deformation between P_4 and P_{14} ($\delta = 0$) to the original height of the damper. Shape change ratio $\xi_{t\,(y)}$—the ratio of the distance in the Y-axis direction between P_4 and P_{14} to the original height of the damper—is used to describe the shape change of the specimen when deformation δ does not equal 0. ξ (red) and $\xi_{t\,(y)}$ (black) are compared and indicated in Figure. A-10 with time t as the X-axis. Seems that ξ is the peak value of $\xi_{t\,(y)}$ in each loading cycle, which means the most obvious shape change normally initiates on the parallel arms when deformation δ returns to 0.

The residual plastic deformation ratio of other pairs of measurement points such as P_1 and P_{17} ($\xi_{(1-17)}$, black), are indicated in Figure. A-11 in comparison with ξ (red). It is worth noting that, the area around the middle part of the damper's parallel arms (P_4 and P_{14}) normally has the maximum residual plastic deformation. Residual plastic deformation ratio ξ seems to be applicable for describing the deformation behavior of U-shape

dampers loaded under complicated loading history.

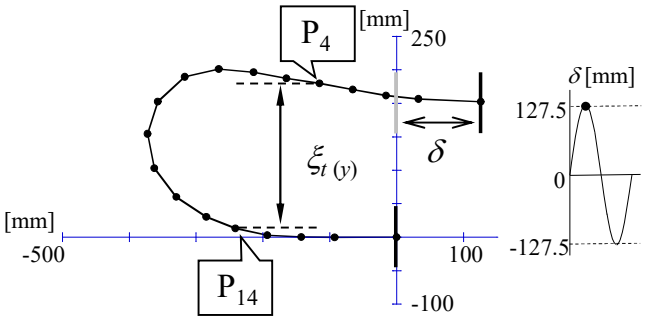

(a) δ = -127.5mm

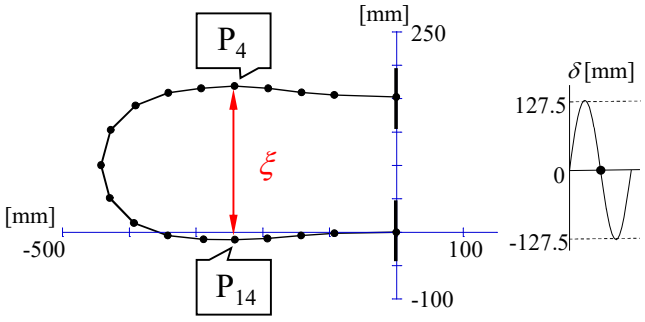

(b) δ = 0mm

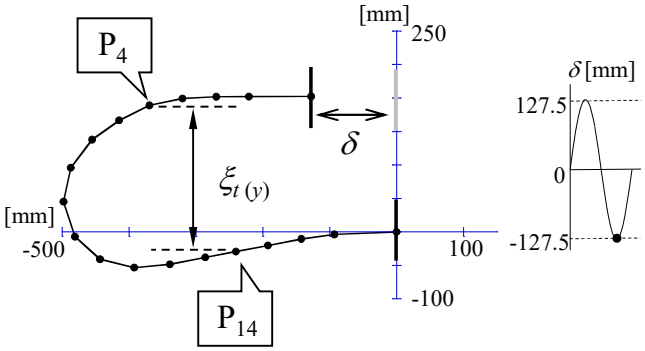

(c) δ = +127.5mm

Figure. A-9 Shape change of U-damper (Loading cycle No. 14, II-7)

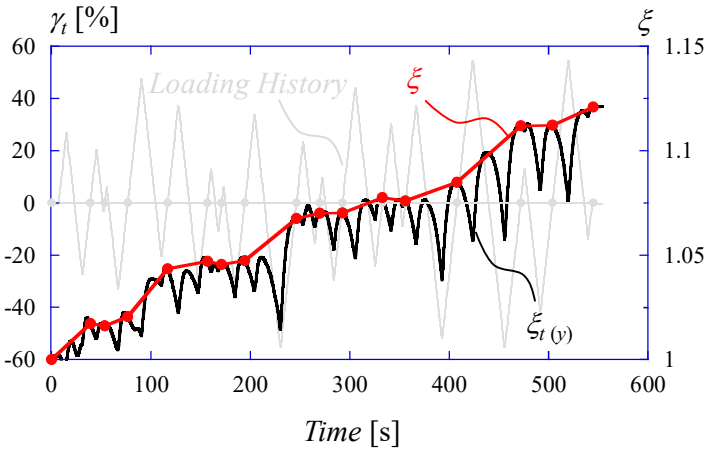

Figure. A-10 Comparison between residual plastic deformation ratio (ξ) and shape change of U-damper during cyclic loading ($\xi_{t\,(y)}$)

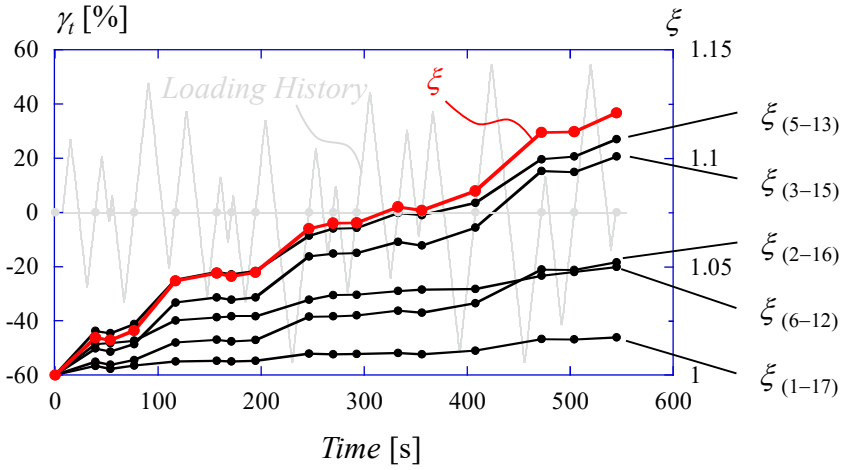

Figure. A-11 Residual plastic deformation of other sections

APPENDIX F. Effect of different low cycle fatigue behavior evaluation equation

Both fatigue curves Eq (A-2)(a) composed by Kishiki et al. (2008) and the simplified one Eq (A-2)(b) are applied in the cumulative damage evaluation of U-shaped steel dampers in the present study. Eq (A-2)(a) is capable of precisely reflecting the fatigue of the dampers under both elastic and plastic deformation amplitude. Thus, this equation was applied in the experimental design of dynamic loading tests Series I and Series II. The loading cycles to fracture corresponding to the variable deformation amplitudes of earthquake-induced excitations can be counted easily through the inverse function of Eq (A-2)(b) (Chapter 4). This determines that Eq (A-2)(b) is adopted in cumulative damage evaluation of U-shaped steel dampers in time-history analysis. The residual plastic deformation-cumulative damage relationship evaluation equations under both constant deformation amplitude and complicated loading history (Eq (2-9), Eq (3-1), and Figure. 3-6) are established based on the estimated value using Eq (A-2)(b) (Chapter 2 and Chapter 3). APPENDIX F indicates the effect of the fatigue curves on the residual plastic deformation-cumulative damage relationship evaluation of U-shaped steel dampers.

As mentioned in APPENDIX B, both Eq (A-2)(a) and (b) were proposed to underestimate the number of cycles until fracture in most cases to exercise the function of "predicting the happening of dampers' fracture". The experimental results of cyclic loading test under constant deformation amplitude (Series I, Table A-1) indicate that fatigue curve Eq (A-2)(b) satisfies the requirements completely. The loading cycles to fracture of single U-shaped elements loaded under constant deformation amplitude are all slightly underestimated by Eq (A-2)(b).

Applying the estimated value of Eq (A-2)(b) to evaluate the residual plastic

deformation-cumulative damage relationship evaluation under constant deformation amplitude (test Series I; Figure. A-12), the error can still be controlled within the range from 0.96 to 1.04, which remains the same as the results using Eq (A-2)(a). Furthermore, for the residual plastic deformation-cumulative damage relationship evaluation under complicated loading histories (test Series II; Figure. A-13, and Figure. A-14), evaluating precision seems not significantly affected by replacing Eq (A-2)(a) with Eq (A-2)(b) as well.

In summary, the residual plastic deformation-cumulative damage relationship of U-shaped steel dampers can be evaluated precisely based on both Eq (A-2)(a) and (b).

Table A-1 Experimental results of cumulative damage under constant deformation amplitude (test Series I)

Damper size	Series	No.	Loading History	D
UD40	II	II-1	Incremental deformation amplitude	1.3
		II-2	Decremental deformation amplitude	1.32
		II-3	Decremental deformation amplitude	1.45
		II-4	Incremental deformation amplitude (Offset)	1.26
		II-5	Incremental + decremental deformation amplitude (Offset)	1.29
		II-6	Approximately random	1.5
		II-7	Approximately random	1.25

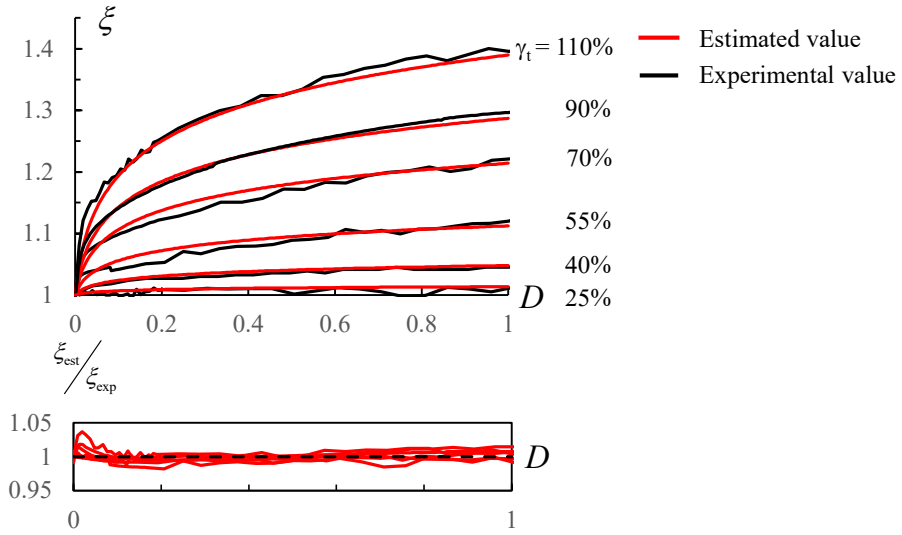

Figure. A-12 ξ-D relationship evaluation using Eq (A-2)(b) and precision analysis

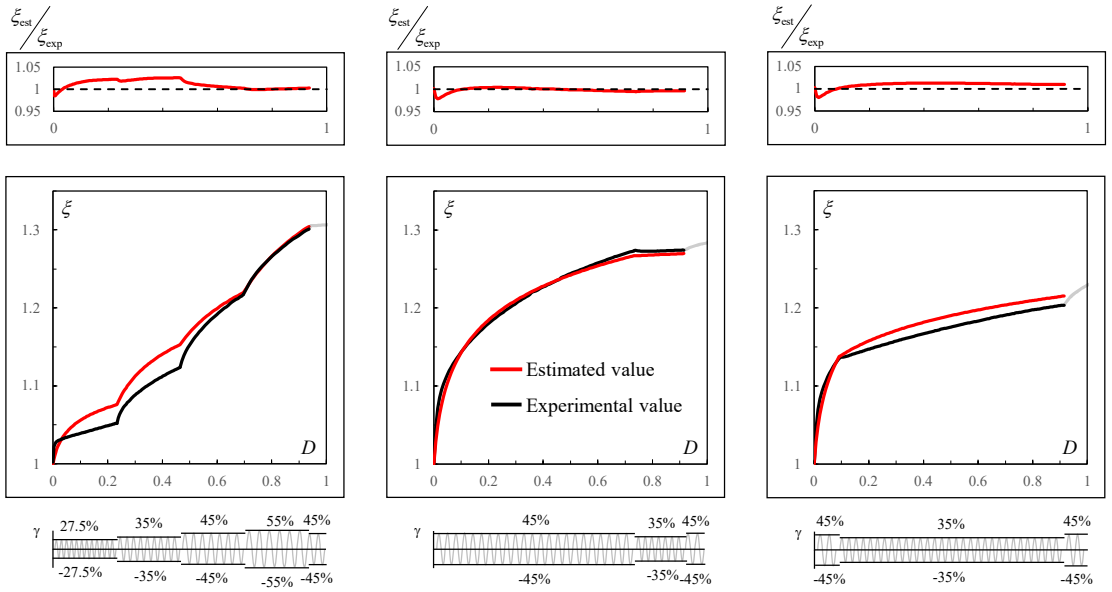

(a) II-1 (b) II-2 (c) II-3

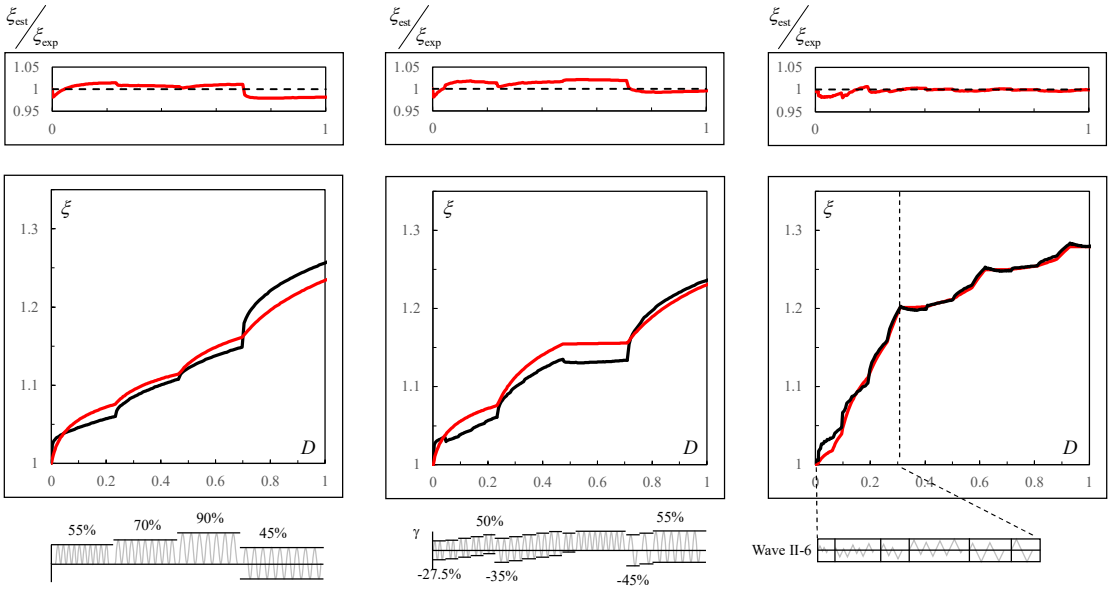

(d) II-4 (e) II-5 (f) II-6

Figure. A-13 *ξ-D* relationship evaluation under complicated loading history (Series II) using Eq (A-2)(b)

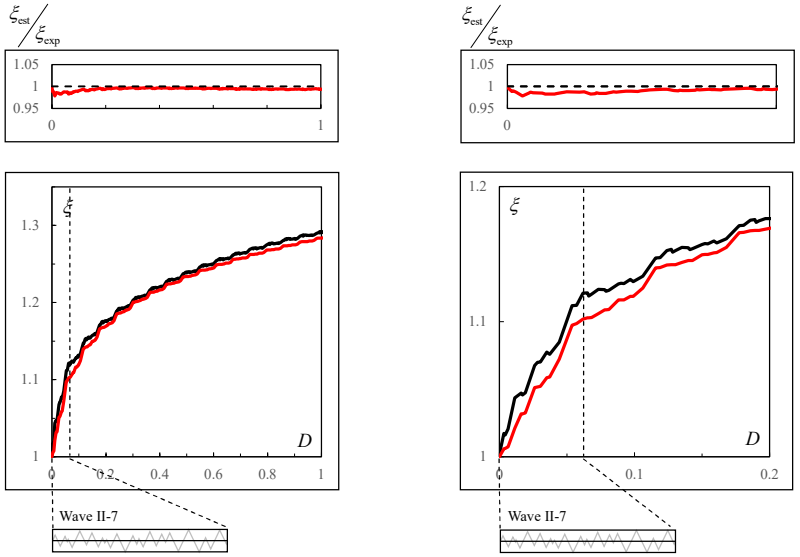

(a) D = 0 ~ 1.0 (b) D = 0 ~ 0.2

Figure. A-14 *ξ-D* relationship evaluation of specimen I-7 using Eq (A-2)(b)

APPENDIX G. Significant duration

Bommer and Martinez-Pereira (1999) [A-6] has summarized more than 30 definitions of ground-motion durations in the literature. Among these definitions, significant duration (termed as SD) is one of the most widely used metrics. SD is defined based on the Arias intensity (Arias, 1970, Eq (A-5)) [A-7].

$$I_A = \frac{\pi}{2g}\int_0^{t_{\max}} a(t)^2\, dt \qquad \text{Eq (A-5)}$$

Where I_A is the Arias intensity; $t_{\max}$ is the total duration of ground motion records; g is acceleration of gravity. Significant durations defined as the time interval over which specified proportions of normalized I_A are accumulated. The time intervals between 5%–75% and 5%–95% of I_A (denoted as SD5–75 and SD5–95, respectively) are commonly used definitions of significant duration. Other time intervals such as 20%–80% of I_A have also been used for some applications. Figure. A-15 shows an example of the computed significant durations using a ground-motion record. It is obvious that SD5–95 is always greater than SD5–75 for a given time history. The cumulative damage caused by a single loading cycle with $\gamma_t < 20\%$ cannot be evaluated using Eq (4-1). Thus, loading cycles with $\gamma_t < 20\%$ were excluded from the evaluation of the cumulative damage to the dampers. Meanwhile, residual plastic deformation caused by loading cycles with $\gamma_t < 25\%$ is not significantly affect the final estimated value of residual plastic deformation ratio ξ. Therefore, in the present study, strong vibration is defined as vibration with γ_t greater than 20%. This causes the duration of the strong vibratory motion to be grossly overestimated by $SD_{5\text{-}95}$. $SD_{5\text{-}75}$ has become a more desirable choice for significant duration estimation.

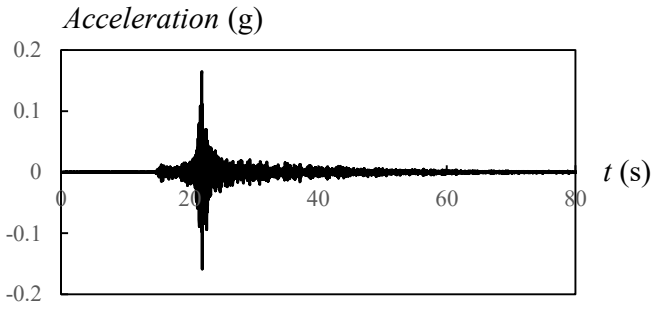

(a) Ground motion record (No. 1 Table A-2)

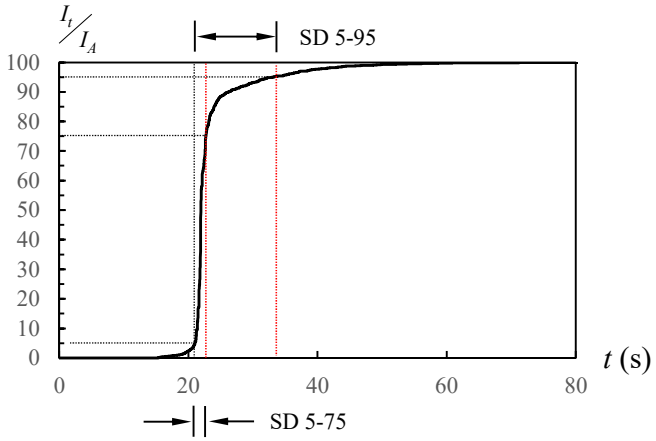

(b) Definition of SD5-75 and SD5-95

Figure. A-15 Significant duration

APPENDIX H. Ground motion records applied in the analytical study.

Ground motion records applied in time-history analysis in Chapter 4 are listed in Table A-2

Table A-2 Experimental results of cumulative damage under constant deformation amplitude (test Series I)

NO.	Record Date (Month/Day/Year)	Record Time	Station Code	Magnitude	Epicenter Distance (km)	EW Component PGA (gal)	NS Component PGA (gal)
1	2011/3/11	14:47:04	FKSH10	9.0	266	768.098	1062.405
2	2011/3/11	14:47:08	TCGH16	9.0	301	1196.698	798.625
3	2011/3/11	14:47:10	IBRH11	9.0	309	826.980	814.855
4	2011/3/11	14:46:48	MYGH10	9.0	174	852.677	870.792
5	2011/3/11	14:47:08	IBRH15	9.0	284	780.754	605.773
6	2011/3/11	14:46:53	FKSH19	9.0	201	856.590	605.806
7	2011/3/11	14:47:05	TCGH13	9.0	282	839.503	554.681
8	2011/3/11	14:46:43	IWTH27	9.0	155	630.297	738.151
9	2011/3/11	14:46:46	IWTH05	9.0	156	654.706	576.866
10	2011/3/11	14:47:04	IBRH12	9.0	265	526.014	604.410
11	2011/3/11	14:46:57	IWTH02	9.0	230	535.771	586.835
12	2011/3/11	14:47:06	TCGH10	9.0	286	600.299	541.251
13	2011/3/11	14:47:04	IBRH16	9.0	272	585.054	503.960
14	2011/3/11	14:46:49	FKSH20	9.0	178	660.456	394.283
15	2011/3/11	14:47:08	IBRH18	9.0	277	591.943	442.018
16	2011/3/11	14:46:55	FKSH18	9.0	216	506.944	577.648
17	2011/3/11	14:46:43	MYGH04	9.0	154	449.898	552.540
18	2011/3/11	14:46:49	IWTH26	9.0	188	512.967	521.076
19	2011/3/11	14:46:56	AKTH04	9.0	222	523.309	356.975
20	2011/3/11	14:47:01	IBRH13	9.0	249	438.193	556.236
21	2011/3/11	14:46:41	MYGH12	9.0	137	459.842	526.517

22	2011/3/11	14:46:58	FKSH09	9.0	230	433.227	424.375
23	2011/3/11	14:46:46	IWTH04	9.0	175	384.203	333.365
24	2011/3/11	14:47:19	IBRH17	9.0	318	338.304	472.234
25	2011/3/11	14:46:44	IWTH23	9.0	158	486.379	354.419
26	2011/3/11	14:46:41	MYGH03	9.0	140	423.576	453.572
27	2011/3/11	14:47:08	TCGH12	9.0	299	345.377	466.173
28	2011/3/11	14:46:57	FKSH12	9.0	225	417.813	355.365
29	2011/3/11	14:46:59	FKSH11	9.0	244	394.439	492.285
30	2011/3/11	14:46:48	MYGH05	9.0	189	407.021	487.700
31	2011/3/11	14:46:55	FKSH14	9.0	205	387.683	355.917
32	2011/3/11	14:47:17	TCGH11	9.0	314	461.564	406.964
33	2011/3/11	14:46:49	IWTH21	9.0	172	413.579	331.318
34	2011/3/11	14:47:02	IBRH14	9.0	258	393.074	378.483
35	2011/3/11	14:46:52	IWTH20	9.0	209	399.395	374.044
36	2011/3/11	14:47:01	FKSH08	9.0	250	294.087	308.995
37	2011/3/11	14:46:50	IWTH18	9.0	183	256.502	332.610
38	2011/3/11	14:46:52	MYGH09	9.0	198	323.302	315.904
39	2011/3/11	14:47:17	TCGH15	9.0	316	322.821	342.480
40	2011/3/11	14:46:57	FKSH16	9.0	221	325.610	204.430
41	2011/3/11	14:47:04	IWTH01	9.0	271	314.999	263.272
42	2011/3/11	14:46:49	IWTH22	9.0	192	324.933	250.891
43	2011/3/11	14:47:21	IBRH10	9.0	338	295.431	274.128
44	2011/3/11	14:46:45	MYGH06	9.0	165	263.394	246.578
45	2011/3/11	14:46:53	FKSH17	9.0	205	288.732	270.562
46	2011/3/11	14:46:53	IWTH28	9.0	201	289.265	265.589
47	2011/3/11	14:46:47	MYGH08	9.0	177	255.981	282.865
48	2011/3/11	14:46:54	IWTH14	9.0	200	229.328	291.571
49	2011/3/11	14:47:01	IWTH12	9.0	259	256.894	283.900
50	2011/3/11	14:47:29	KNGH10	9.0	415	276.953	209.377
51	2011/3/11	14:47:24	SITH06	9.0	387	254.014	225.361
52	2011/3/11	14:47:15	TCGH14	9.0	335	210.972	190.977
53	2011/3/11	14:46:59	YMTH04	9.0	225	222.392	219.044
54	2011/3/11	14:47:23	CHBH13	9.0	340	233.965	244.478
55	2011/3/11	14:47:39	CHBH04	9.0	360	234.159	203.757
56	2011/3/11	14:47:17	IBRH07	9.0	328	191.503	165.412
57	2011/3/11	14:46:56	YMTH01	9.0	219	180.526	196.257

58	2011/3/11	14:47:27	GNMH12	9.0	413	195.735	147.575
59	2011/3/11	14:47:15	IBRH19	9.0	323	210.613	191.203
60	2011/3/11	14:47:07	FKSH05	9.0	280	180.550	174.797
61	2011/3/11	14:46:59	YMTH06	9.0	235	202.253	147.674
62	2011/3/11	14:46:58	YMTH07	9.0	250	208.130	147.177
63	2011/3/11	14:47:16	IBRH20	9.0	316	187.607	216.148
64	2011/3/11	14:47:29	SITH11	9.0	405	203.783	200.449
65	2011/3/11	14:46:54	IWTH15	9.0	227	196.959	185.123
66	2011/3/11	14:47:20	GNMH05	9.0	382	199.670	172.249
67	2011/3/11	14:46:50	IWTH24	9.0	202	181.370	188.006
68	2011/3/11	14:47:09	AOMH16	9.0	303	153.883	200.853
69	2011/3/11	14:47:15	TCGH07	9.0	330	188.323	147.660
70	2011/3/11	14:46:55	IWTH03	9.0	216	183.639	163.940
71	2011/3/11	14:47:21	SITH01	9.0	368	164.000	177.175
72	2011/3/11	14:47:06	FKSH04	9.0	278	177.197	170.684
73	2011/3/11	14:47:17	CHBH14	9.0	319	122.344	170.352
74	2011/3/11	14:47:25	SITH10	9.0	399	136.406	152.036
75	2011/3/11	14:47:03	IWTH11	9.0	263	151.311	142.562
76	2011/3/11	14:47:11	TCGH09	9.0	301	142.567	151.025
77	2011/3/11	14:47:21	CHBH10	9.0	367	131.396	106.529
78	2011/3/11	14:47:03	IWTH06	9.0	281	158.620	146.525
79	2011/3/11	14:46:52	IWTH17	9.0	203	158.750	126.998
80	2011/3/11	14:47:28	TKYH12	9.0	419	105.914	157.180
81	2011/3/11	14:47:08	AOMH13	9.0	301	130.356	130.492
82	2011/3/11	14:46:57	YMTH02	9.0	229	149.633	139.739
83	2011/3/11	14:46:56	IWTH16	9.0	238	154.811	114.626
84	2011/3/11	14:47:06	FKSH03	9.0	279	115.855	133.003
85	2011/3/11	14:47:31	KNGH11	9.0	433	123.558	139.108
86	2003/9/26	4:50:39	KSRH03	8.0	184	299.515	806.160
87	2003/9/26	4:50:38	KSRH10	8.0	180	580.440	534.579
88	2003/9/26	4:50:44	NMRH02	8.0	223	455.315	514.111
89	2003/9/26	4:50:27	TKCH08	8.0	109	499.732	416.056
90	2003/9/26	4:50:32	KSRH07	8.0	152	500.248	339.595
91	2003/9/26	4:50:41	NMRH04	8.0	199	428.320	437.754
92	2003/9/26	4:50:34	TKCH05	8.0	154	406.141	357.185
93	2003/9/26	4:50:32	KSRH02	8.0	148	404.614	373.116

94	2003/9/26	4:50:31	KSRH09	8.0	134	391.698	368.996
95	2003/9/26	4:50:28	TKCH07	8.0	123	403.939	366.731
96	2003/9/26	4:50:39	NMRH05	8.0	189	341.519	391.309
97	2003/9/26	4:50:34	KSRH06	8.0	163	319.383	377.144
98	2003/9/26	4:50:44	IBUH03	8.0	206	376.509	255.856
99	2003/9/26	4:50:36	KSRH04	8.0	167	334.004	249.714
100	2003/9/26	4:50:36	KSRH05	8.0	164	326.634	274.541
101	2003/9/26	4:50:34	TKCH11	8.0	156	254.425	228.749
102	2003/9/26	4:50:38	TKCH04	8.0	182	228.042	215.912
103	2003/9/26	4:50:39	KKWH08	8.0	182	246.115	170.633
104	2003/9/26	4:50:41	HDKH04	8.0	187	216.149	140.675
105	2003/9/26	4:50:35	HDKH06	8.0	156	209.253	188.678
106	2003/9/26	4:50:26	HDKH07	8.0	104	198.580	168.470
107	2003/9/26	4:50:47	ABSH07	8.0	244	173.793	175.461
108	2003/9/26	4:50:42	HDKH01	8.0	184	137.193	186.080
109	2003/9/26	4:50:33	TKCH06	8.0	149	148.233	162.410
110	2003/9/26	4:50:38	TKCH02	8.0	179	183.385	146.862
111	2003/9/26	4:50:36	TKCH03	8.0	174	180.371	134.908
112	2003/9/26	4:50:46	IBUH01	8.0	222	139.890	124.683
113	2003/9/26	4:50:51	IBUH06	8.0	264	139.046	150.383
114	2003/9/26	4:50:39	KSRH01	8.0	184	158.981	151.573
115	2003/9/26	4:50:38	TKCH01	8.0	190	132.272	133.296
116	2011/3/11	15:12:08	IBRH18	7.7	65	604.145	306.325
117	2011/3/11	15:12:08	TCGH16	7.7	117	344.648	283.290
118	2011/3/11	15:12:04	IBRH16	7.7	98	313.347	234.990
119	2011/3/11	15:12:04	FKSH10	7.7	157	196.731	293.956
120	2011/3/11	15:12:10	IBRH11	7.7	105	287.653	272.668
121	2011/3/11	15:12:08	IBRH15	7.7	100	206.720	286.827
122	2011/3/11	15:15:50	IBRH17	7.7	86	198.359	218.484
123	2011/3/11	15:12:16	IBRH20	7.7	57	228.084	168.051
124	2011/3/11	15:12:04	IBRH12	7.7	117	199.702	235.068
125	2011/3/11	15:12:16	IBRH21	7.7	105	193.469	137.493
126	2011/3/11	15:12:17	TCGH11	7.7	150	198.748	169.056
127	2011/3/11	15:12:36	CHBH14	7.7	58	125.499	179.197
128	2011/3/11	15:12:01	IBRH13	7.7	98	144.527	182.233
129	2011/3/11	15:12:05	TCGH13	7.7	120	157.388	152.810

130	2011/3/11	15:12:06	TCGH10	7.7	139	148.716	136.689
131	2011/3/11	15:15:50	CHBH13	7.7	92	127.462	151.710
132	2011/3/11	15:15:53	IBRH10	7.7	115	117.001	132.535
133	2004/9/5	23:57:42	MIEH05	7.4	136	233.765	226.270
134	2004/9/5	23:57:46	NARH05	7.4	175	187.489	159.349
135	2011/3/11	15:06:57	IWTH02	7.4	120	401.277	320.161
136	2011/3/11	15:07:04	IWTH01	7.4	130	244.491	165.664
137	2011/3/11	15:07:17	AOMH05	7.4	182	246.415	154.642
138	2011/3/11	15:07:09	AOMH16	7.4	160	166.000	167.776
139	2011/3/11	15:07:01	IWTH12	7.4	121	164.893	105.662
140	2016/11/22	5:59:59	FKSH14	7.4	67	182.376	250.706
141	2016/11/22	6:00:04	FKSH12	7.4	93	153.861	190.156
142	2016/11/22	6:00:11	FKSH10	7.4	136	142.948	173.196
143	2016/11/22	6:00:13	TCGH16	7.4	163	171.313	83.464
144	2016/11/22	6:00:11	TCGH13	7.4	144	95.131	155.039
145	2016/11/22	6:00:08	MYGH07	7.4	125	152.452	133.681
146	2016/11/22	6:00:14	IBRH11	7.4	170	133.666	142.631
147	2000/10/6	13:30:00	TTRH02	7.3	7	753.026	927.178
148	2000/10/6	13:30:00	SMNH01	7.3	8	607.058	720.366
149	2000/10/6	13:30:00	SMNH02	7.3	24	314.945	563.951
150	2000/10/6	13:30:00	OKYH14	7.3	45	442.991	260.328
151	2000/10/6	13:30:00	HRSH03	7.3	86	341.141	224.775
152	2000/10/6	13:30:00	OKYH09	7.3	32	283.756	181.806
153	2000/10/6	13:30:00	OKYH08	7.3	41	238.467	224.851
154	2000/10/6	13:30:00	HRSH06	7.3	56	240.323	185.052
155	2000/10/6	13:30:28	OKYH10	7.3	53	131.752	280.663
156	2000/10/6	13:30:27	SMNH12	7.3	46	258.577	227.174
157	2000/10/6	13:30:25	SMNH10	7.3	31	226.415	155.130
158	2000/10/6	13:30:25	TTRH04	7.3	33	207.152	184.383
159	2000/10/6	13:30:23	OKYH07	7.3	26	127.080	179.669
160	2000/10/6	13:30:36	OKYH01	7.3	99	180.702	97.379
161	2000/10/6	13:30:37	HRSH01	7.3	105	169.288	158.318
162	2000/10/6	13:30:33	HRSH05	7.3	80	131.040	117.268
163	2000/10/6	13:30:29	SMNH03	7.3	57	154.626	154.792
164	2000/10/6	13:30:32	OKYH05	7.3	65	149.029	107.452
165	2012/12/7	17:19:09	IWTH02	7.3	294	206.620	315.230

166	2012/12/7	17:19:15	IBRH11	7.3	378	230.113	186.727
167	2012/12/7	17:19:22	AOMH05	7.3	395	146.694	151.475
168	2012/12/7	17:19:15	TCGH16	7.3	374	181.515	118.670
169	2012/12/7	17:19:00	IWTH27	7.3	233	111.589	160.401
170	2012/12/7	17:19:14	IWTH01	7.3	329	138.126	100.573
171	2016/4/16	1:25:08	KMMH16	7.3	7	1156.946	653.017
172	2016/4/16	1:25:10	KMMH03	7.3	28	227.640	786.576
173	2016/4/16	1:25:14	KMMH02	7.3	50	660.389	302.731
174	2016/4/16	1:24:20	KMMH14	7.3	13	402.223	457.322
175	2016/4/16	1:25:18	OITH11	7.3	72	518.752	559.415
176	2016/4/16	1:25:12	KMMH01	7.3	40	208.778	201.128
177	2016/4/16	1:25:11	KMMH09	7.3	32	200.010	240.424
178	2016/4/16	1:25:16	KMMH12	7.3	61	155.069	217.353
179	2016/4/16	1:25:17	KMMH10	7.3	73	176.318	130.727
180	2016/4/16	1:25:11	KMMH06	7.3	32	162.473	117.976
181	2016/4/16	1:25:16	MYZH04	7.3	60	164.491	106.979
182	2016/4/16	1:25:18	SAGH04	7.3	76	97.637	143.857
183	2005/8/16	11:46:42	MYGH11	7.2	91	301.231	462.050
184	2005/8/16	11:46:46	MYGH10	7.2	124	408.911	301.961
185	2005/8/16	11:46:58	IWTH02	7.2	201	325.720	197.527
186	2005/8/16	11:46:45	MYGH01	7.2	113	216.333	287.995
187	2005/8/16	11:46:49	IWTH26	7.2	144	239.309	189.233
188	2005/8/16	11:46:44	MYGH04	7.2	109	225.414	267.029
189	2005/8/16	11:46:42	MYGH12	7.2	91	236.370	254.812
190	2005/8/16	11:46:45	IWTH05	7.2	113	237.665	223.306
191	2005/8/16	11:46:43	MYGH03	7.2	102	222.485	169.146
192	2005/8/16	11:46:55	IWTH14	7.2	180	110.063	230.750
193	2005/8/16	11:46:46	IWTH27	7.2	117	214.705	211.048
194	2005/8/16	11:46:54	FKSH12	7.2	183	212.037	166.525
195	2005/8/16	11:46:53	IWTH20	7.2	170	194.074	161.050
196	2005/8/16	11:46:52	FKSH19	7.2	156	197.411	180.549
197	2005/8/16	11:46:49	IWTH04	7.2	138	135.838	154.236
198	2005/8/16	11:46:47	IWTH23	7.2	131	154.933	167.701
199	2005/8/16	11:46:53	FKSH18	7.2	170	139.251	163.998
200	2005/8/16	11:46:49	MYGH05	7.2	139	157.770	126.507
201	2005/8/16	11:46:50	MYGH09	7.2	148	109.876	148.771

202	2008/6/14	8:43:46	IWTH25	7.2	3	1432.594	1143.231
203	2008/6/14	8:43:49	AKTH04	7.2	22	2449.245	1318.461
204	2008/6/14	8:43:48	IWTH26	7.2	12	1055.515	888.277
205	2008/6/14	8:43:50	IWTH24	7.2	22	434.580	502.915
206	2008/6/14	8:43:51	MYGH02	7.2	27	229.600	254.437
207	2008/6/14	8:43:51	IWTH27	7.2	56	235.493	216.795
208	2008/6/14	8:43:51	AKTH19	7.2	40	161.118	248.091
209	2008/6/14	8:43:51	IWTH20	7.2	38	240.304	249.258
210	2008/6/14	8:43:51	IWTH05	7.2	45	176.120	211.279
211	2008/6/14	8:43:51	MYGH04	7.2	47	150.857	229.470
212	2008/6/14	8:43:51	IWTH22	7.2	50	161.519	207.155
213	2008/6/14	8:43:51	MYGH10	7.2	121	203.597	152.358
214	2008/6/14	8:43:51	IWTH02	7.2	98	178.390	162.878
215	2008/6/14	8:43:51	IWTH04	7.2	47	158.769	125.552
216	2008/6/14	8:43:51	AKTH06	7.2	34	185.671	179.888
217	2008/6/14	8:43:51	MYGH11	7.2	70	120.273	182.430
218	2008/6/14	8:43:51	IWTH14	7.2	119	129.607	170.680
219	2008/6/14	8:43:51	IWTH19	7.2	49	136.824	145.182
220	2003/9/26	6:08:09	HDKH03	7.1	148	175.031	136.879
221	2003/9/26	6:08:36	IBUH01	7.1	201	163.526	121.193
222	2003/9/26	6:08:39	IBUH06	7.1	236	122.999	147.829
223	2003/9/26	6:07:34	TKCH08	7.1	97	169.262	130.774
224	2003/9/26	6:08:42	IBUH04	7.1	271	167.134	71.332
225	2003/9/26	6:07:39	HDKH07	7.1	80	146.195	107.912
226	2004/11/29	3:32:29	KSRH06	7.1	75	562.546	756.457
227	2004/11/29	3:32:26	KSRH04	7.1	57	377.480	194.234
228	2004/11/29	3:32:24	KSRH10	7.1	32	274.012	364.090
229	2004/11/29	3:32:31	KSRH05	7.1	91	315.666	337.521
230	2004/11/29	3:32:29	KSRH03	7.1	72	204.226	282.473
231	2004/11/29	3:32:31	KSRH02	7.1	96	265.877	234.092
232	2004/11/29	3:32:30	NMRH02	7.1	85	252.892	167.012
233	2004/11/29	3:32:26	NMRH04	7.1	52	183.581	158.031
234	2004/11/29	3:32:29	KSRH07	7.1	80	122.956	123.086
235	2004/11/29	3:32:28	NMRH03	7.1	72	116.235	118.877
236	2011/4/7	23:33:00	IWTH27	7.1	98	782.814	795.532
237	2011/4/7	23:33:00	IWTH05	7.1	89	571.549	836.249

238	2011/4/7	23:33:12	IWTH02	7.1	186	558.401	649.455
239	2011/4/7	23:33:00	MYGH10	7.1	95	756.913	542.623
240	2011/4/7	23:32:58	MYGH04	7.1	83	629.313	539.800
241	2011/4/7	23:32:58	MYGH03	7.1	83	510.339	674.815
242	2011/4/7	23:33:03	IWTH26	7.1	117	434.512	533.291
243	2011/4/7	23:33:03	IWTH04	7.1	118	431.876	581.137
244	2011/4/7	23:33:03	IWTH23	7.1	119	483.476	507.320
245	2011/4/7	23:33:05	IWTH21	7.1	141	409.782	411.243
246	2011/4/7	23:33:01	MYGH05	7.1	108	373.486	445.228
247	2011/4/7	23:33:04	IWTH28	7.1	128	395.642	417.934
248	2011/4/7	23:32:59	MYGH06	7.1	86	371.240	370.132
249	2011/4/7	23:33:06	IWTH18	7.1	141	331.196	341.077
250	2011/4/7	23:33:07	AKTH04	7.1	150	346.361	335.271
251	2011/4/7	23:33:07	IWTH20	7.1	148	344.557	268.359
252	2011/4/7	23:33:10	IWTH14	7.1	171	219.506	305.117
253	2011/4/7	23:33:05	IWTH22	7.1	137	320.997	238.158
254	2011/4/7	23:33:09	FKSH12	7.1	162	203.478	277.170
255	2011/4/7	23:33:05	FKSH19	7.1	133	254.526	267.805
256	2011/4/7	23:33:00	MYGH08	7.1	95	199.747	249.585
257	2011/4/7	23:33:18	IWTH01	7.1	231	218.394	252.034
258	2011/4/7	23:33:11	IWTH03	7.1	179	199.692	191.379
259	2011/4/7	23:33:03	MYGH09	7.1	118	238.276	169.404
260	2011/4/7	23:33:05	IWTH24	7.1	136	231.001	195.767
261	2011/4/7	23:33:07	FKSH18	7.1	145	173.264	213.131
262	2011/4/7	23:33:09	IWTH17	7.1	162	112.044	176.431
263	2011/4/7	23:33:17	IBRH16	7.1	220	203.022	131.817
264	2011/4/7	23:33:04	FKSH17	7.1	131	175.596	149.489
265	2011/4/7	23:33:10	IWTH15	7.1	172	143.489	194.726
266	2011/4/7	23:33:16	IWTH12	7.1	221	166.333	160.877
267	2011/4/7	23:33:06	FKSH16	7.1	144	173.740	96.214
268	2011/4/7	23:33:05	YMTH01	7.1	136	144.221	163.439
269	2011/4/7	23:33:07	YMTH06	7.1	155	148.623	106.051
270	2011/4/7	23:33:09	FKSH09	7.1	162	137.097	150.180
271	2003/5/26	18:24:47	IWTH04	7.0	48	722.976	729.625
272	2003/5/26	18:24:45	IWTH27	7.0	28	556.093	888.060
273	2003/5/26	18:24:45	MYGH03	7.0	13	650.758	809.059

274	2003/5/26	18:24:50	IWTH21	7.0	77	586.219	549.897
275	2003/5/26	18:24:54	IWTH02	7.0	116	674.510	795.582
276	2003/5/26	18:24:45	MYGH04	7.0	31	502.552	664.727
277	2003/5/26	18:24:48	IWTH26	7.0	61	521.295	483.528
278	2003/5/26	18:24:50	MYGH05	7.0	82	579.017	614.980
279	2003/5/26	18:24:45	IWTH05	7.0	29	501.657	570.648
280	2003/5/26	18:24:49	IWTH18	7.0	73	434.641	461.888
281	2003/5/26	18:24:53	IWTH14	7.0	106	296.201	458.662
282	2003/5/26	18:24:47	IWTH23	7.0	53	529.373	419.983
283	2003/5/26	18:24:45	MYGH12	7.0	28	391.235	346.445
284	2003/5/26	18:24:46	MYGH11	7.0	44	435.424	359.089
285	2003/5/26	18:25:00	IWTH01	7.0	161	386.897	243.773
286	2003/5/26	18:24:49	IWTH20	7.0	81	317.517	291.327
287	2003/5/26	18:24:51	IWTH19	7.0	93	373.018	353.645
288	2003/5/26	18:24:54	MYGH07	7.0	114	305.740	239.466
289	2003/5/26	18:24:48	IWTH25	7.0	74	287.349	316.616
290	2003/5/26	18:24:52	IWTH15	7.0	103	268.816	328.131
291	2003/5/26	18:24:53	IWTH03	7.0	110	272.020	299.455
292	2003/5/26	18:24:48	IWTH22	7.0	67	261.403	246.771
293	2003/5/26	18:24:49	IWTH24	7.0	72	268.786	226.377
294	2003/5/26	18:24:58	IWTH12	7.0	151	199.298	254.180
295	2003/5/26	18:24:54	MYGH10	7.0	118	223.449	221.217
296	2003/5/26	18:24:50	MYGH01	7.0	87	180.074	196.855
297	2003/5/26	18:24:51	IWTH17	7.0	93	184.195	199.439
298	2003/5/26	18:25:05	FKSH12	7.0	202	206.800	136.301
299	2003/5/26	18:25:01	IWTH06	7.0	167	179.909	127.658
300	2003/5/26	18:24:57	IWTH09	7.0	142	138.296	131.264
301	2003/5/26	18:24:55	AKTH17	7.0	124	150.336	157.754
302	2005/3/20	10:53:49	FKOH03	7.0	40	203.213	249.519
303	2005/3/20	10:53:53	FKOH08	7.0	68	211.445	240.024
304	2005/3/20	10:53:48	SAGH03	7.0	37	201.856	215.690
305	2005/3/20	10:53:49	SAGH04	7.0	46	114.518	194.754
306	2005/3/20	10:53:54	FKOH05	7.0	76	145.744	165.740
307	2005/3/20	10:53:48	FKOH09	7.0	36	143.559	140.024
308	2005/3/20	10:53:57	NGSH01	7.0	90	180.172	110.511
309	2005/3/20	10:53:52	FKOH04	7.0	57	163.916	132.573

310	2005/3/20	10:53:52	SAGH02	7.0	59	174.206	106.938
311	2005/3/20	10:53:48	SAGH01	7.0	37	141.833	125.447
312	2008/5/8	1:45:41	TCGH16	7.0	142	108.018	135.839
313	2011/4/11	17:16:18	FKSH12	7.0	31	416.912	510.316
314	2011/4/11	17:16:16	IBRH13	7.0	19	445.589	362.748
315	2011/4/11	17:16:23	IBRH18	7.0	65	467.749	188.040
316	2011/4/11	17:16:22	FKSH10	7.0	57	322.378	322.774
317	2011/4/11	17:16:19	FKSH11	7.0	41	338.363	264.062
318	2011/4/11	17:16:18	IBRH14	7.0	30	244.378	243.940
319	2011/4/11	17:16:20	IBRH16	7.0	42	200.561	292.333
320	2011/4/11	17:16:21	FKSH09	7.0	50	294.197	263.173
321	2011/4/11	17:16:18	IBRH12	7.0	34	198.252	219.118
322	2011/4/11	17:16:24	TCGH16	7.0	69	257.613	230.024
323	2011/4/11	17:16:21	TCGH13	7.0	50	252.242	162.335
324	2011/4/11	17:16:25	IBRH11	7.0	80	236.972	169.078
325	2011/4/11	17:16:22	TCGH10	7.0	59	192.244	208.882
326	2011/4/11	17:16:21	IBRH15	7.0	54	150.666	188.687
327	2011/4/11	17:16:23	FKSH18	7.0	62	144.394	194.645
328	2011/4/11	17:16:22	FKSH08	7.0	55	150.795	170.899
329	2011/4/11	17:16:22	FKSH19	7.0	58	147.431	148.677
330	2011/4/11	17:16:24	TCGH12	7.0	67	137.782	168.547
331	2011/4/11	17:16:30	IBRH17	7.0	101	151.463	159.660
332	2011/4/11	17:16:26	FKSH05	7.0	79	141.756	144.414
333	2011/4/11	17:16:17	FKSH14	7.0	28	139.027	116.932
334	2004/9/5	19:07:34	NARH05	6.9	170	203.861	153.368
335	2004/9/5	19:07:29	MIEH05	6.9	128	126.935	118.461
336	2004/12/6	23:15:22	KSRH10	6.9	44	437.248	334.700
337	2004/12/6	23:15:27	KSRH06	6.9	85	381.468	376.309
338	2004/12/6	23:15:29	KSRH05	6.9	101	265.279	193.932
339	2004/12/6	23:15:27	KSRH03	6.9	83	139.002	257.455
340	2004/12/6	23:15:26	NMRH05	6.9	75	242.590	161.552
341	2004/12/6	23:15:25	KSRH04	6.9	68	173.371	176.469
342	2004/12/6	23:15:28	NMRH02	6.9	97	190.124	134.057
343	2004/12/6	23:15:25	NMRH04	6.9	64	142.259	132.113
344	2007/3/25	9:42:05	ISKH02	6.9	35	359.337	274.265
345	2007/3/25	9:42:10	ISKH01	6.9	63	123.075	359.311

346	2007/3/25	9:42:17	ISKH09	6.9	106	179.342	179.340
347	2011/6/23	6:51:08	IWTH02	6.9	104	418.393	219.607
348	2011/6/23	6:51:09	IWTH01	6.9	111	198.024	142.539
349	2011/6/23	6:51:16	AOMH05	6.9	162	178.589	213.201
350	2004/10/23	17:56:04	NIGH01	6.8	15	655.346	818.250
351	2004/10/23	17:56:05	NIGH11	6.8	17	587.851	454.426
352	2004/10/23	17:56:09	NIGH06	6.8	44	409.766	356.745
353	2004/10/23	17:56:04	NIGH12	6.8	13	345.430	409.975
354	2004/10/23	17:56:08	NIGH09	6.8	36	390.056	368.367
355	2004/10/23	17:56:08	FKSH21	6.8	40	361.727	246.517
356	2004/10/23	17:56:06	NIGH15	6.8	29	182.627	242.773
357	2004/10/23	17:56:10	NIGH10	6.8	52	131.375	214.156
358	2004/10/23	17:56:12	FKSH06	6.8	59	147.469	125.924
359	2004/10/23	17:56:13	TCGH07	6.8	69	100.465	160.414
360	2004/10/23	17:56:11	FKSH07	6.8	55	101.234	149.237
361	2004/10/23	17:56:13	NIGH08	6.8	68	139.834	125.508
362	2007/7/16	10:13:34	NIGH13	6.8	59	169.518	264.107
363	2007/7/16	10:13:32	NIGH12	6.8	50	195.585	114.491
364	2007/7/16	10:13:32	NIGH11	6.8	44	133.082	163.057
365	2007/7/16	10:13:32	NIGH06	6.8	42	149.948	147.917
366	2007/7/16	10:13:29	NIGH01	6.8	29	120.962	151.222
367	2008/7/24	0:26:35	IWTH02	6.8	24	683.841	1019.271
368	2008/7/24	0:26:36	IWTH12	6.8	50	669.922	716.204
369	2008/7/24	0:26:34	IWTH03	6.8	8	548.519	475.028
370	2008/7/24	0:26:35	IWTH21	6.8	38	444.708	469.152
371	2008/7/24	0:26:35	IWTH14	6.8	23	317.355	486.494
372	2008/7/24	0:26:35	IWTH09	6.8	40	524.084	421.565
373	2008/7/24	0:26:35	IWTH18	6.8	30	389.574	378.330
374	2008/7/24	0:26:36	IWTH08	6.8	61	384.351	314.377
375	2008/7/24	0:26:36	IWTH23	6.8	53	399.121	399.585
376	2008/7/24	0:26:36	IWTH27	6.8	78	433.086	300.912
377	2008/7/24	0:26:35	IWTH17	6.8	10	324.874	309.531
378	2008/7/24	0:26:36	IWTH07	6.8	60	218.983	384.198
379	2008/7/24	0:26:36	AKTH04	6.8	101	221.288	301.896
380	2008/7/24	0:26:36	AOMH17	6.8	84	297.595	215.472
381	2008/7/24	0:26:36	AKTH14	6.8	80	197.033	280.610

382	2008/7/24	0:26:36	IWTH05	6.8	99	318.826	195.907
383	2008/7/24	0:26:36	IWTH04	6.8	65	241.229	303.966
384	2008/7/24	0:26:36	MYGH03	6.8	90	218.105	312.670
385	2008/7/24	0:26:36	IWTH01	6.8	62	246.781	268.813
386	2008/7/24	0:26:36	IWTH19	6.8	63	222.722	244.993
387	2008/7/24	0:26:36	IWTH22	6.8	53	252.276	182.383
388	2008/7/24	0:26:36	IWTH26	6.8	101	239.714	148.564
389	2008/7/24	0:26:36	AOMH05	6.8	133	249.425	185.646
390	2008/7/24	0:26:36	MYGH04	6.8	108	191.038	226.613
391	2008/7/24	0:26:36	AOMH16	6.8	93	222.541	197.406
392	2008/7/24	0:26:35	IWTH13	6.8	24	207.434	228.985
393	2008/7/24	0:26:36	IWTH20	6.8	66	191.588	181.608
394	2008/7/24	0:26:36	AOMH12	6.8	103	156.173	179.413
395	2008/7/24	0:26:36	MYGH11	6.8	137	194.175	148.564
396	2008/7/24	0:26:36	IWTH06	6.8	71	186.436	168.945
397	2008/7/24	0:26:36	IWTH15	6.8	48	184.149	151.674
398	2008/7/24	0:26:36	AOMH13	6.8	95	144.122	197.642
399	2008/7/24	0:26:36	AOMH18	6.8	82	105.844	153.475
400	2008/7/24	0:26:37	MYGH01	6.8	175	87.520	151.892
401	2008/7/24	0:26:36	IWTH11	6.8	54	140.757	127.721
402	2008/7/24	0:26:40	IWTH25	6.8	104	115.330	124.028
403	2015/5/13	6:13:09	IWTH27	6.8	57	210.216	149.014
404	2015/5/13	6:13:10	MYGH13	6.8	66	140.160	183.378
405	2015/5/13	6:13:18	IWTH02	6.8	126	118.258	175.709
406	2015/5/13	6:13:09	IWTH23	6.8	54	120.654	168.122
407	2015/5/13	6:13:11	MYGH04	6.8	72	79.332	149.552
408	2015/5/13	6:13:08	MYGH03	6.8	45	116.832	140.679
409	2010/3/14	17:08:19	MYGH01	6.7	92	131.370	152.859
410	2011/3/11	20:37:00	IWTH02	6.7	129	274.643	327.960
411	2011/3/11	20:37:04	IWTH01	6.7	162	190.571	84.931
412	2011/3/11	20:36:51	IWTH23	6.7	70	139.027	127.230
413	2011/3/12	3:59:18	NGNH29	6.7	16	323.809	279.523
414	2011/3/12	3:59:20	NIGH14	6.7	23	346.101	300.030
415	2011/3/12	3:59:20	NIGH11	6.7	25	158.368	238.511
416	2011/3/12	3:59:31	NIGH06	6.7	85	145.829	201.609
417	2011/3/12	3:59:21	NIGH19	6.7	26	127.317	139.842

418	2011/3/12	3:59:24	GNMH13	6.7	44	117.574	160.039
419	2011/3/12	3:59:19	NIGH13	6.7	19	135.939	143.138
420	2014/11/22	22:08:21	NGNH28	6.7	19	178.462	200.823
421	2014/11/22	22:08:21	NGNH27	6.7	19	152.061	139.631
422	2014/11/22	22:08:22	NIGH17	6.7	26	113.872	115.738
423	2016/1/14	12:25:42	HDKH07	6.7	21	160.683	114.290
424	2012/3/27	20:00:49	IWTH14	6.6	37	191.795	218.739
425	2012/3/27	20:00:51	IWTH21	6.6	50	164.408	177.195
426	2012/3/27	20:00:57	IWTH02	6.6	81	211.015	128.619
427	2012/3/27	20:00:57	IWTH12	6.6	87	168.653	102.339
428	2012/3/27	20:01:00	IWTH01	6.6	97	148.661	84.918
429	2012/3/27	20:01:08	AKTH04	6.6	156	122.849	99.722
430	2012/3/27	20:01:05	AKTH14	6.6	133	82.652	150.253
431	2012/3/27	20:00:55	IWTH23	6.6	73	126.630	139.479
432	2012/3/27	20:01:01	IWTH27	6.6	110	140.561	64.923
433	2016/10/21	14:07:28	OKYH09	6.6	27	217.844	177.611
434	2016/10/21	14:07:27	TTRH04	6.6	23	210.554	159.398
435	2016/10/21	14:07:25	TTRH07	6.6	10	185.535	178.155
436	2016/10/21	14:07:28	TTRH03	6.6	33	162.582	197.018
437	2016/10/21	14:07:28	TTRH06	6.6	31	101.789	159.762
438	2016/10/21	14:07:30	OKYH11	6.6	42	111.308	122.698
439	2004/10/23	18:31:00	NIGH11	6.5	22	533.969	741.341
440	2004/10/23	18:34:09	NIGH12	6.5	10	363.994	545.156
441	2004/10/23	18:34:18	NGNH29	6.5	62	216.086	345.272
442	2004/10/23	18:34:12	NIGH09	6.5	31	291.610	186.019
443	2004/10/23	18:31:05	NIGH01	6.5	14	273.865	321.718
444	2004/10/23	18:34:13	FKSH21	6.5	34	289.597	212.003
445	2004/10/23	18:34:28	NIGH06	6.5	40	219.164	258.283
446	2004/10/23	18:34:17	NIGH13	6.5	55	234.580	180.822
447	2004/10/23	18:34:12	NIGH15	6.5	29	139.765	211.438
448	2004/10/23	18:34:15	NIGH10	6.5	47	132.655	175.885
449	2004/10/23	18:34:16	FKSH07	6.5	51	121.849	176.486
450	2004/10/23	18:34:15	NIGH07	6.5	50	134.714	121.341
451	2009/8/11	5:07:12	SZOH33	6.5	29	431.576	429.009
452	2009/8/11	5:07:11	SZOH39	6.5	25	294.810	519.361
453	2009/8/11	5:07:14	SZOH42	6.5	43	442.631	332.367

454	2009/8/11	5:07:13	SZOH34	6.5	39	294.629	275.475
455	2009/8/11	5:07:12	SZOH36	6.5	31	217.338	291.397
456	2009/8/11	5:07:11	SZOH43	6.5	21	223.924	247.082
457	2009/8/11	5:07:14	SZOH37	6.5	47	250.964	177.304
458	2009/8/11	5:07:14	SZOH38	6.5	55	128.404	173.857
459	2009/8/11	5:07:14	SZOH35	6.5	57	91.201	165.724
460	2009/8/11	5:07:12	SZOH41	6.5	33	132.011	143.470
461	2009/8/11	5:07:14	NGNH14	6.5	99	148.097	146.589
462	2009/8/11	5:07:14	KNGH19	6.5	86	171.696	81.380
463	2009/8/11	5:07:14	SZOH31	6.5	42	139.868	148.549
464	2009/8/11	5:07:14	NGNH25	6.5	77	126.079	114.423
465	2011/3/11	16:28:50	IWTH27	6.5	65	264.456	250.499
466	2011/3/11	16:28:52	IWTH23	6.5	48	181.877	177.324
467	2011/3/11	16:25:50	MYGH05	6.5	140	129.796	119.795
468	2011/3/11	16:29:07	IWTH02	6.5	117	121.654	119.911
469	2011/3/11	16:28:48	MYGH03	6.5	57	129.966	140.458
470	2011/3/28	7:24:13	MYGH04	6.5	97	116.440	148.511
471	2011/3/28	7:24:14	IWTH23	6.5	107	142.144	103.675
472	2011/3/28	7:24:16	IWTH05	6.5	99	138.010	119.894
473	2011/7/31	3:54:04	FKSH12	6.5	68	304.503	363.271
474	2011/7/31	3:54:06	FKSH18	6.5	89	364.705	325.831
475	2011/7/31	3:54:03	IBRH13	6.5	59	281.190	299.520
476	2011/7/31	3:54:05	IBRH16	6.5	79	234.738	207.520
477	2011/7/31	3:54:00	FKSH14	6.5	26	119.008	180.276
478	2011/7/31	3:54:05	FKSH19	6.5	77	162.432	165.093
479	2011/7/31	3:54:08	FKSH10	6.5	104	120.585	192.206
480	2011/7/31	3:54:09	IBRH11	6.5	113	182.251	168.074
481	2011/7/31	3:54:06	IBRH15	6.5	91	131.304	153.096
482	2011/7/31	3:54:03	IBRH14	6.5	64	157.718	111.887
483	2011/7/31	3:54:09	TCGH10	6.5	107	115.409	129.775
484	2011/8/19	14:36:47	MYGH10	6.5	86	256.244	231.324
485	2013/2/2	23:17:56	KSRH06	6.5	114	545.101	694.844
486	2013/2/2	23:17:55	KSRH07	6.5	102	574.692	324.475
487	2013/2/2	23:17:56	KSRH05	6.5	103	501.567	321.915
488	2013/2/2	23:17:53	KSRH09	6.5	69	246.399	338.047
489	2013/2/2	23:17:52	TKCH07	6.5	27	303.000	250.927

490	2013/2/2	23:17:50	TKCH08	6.5	25	242.340	294.528
491	2013/2/2	23:17:52	TKCH05	6.5	56	252.734	244.298
492	2013/2/2	23:17:54	KSRH02	6.5	86	207.653	262.082
493	2013/2/2	23:17:50	TKCH11	6.5	34	220.140	267.411
494	2013/2/2	23:18:01	KSRH10	6.5	164	173.301	241.758
495	2013/2/2	23:18:04	NMRH02	6.5	178	242.493	114.345
496	2013/2/2	23:17:59	KSRH03	6.5	137	171.058	177.167
497	2013/2/2	23:18:00	NMRH05	6.5	149	165.372	141.860
498	2013/2/2	23:17:53	KSRH08	6.5	75	135.971	162.069
499	2013/2/2	23:17:55	HDKH03	6.5	73	137.444	139.200
500	2013/2/2	23:17:52	TKCH04	6.5	58	136.925	136.062
501	2016/4/14	21:26:36	KMMH16	6.5	6	925.025	759.771
502	2016/4/14	21:26:37	KMMH14	6.5	13	218.997	328.222
503	2016/4/14	21:26:40	KMMH07	6.5	27	150.694	166.211
504	2016/4/14	21:26:39	KMMH03	6.5	28	123.609	125.446
505	2016/4/14	21:26:40	KMMH09	6.5	29	140.442	118.073
506	2016/4/14	21:26:43	KMMH02	6.5	48	143.397	142.135
507	2001/3/24	15:28:05	HRSH01	6.4	40	492.962	460.976
508	2001/3/24	15:28:05	EHMH05	6.4	47	504.428	506.448
509	2001/3/24	15:28:07	HRSH03	6.4	59	554.513	374.847
510	2001/3/24	15:28:06	EHMH02	6.4	53	396.845	285.411
511	2001/3/24	15:28:08	KOCH05	6.4	67	296.661	328.511
512	2001/3/24	15:28:03	HRSH07	6.4	19	336.100	285.005
513	2001/3/24	15:28:08	EHMH08	6.4	70	287.265	241.281
514	2001/3/24	15:28:05	EHMH04	6.4	41	328.479	313.913
515	2001/3/24	15:28:06	HRSH02	6.4	52	308.453	228.622
516	2001/3/24	15:28:10	HRSH06	6.4	90	291.033	215.908
517	2001/3/24	15:28:06	YMGH03	6.4	54	218.979	206.540
518	2001/3/24	15:28:09	EHMH07	6.4	69	234.718	197.076
519	2001/3/24	15:28:11	KGWH02	6.4	93	182.782	236.510
520	2001/3/24	15:28:09	HRSH10	6.4	75	185.921	234.124
521	2001/3/24	15:28:10	SMNH05	6.4	83	214.111	207.177
522	2001/3/24	15:28:11	EHMH06	6.4	88	154.146	198.776
523	2001/3/24	15:28:13	KGWH01	6.4	115	166.743	197.546
524	2001/3/24	15:28:08	HRSH09	6.4	68	218.201	123.873
525	2001/3/24	15:28:06	HRSH08	6.4	58	181.727	123.088

526	2001/3/24	15:28:10	EHMH03	6.4	90	202.694	156.545
527	2001/3/24	15:28:08	YMGH05	6.4	66	145.040	161.338
528	2001/3/24	15:28:10	SMNH07	6.4	88	156.586	164.936
529	2001/3/24	15:28:16	TKSH02	6.4	129	129.424	168.441
530	2001/3/24	15:28:10	SMNH08	6.4	88	136.871	137.241
531	2001/3/24	15:28:09	KOCH02	6.4	76	124.344	137.465
532	2001/12/2	22:02:14	IWTH14	6.4	67	147.975	271.659
533	2001/12/2	22:02:13	IWTH18	6.4	36	250.848	216.437
534	2001/12/2	22:02:14	IWTH02	6.4	49	248.501	215.261
535	2001/12/2	22:02:14	IWTH21	6.4	58	220.754	210.809
536	2001/12/2	22:02:14	MYGH04	6.4	68	151.711	211.757
537	2001/12/2	22:02:12	IWTH22	6.4	8	157.117	155.227
538	2001/12/2	22:02:14	IWTH23	6.4	50	161.890	119.096
539	2001/12/2	22:02:16	IWTH12	6.4	85	103.527	111.940
540	2001/12/2	22:02:14	MYGH03	6.4	62	144.834	115.193
541	2001/12/2	22:02:13	IWTH04	6.4	26	140.053	120.454
542	2005/1/18	23:09:19	KSRH06	6.4	61	128.192	224.016
543	2005/1/18	23:09:19	NMRH04	6.4	59	97.306	158.131
544	2005/1/18	23:09:20	KSRH03	6.4	65	158.006	136.163
545	2011/3/11	15:06:44	IWTH23	6.4	56	217.623	211.065
546	2011/3/11	15:06:43	IWTH27	6.4	75	123.360	174.529
547	2011/3/15	22:31:50	SZOH37	6.4	18	475.922	362.549
548	2011/3/15	22:31:53	KNGH20	6.4	38	201.139	200.747
549	2011/3/15	22:31:52	YMNH14	6.4	32	185.028	138.918
550	2011/3/15	22:31:51	YMNH15	6.4	27	138.980	187.690
551	2011/3/15	22:31:53	SZOH34	6.4	33	186.799	130.829
552	2011/4/12	14:07:46	FKSH12	6.4	19	416.419	347.075
553	2011/4/12	14:07:49	IBRH12	6.4	38	247.760	364.523
554	2011/4/12	14:07:48	IBRH13	6.4	29	216.651	324.302
555	2011/4/12	14:07:50	FKSH19	6.4	47	329.965	194.863
556	2011/4/12	14:07:51	IBRH16	6.4	51	242.343	176.813
557	2011/4/12	14:07:48	FKSH11	6.4	32	214.684	170.258
558	2011/4/12	14:07:49	FKSH09	6.4	39	146.793	195.681
559	2011/4/12	14:07:49	IBRH14	6.4	41	146.734	186.993
560	2011/7/23	13:34:34	IWTH23	6.4	50	155.792	134.880
561	2011/7/23	13:34:43	IWTH02	6.4	122	165.981	118.591

562	2011/7/23	13:34:34	IWTH27	6.4	51	140.102	158.560
563	2016/4/15	0:03:27	KMMH16	6.4	11	590.160	353.195
564	2016/4/15	0:03:48	KMMH14	6.4	8	323.927	353.275
565	2004/10/23	18:01:04	NIGH01	6.3	12	501.752	742.318
566	2004/10/23	18:01:09	NIGH06	6.3	34	133.363	232.009
567	2004/10/23	18:01:09	NIGH09	6.3	24	173.337	159.364
568	2004/10/23	18:01:04	NIGH12	6.3	14	138.687	163.083
569	2004/10/23	18:01:08	FKSH21	6.3	30	175.499	133.712
570	2004/10/23	18:01:24	NIGH10	6.3	40	85.437	132.789
571	2011/7/25	3:51:38	MYGH10	6.3	70	257.052	332.138
572	2011/7/25	3:51:41	FKSH18	6.3	99	139.963	146.443
573	2011/7/25	3:51:39	FKSH19	6.3	84	159.435	114.058
574	2013/2/25	16:23:54	TCGH07	6.3	4	834.984	1224.321
575	2013/4/13	5:33:21	HYGH01	6.3	14	167.700	159.632
576	2016/12/28	21:38:51	IBRH13	6.3	8	730.050	760.452
577	2016/12/28	21:38:51	IBRH14	6.3	4	354.048	393.730
578	2016/12/28	21:38:53	IBRH06	6.3	19	307.515	366.303
579	2016/12/28	21:38:55	TCGH13	6.3	35	157.135	146.290
580	2016/12/28	21:39:00	FKSH10	6.3	65	123.917	153.144
581	2016/12/28	21:38:52	IBRH16	6.3	18	105.012	135.020
582	2003/7/26	7:13:42	MYGH07	6.2	53	139.958	139.729
583	2003/7/26	7:13:37	MYGH06	6.2	22	125.533	126.336
584	2003/7/26	7:13:39	MYGH12	6.2	35	119.848	143.705
585	2006/6/12	5:02:03	HRSH03	6.2	222	173.900	175.048
586	2006/6/12	5:01:57	KOCH05	6.2	171	159.776	184.218
587	2010/6/13	12:33:13	MYGH10	6.2	100	137.742	143.460
588	2010/6/13	12:33:10	FKSH20	6.2	72	119.455	109.092
589	2011/3/12	22:15:12	FKSH12	6.2	76	119.111	140.054
590	2011/3/14	10:02:47	IBRH18	6.2	47	195.558	187.003
591	2011/3/14	10:02:50	IBRH16	6.2	68	155.767	147.876
592	2011/3/14	10:02:54	TCGH16	6.2	95	101.245	109.647
593	2011/3/24	17:21:11	IWTH27	6.2	72	119.653	156.055
594	2011/3/24	17:21:13	IWTH05	6.2	90	182.842	113.709
595	2011/3/24	17:21:13	IWTH04	6.2	84	101.497	136.312
596	2011/8/1	23:58:15	SZOH39	6.2	23	231.684	208.303
597	2011/8/1	23:58:18	SZOH36	6.2	39	208.295	207.310

598	2011/8/1	23:58:18	SZOH33	6.2	38	118.555	138.546
599	2012/6/18	5:32:31	IWTH23	6.2	50	142.837	126.306
600	2014/3/14	2:07:06	EHMH12	6.2	64	226.850	149.252
601	2014/3/14	2:07:08	HRSH07	6.2	96	167.486	176.852
602	2014/3/14	2:07:08	HRSH13	6.2	92	190.009	155.555
603	2014/3/14	2:07:06	EHMH11	6.2	67	169.284	125.838
604	2014/3/14	2:07:11	EHMH02	6.2	121	118.942	144.973
605	2014/3/14	2:07:06	HRSH14	6.2	75	88.363	163.028
606	2014/3/14	2:07:07	EHMH05	6.2	85	143.131	140.223
607	2014/3/14	2:07:12	HRSH10	6.2	125	107.680	157.768
608	2014/3/14	2:07:03	YMGH15	6.2	32	84.317	151.976
609	2014/3/14	2:07:07	EHMH07	6.2	82	144.169	76.719
610	2002/11/3	12:37:58	MYGH11	6.1	81	145.152	214.072
611	2002/11/3	12:37:57	MYGH04	6.1	72	95.047	214.263
612	2002/11/3	12:37:54	MYGH03	6.1	44	128.300	165.733
613	2002/11/3	12:37:55	IWTH23	6.1	50	122.769	135.395
614	2002/11/3	12:37:57	IWTH05	6.1	68	102.476	118.723
615	2004/10/27	10:40:56	NIGH01	6.1	20	442.553	399.588
616	2004/10/27	10:40:53	NIGH12	6.1	9	336.859	397.214
617	2004/10/27	10:40:56	FKSH21	6.1	26	300.134	411.291
618	2004/10/27	10:40:56	NIGH09	6.1	29	287.207	219.538
619	2004/10/27	10:40:59	NIGH06	6.1	40	184.464	198.453
620	2004/10/27	10:40:56	NIGH15	6.1	27	89.063	214.508
621	2004/10/27	10:40:58	NIGH11	6.1	29	194.378	108.214
622	2004/10/27	10:41:01	NIGH08	6.1	57	120.911	182.062
623	2004/10/27	10:40:57	NIGH14	6.1	33	119.814	172.908
624	2004/10/27	10:40:59	FKSH07	6.1	44	120.701	136.940
625	2004/10/27	10:41:01	TCGH07	6.1	59	141.802	100.541
626	2004/12/14	14:56:13	RMIH05	6.1	9	236.099	340.433
627	2004/12/14	14:56:17	SRCH02	6.1	36	268.915	187.459
628	2011/3/11	17:37:03	FKSH20	6.1	30	194.840	159.609
629	2011/3/11	17:40:47	MYGH10	6.1	68	194.987	220.871
630	2011/3/11	17:39:55	FKSH19	6.1	53	179.801	186.829
631	2011/3/19	18:56:20	IBRH13	6.1	1	526.091	1026.463
632	2011/3/19	18:56:22	IBRH14	6.1	10	382.583	407.210
633	2011/3/19	18:56:27	IBRH12	6.1	23	168.451	145.192

634	2011/3/19	18:56:30	TCGH16	6.1	51	210.413	106.835
635	2011/3/19	18:56:24	IBRH16	6.1	22	184.066	187.667
636	2011/3/19	18:56:37	IBRH11	6.1	60	139.692	154.187
637	2011/3/19	18:56:28	TCGH13	6.1	35	132.513	127.817
638	2011/3/19	18:56:33	IBRH18	6.1	47	148.428	96.652
639	2011/3/19	18:56:37	FKSH10	6.1	60	133.913	123.837
640	2011/3/31	16:15:40	IWTH27	6.1	51	129.250	139.422
641	2011/3/31	16:15:40	IWTH23	6.1	50	151.460	82.394
642	2011/8/12	3:22:16	FKSH12	6.1	59	170.796	153.968
643	2011/8/12	3:22:13	FKSH14	6.1	18	148.294	140.119
644	2011/8/12	3:22:18	FKSH09	6.1	78	176.308	82.502
645	2011/8/12	3:22:19	FKSH18	6.1	80	158.223	149.409
646	2011/8/12	3:22:17	FKSH19	6.1	68	144.457	157.435
647	2011/8/12	3:22:16	IBRH13	6.1	56	91.286	152.616
648	2012/3/14	21:05:07	CHBH14	6.1	10	187.184	167.297
649	2012/5/24	0:02:44	AOMH05	6.1	101	165.762	138.720
650	2012/8/25	23:16:25	TKCH08	6.1	18	490.466	315.525
651	2012/8/25	23:16:26	HDKH07	6.1	27	169.400	112.943
652	2014/8/10	12:43:35	AOMH05	6.1	104	122.806	140.267
653	2017/9/27	5:22:28	IWTH02	6.1	104	98.441	134.989
654	2018/6/18	7:58:37	KYTH07	6.1	13	258.986	326.450
655	2018/6/18	7:58:38	OSKH05	6.1	17	223.036	262.420
656	2018/6/18	7:58:38	KYTH08	6.1	21	191.705	119.439
657	2018/6/18	7:58:39	OSKH02	6.1	29	120.354	178.124
658	2018/6/18	7:58:37	OSKH04	6.1	12	131.333	131.218
659	2000/7/21	3:39:00	IBRH09	6.0	67	113.530	145.731
660	2000/7/21	3:39:35	TCGH13	6.0	85	151.001	127.885
661	2000/7/21	3:39:00	FKSH10	6.0	114	98.084	147.403
662	2004/10/23	18:11:04	NIGH01	6.0	20	272.204	236.577
663	2004/10/23	18:11:08	NIGH11	6.0	12	345.853	317.828
664	2004/10/23	18:11:49	NIGH06	6.0	49	168.368	202.758
665	2004/10/23	18:11:14	NIGH12	6.0	14	171.466	177.258
666	2004/10/23	18:11:30	NIGH09	6.0	41	163.933	150.703
667	2004/11/29	3:36:44	KSRH10	6.0	37	194.185	203.918
668	2011/3/11	16:30:14	FKSH19	6.0	51	163.376	105.032
669	2011/3/23	7:12:33	FKSH12	6.0	24	140.429	252.174

670	2013/5/18	14:48:12	MYGH10	6.0	70	141.196	210.945
671	2013/5/18	14:48:16	MYGH07	6.0	101	146.012	100.090
672	2013/5/18	14:48:14	FKSH19	6.0	84	127.641	102.886
673	2013/8/4	12:29:04	MYGH13	6.0	68	154.884	318.996
674	2013/8/4	12:29:08	MYGH07	6.0	102	238.118	213.564
675	2013/8/4	12:29:03	MYGH11	6.0	56	108.044	203.430
676	2013/8/4	12:29:06	MYGH03	6.0	85	164.541	110.560
677	2013/8/4	12:29:06	IWTH05	6.0	87	118.061	147.088
678	2001/4/27	2:49:17	NMRH02	5.9	104	205.028	143.454
679	2001/4/27	2:49:17	NMRH05	5.9	96	135.970	131.045
680	2004/11/8	11:16:01	NIGH01	5.9	13	262.365	224.592
681	2011/3/12	4:30:14	NGNH29	5.9	12	214.797	393.177
682	2011/4/11	20:42:40	FKSH12	5.9	29	130.657	172.682
683	2011/4/11	20:42:41	IBRH12	5.9	31	185.877	167.285
684	2011/4/11	20:42:41	FKSH11	5.9	37	144.979	141.517
685	2011/4/11	20:42:43	FKSH09	5.9	47	104.668	133.834
686	2011/4/16	11:19:43	IBRH11	5.9	18	262.080	176.242
687	2012/4/1	23:04:36	FKSH12	5.9	52	177.480	123.776
688	2012/4/1	23:04:38	FKSH18	5.9	70	103.315	159.428
689	2013/4/17	21:03:42	MYGH13	5.9	32	115.433	285.409
690	2013/4/17	21:03:44	MYGH03	5.9	51	170.012	123.578
691	2013/9/20	2:25:12	IBRH06	5.9	19	342.878	321.386
692	2013/9/20	2:25:13	FKSH14	5.9	25	197.962	272.801
693	2013/9/20	2:25:13	FKSH12	5.9	22	85.908	255.727
694	2013/9/20	2:25:16	IBRH12	5.9	41	184.028	170.787
695	2013/9/20	2:25:18	FKSH20	5.9	55	172.814	135.011
696	2014/7/5	7:42:13	IWTH14	5.9	21	148.602	145.947
697	2016/4/16	1:45:08	KMMH16	5.9	10	384.504	371.539
698	2016/4/16	1:45:14	KMMH02	5.9	33	348.187	272.890
699	2016/4/16	1:42:59	KMMH03	5.9	16	183.434	162.469
700	2016/4/16	1:44:11	KMMH01	5.9	33	155.502	155.976
701	2016/4/16	1:43:28	OITH11	5.9	55	133.159	123.271
702	2016/4/16	3:02:39	KMMH02	5.9	18	127.432	148.564
703	2016/11/12	6:43:10	MYGH13	5.9	31	122.490	311.233
704	2016/11/12	6:43:12	IWTH05	5.9	50	157.274	179.687
705	2017/10/6	23:56:55	IBRH12	5.9	80	158.089	231.536

706	2017/10/6	23:56:54	FKSH09	5.9	71	99.447	180.138
707	2017/10/6	23:56:54	FKSH18	5.9	71	136.825	69.517
708	2004/4/12	3:06:23	KSRH10	5.8	43	138.911	185.885
709	2004/4/12	3:06:26	KSRH03	5.8	68	167.536	105.314
710	2004/8/10	15:13:40	IWTH14	5.8	21	144.330	140.906
711	2004/8/10	15:13:44	IWTH02	5.8	66	115.848	128.377
712	2004/10/25	6:05:04	FKSH21	5.8	33	217.298	332.183
713	2004/10/25	6:05:01	NIGH01	5.8	12	354.611	243.514
714	2004/10/25	6:05:02	NIGH12	5.8	12	190.716	247.516
715	2004/10/25	6:05:04	NIGH09	5.8	28	147.412	150.012
716	2005/4/20	6:11:33	FKOH03	5.8	28	290.285	264.603
717	2005/4/20	6:11:37	FKOH08	5.8	55	144.540	118.641
718	2006/4/21	2:50:42	SZOH35	5.8	10	141.860	129.887
719	2011/3/11	14:52:01	IBRH13	5.8	103	780.320	669.665
720	2011/3/11	14:52:02	IBRH14	5.8	113	196.108	212.077
721	2011/3/11	14:52:04	IBRH12	5.8	116	180.136	203.172
722	2011/3/11	14:52:04	FKSH10	5.8	116	132.643	213.048
723	2011/3/11	14:51:49	FKSH20	5.8	30	146.888	81.224
724	2011/3/20	21:03:56	IWTH18	5.8	41	102.728	169.240
725	2011/3/23	7:35:00	FKSH12	5.8	25	145.662	267.700
726	2011/3/23	7:35:03	IBRH13	5.8	34	98.044	188.608
727	2011/8/1	22:45:01	IWTH02	5.8	75	120.176	190.892
728	2011/8/1	22:44:56	IWTH14	5.8	31	118.114	177.463
729	2014/6/16	5:15:02	FKSH12	5.8	55	174.528	126.944
730	2014/6/16	5:15:04	FKSH18	5.8	72	191.285	96.635
731	2014/6/16	5:15:04	FKSH09	5.8	72	175.897	146.428
732	2014/6/16	5:15:07	MYGH10	5.8	99	142.265	119.193
733	2016/4/14	22:05:02	KMMH16	5.8	4	559.833	464.685
734	2016/4/14	22:06:31	KMMH14	5.8	18	87.575	176.308
735	2016/4/16	3:55:56	KMMH02	5.8	16	231.503	197.069
736	2016/4/18	20:42:01	KMMH02	5.8	18	152.107	161.942
737	2018/4/9	1:32:34	SMNH04	5.8	14	181.793	551.643
738	2018/4/9	1:32:34	SMNH03	5.8	11	188.967	290.121
739	2018/4/9	1:32:37	SMNH16	5.8	31	130.315	153.469
740	2002/11/4	13:36:15	KMMH05	5.7	86	204.146	220.593
741	2002/11/4	13:36:08	MYZH15	5.7	27	207.857	175.821

742	2002/11/4	13:36:07	MYZH16	5.7	19	95.886	204.837
743	2004/10/6	23:40:54	IBRH09	5.7	55	129.822	113.333
744	2004/10/23	19:42:35	NIGH01	5.7	15	160.257	235.352
745	2008/6/14	9:18:46	IWTH25	5.7	22	210.323	781.934
746	2008/6/14	9:20:05	MYGH02	5.7	3	346.242	445.812
747	2008/6/14	9:20:11	AKTH06	5.7	19	151.755	108.566
748	2010/9/29	16:59:59	FKSH10	5.7	15	131.898	137.783
749	2011/4/13	10:08:01	IBRH13	5.7	18	163.123	200.522
750	2015/2/17	13:46:52	IWTH02	5.7	69	186.160	217.354
751	2015/2/17	13:46:50	IWTH03	5.7	50	149.140	83.484
752	2015/7/10	3:33:04	AOMH17	5.7	22	147.572	139.759
753	2015/7/10	3:33:06	IWTH02	5.7	61	112.025	161.539
754	2017/2/28	16:49:15	FKSH18	5.7	73	166.928	226.276
755	2017/2/28	16:49:11	FKSH20	5.7	34	150.261	103.787
756	2017/2/28	16:49:18	MYGH07	5.7	98	104.053	114.757
757	2001/4/25	23:40:17	EHMH01	5.6	35	158.565	151.421
758	2004/11/27	7:42:46	TKCH08	5.6	19	160.389	163.934
759	2011/4/12	7:26:20	NGNH29	5.6	18	116.582	161.684
760	2011/7/8	3:35:53	FKSH12	5.6	51	107.584	137.816
761	2011/10/10	11:46:11	FKSH18	5.6	84	100.919	299.708
762	2012/4/30	0:02:24	IWTH14	5.6	30	113.918	192.254
763	2012/8/30	4:05:25	IWTH05	5.6	71	156.071	156.590
764	2012/8/30	4:05:25	MYGH04	5.6	66	159.582	196.861
765	2012/10/25	19:32:39	MYGH04	5.6	72	63.929	165.924
766	2012/10/25	19:32:37	MYGH11	5.6	52	118.220	119.773
767	2014/7/8	18:05:27	IBUH05	5.6	12	330.943	239.205
768	2014/7/8	18:05:27	IBUH07	5.6	17	191.934	171.505
769	2014/9/16	12:28:40	IBRH11	5.6	40	185.080	192.866
770	2014/9/16	12:28:43	SITH11	5.6	59	115.578	159.457
771	2014/9/16	12:28:43	TCGH11	5.6	69	143.880	156.453
772	2014/9/16	12:28:43	SITH10	5.6	59	132.961	151.235
773	2014/9/16	12:28:46	GNMH12	5.6	86	124.287	119.438
774	2014/9/16	12:28:42	TCGH14	5.6	55	158.740	119.230
775	2014/9/16	12:28:43	IBRH15	5.6	65	115.069	121.170
776	2014/9/16	12:28:42	SITH06	5.6	52	133.467	112.359
777	2017/6/25	7:02:17	NGNH18	5.6	7	573.387	356.707

778	2017/6/25	7:02:18	NGNH20	5.6	15	321.012	139.918
779	2000/10/8	13:17:58	SMNH02	5.5	11	161.638	285.466
780	2000/10/31	1:43:01	MIEH05	5.5	29	224.064	543.557
781	2000/10/31	1:43:05	MIEH10	5.5	60	148.551	127.854
782	2000/10/31	1:43:01	NARH05	5.5	33	137.083	157.573
783	2000/10/31	1:43:01	MIEH03	5.5	29	130.733	133.890
784	2002/2/12	22:44:54	IBRH11	5.5	88	208.527	159.190
785	2002/2/12	22:44:51	IBRH09	5.5	67	148.511	127.601
786	2010/3/13	21:46:43	FKSH18	5.5	84	158.823	119.457
787	2010/3/13	21:46:42	MYGH01	5.5	81	144.374	121.144
788	2010/10/14	22:59:04	TKCH08	5.5	21	142.723	152.933
789	2011/2/27	5:38:05	GIFH14	5.5	12	219.835	213.850
790	2011/2/27	5:38:05	GIFH16	5.5	12	199.669	116.870
791	2011/4/13	4:38:02	IWTH02	5.5	79	154.846	79.707
792	2011/7/5	19:18:44	WKYH01	5.5	2	1064.490	754.203
793	2012/7/30	7:05:19	IWTH27	5.5	82	120.715	173.434
794	2014/4/3	8:22:58	IWTH27	5.5	25	277.210	192.996
795	2014/6/15	2:31:59	IWTH14	5.5	79	68.739	161.868
796	2015/5/25	14:28:22	IBRH17	5.5	61	148.640	357.517
797	2015/5/25	14:28:26	IBRH18	5.5	95	160.346	137.470
798	2015/5/25	14:28:22	IBRH11	5.5	57	136.413	134.360
799	2016/4/19	17:52:15	KMMH07	5.5	12	142.370	146.813
800	2016/5/16	21:23:11	IBRH17	5.5	39	94.475	151.505
801	2017/8/2	2:02:09	IBRH13	5.5	4	261.585	352.087
802	2017/8/2	2:02:10	IBRH06	5.5	14	278.215	198.252
803	2017/8/2	2:02:10	IBRH14	5.5	12	163.552	261.869
804	2017/8/2	2:02:17	FKSH10	5.5	56	133.452	203.930
805	2017/8/2	2:02:11	IBRH12	5.5	20	161.232	151.981
806	2017/8/2	2:02:13	TCGH13	5.5	33	123.871	146.477
807	1999/8/21	5:33:00	NARH01	5.4	20	157.562	117.967
808	2001/4/3	4:54:31	IWTH08	5.4	39	120.478	140.468
809	2001/4/3	4:54:35	IWTH06	5.4	72	86.974	123.523
810	2004/1/6	14:51:01	MIEH06	5.4	39	251.906	87.302
811	2005/2/16	4:46:46	IBRH17	5.4	38	170.603	254.219
812	2005/2/16	4:46:49	IBRH09	5.4	61	171.947	137.783
813	2005/2/16	4:46:48	IBRH08	5.4	61	143.795	130.525

814	2005/2/16	4:46:44	IBRH10	5.4	12	87.844	127.014
815	2007/4/15	12:19:33	MIEH10	5.4	4	374.024	849.568
816	2007/4/15	12:19:35	MIEH01	5.4	22	261.309	198.615
817	2007/4/15	12:19:34	MIEH02	5.4	12	217.073	189.807
818	2007/4/15	12:19:36	MIEH03	5.4	27	148.778	144.720
819	2009/4/28	20:21:32	KSRH10	5.4	69	163.732	163.136
820	2011/3/12	15:18:51	IWTH23	5.4	59	149.524	188.055
821	2011/4/3	16:38:58	MYGH10	5.4	75	81.902	152.935
822	2011/11/21	19:16:32	HRSH06	5.4	5	223.442	361.771
823	2011/11/21	19:16:38	HRSH03	5.4	45	224.824	130.250
824	2011/11/21	19:16:34	SMNH05	5.4	23	105.118	194.041
825	2012/1/28	7:42:22	YMNH11	5.4	15	188.582	161.492
826	2012/1/28	7:43:19	KNGH18	5.4	22	102.735	168.126
827	2012/1/28	7:43:18	KNGH20	5.4	19	151.776	106.081
828	2012/3/10	2:25:32	IBRH13	5.4	9	304.414	691.192
829	2012/3/10	2:25:32	IBRH14	5.4	6	390.507	228.969
830	2013/12/31	10:03:02	IBRH14	5.4	7	290.893	279.300
831	2013/12/31	10:03:02	IBRH13	5.4	13	132.957	157.789
832	2016/4/16	9:48:36	KMMH03	5.4	17	103.813	75.975
833	2016/4/16	9:48:35	KMMH16	5.4	6	114.679	181.133
834	2016/4/16	9:48:39	KMMH02	5.4	37	162.139	64.968
835	2016/4/16	16:02:03	KMMH14	5.4	8	135.827	189.073
836	2016/7/27	23:47:27	IBRH11	5.4	43	128.283	164.638
837	2016/11/19	11:48:10	WKYH01	5.4	28	240.332	240.564
838	2016/11/19	11:48:14	MIEH05	5.4	70	169.430	225.273
839	2016/11/19	11:48:10	WKYH10	5.4	23	162.791	114.270
840	2018/4/14	4:00:16	NMRH02	5.4	80	268.665	153.945
841	2018/4/14	4:00:13	NMRH04	5.4	52	144.318	76.161
842	2018/4/14	4:00:15	NMRH03	5.4	71	115.446	115.106
843	2002/1/27	16:09:27	IWTH23	5.3	51	190.773	125.053
844	2002/1/27	16:09:26	IWTH21	5.3	45	167.784	151.648
845	2002/9/16	10:10:52	TTRH07	5.3	1	181.729	265.005
846	2002/9/16	10:10:55	TTRH03	5.3	23	156.615	181.884
847	2002/9/16	10:10:53	TTRH04	5.3	15	101.868	82.822
848	2004/2/4	15:08:39	IWTH14	5.3	44	127.487	85.261
849	2004/10/23	19:33:33	NIGH11	5.3	9	321.774	249.681

850	2004/10/23	23:33:43	NIGH12	5.3	12	155.183	179.139
851	2004/10/23	23:34:53	FKSH21	5.3	36	177.467	137.432
852	2004/10/23	23:33:33	NIGH01	5.3	12	98.881	154.650
853	2004/11/10	3:43:11	NIGH01	5.3	12	165.359	225.551
854	2007/3/25	18:11:49	ISKH05	5.3	15	306.265	263.123
855	2007/3/25	18:11:52	ISKH03	5.3	36	170.764	126.379
856	2007/3/25	18:11:50	ISKH02	5.3	19	144.285	86.110
857	2007/4/26	9:03:04	EHMH03	5.3	7	228.001	184.808
858	2007/4/26	9:03:04	KOCH13	5.3	15	204.603	253.437
859	2007/4/26	9:03:06	KGWH02	5.3	36	125.619	159.926
860	2007/4/26	9:03:08	KGWH01	5.3	50	151.844	154.194
861	2008/6/16	23:14:39	IWTH25	5.3	2	547.286	687.711
862	2008/6/16	23:14:42	AKTH04	5.3	23	221.759	116.228
863	2008/6/16	23:14:41	IWTH26	5.3	14	184.908	214.552
864	2011/3/19	8:49:33	IBRH13	5.3	11	289.692	301.118
865	2011/3/19	8:48:14	IBRH14	5.3	18	150.468	110.586
866	2011/4/30	14:06:40	FKSH14	5.3	41	145.921	139.056
867	2011/11/20	10:23:42	IBRH14	5.3	4	385.980	484.459
868	2011/11/20	10:23:43	IBRH13	5.3	10	165.504	280.272
869	2012/3/1	7:32:41	IBRH18	5.3	8	223.082	174.758
870	2012/3/1	7:32:44	IBRH11	5.3	44	192.798	116.562
871	2016/10/20	11:50:00	CHBH06	5.3	16	96.426	170.671
872	2016/10/20	11:50:01	IBRH20	5.3	19	73.954	139.894
873	2017/7/11	11:56:39	KGSH09	5.3	18	260.162	460.185
874	2017/7/11	11:56:39	KGSH10	5.3	20	182.382	102.584
875	2017/7/11	11:56:42	KGSH07	5.3	37	145.818	176.794
876	2004/11/4	8:57:33	NIGH01	5.2	2	164.001	215.048
877	2008/3/8	1:55:08	IBRH11	5.2	43	118.165	118.836
878	2008/7/5	16:49:16	IBRH11	5.2	79	173.054	224.621
879	2008/7/5	16:49:13	IBRH16	5.2	50	175.168	201.686
880	2008/8/22	19:59:59	IBRH15	5.2	31	151.617	148.522
881	2008/8/22	19:59:59	IBRH16	5.2	29	188.852	144.907
882	2008/8/22	20:00:00	IBRH11	5.2	43	161.740	153.282
883	2008/8/22	19:59:58	IBRH18	5.2	9	170.177	144.690
884	2009/2/18	6:47:09	GIFH12	5.2	11	344.004	363.457
885	2010/7/4	4:33:14	IWTH26	5.2	10	214.828	194.550

886	2011/6/4	1:57:34	SMNH12	5.2	19	211.303	219.166
887	2011/6/4	1:57:34	SMNH04	5.2	13	86.021	155.877
888	2011/9/21	22:30:59	IBRH13	5.2	6	379.192	357.300
889	2011/9/21	22:30:59	IBRH14	5.2	6	347.628	220.361
890	2011/9/21	22:31:02	IBRH12	5.2	26	125.524	87.312
891	2012/2/19	14:54:52	IBRH14	5.2	7	191.573	210.645
892	2012/2/19	14:54:51	IBRH13	5.2	5	183.764	142.662
893	2012/7/10	12:48:59	NGNH07	5.2	10	192.704	135.046
894	2012/8/22	10:33:14	TKCH08	5.2	18	148.745	108.863
895	2012/8/26	3:37:15	FKSH19	5.2	64	131.899	105.783
896	2012/11/24	5:21:40	MYGH11	5.2	52	80.809	206.327
897	2012/12/21	17:07:30	IWTH27	5.2	50	100.386	151.961
898	2012/12/21	17:07:28	MYGH13	5.2	35	84.699	134.984
899	2013/7/23	12:02:15	FKSH12	5.2	16	190.111	168.933
900	2015/8/6	18:22:40	IBRH12	5.2	52	159.612	117.989
901	2015/8/6	18:22:39	IBRH11	5.2	44	153.439	141.053
902	2015/8/6	18:22:38	IBRH15	5.2	31	148.151	89.625
903	2015/8/6	18:22:38	IBRH16	5.2	30	164.944	119.363
904	2015/8/6	18:22:37	IBRH18	5.2	8	144.271	76.712
905	2016/8/31	19:46:06	KMMH14	5.2	16	97.119	141.502
906	1999/4/25	21:27:00	IBRH09	5.1	25	161.553	169.781
907	2001/1/4	13:18:25	NIGH14	5.1	11	244.533	316.093
908	2001/1/4	13:18:28	NIGH11	5.1	24	203.190	133.089
909	2001/1/4	13:18:26	NIGH19	5.1	17	111.445	115.081
910	2001/4/3	23:57:23	NGNH14	5.1	56	120.365	134.874
911	2001/8/25	22:21:29	KYTH04	5.1	16	189.693	118.476
912	2004/11/8	11:32:21	NIGH09	5.1	18	194.838	142.949
913	2004/11/8	11:32:20	NIGH01	5.1	15	129.029	191.975
914	2004/11/8	11:32:24	NIGH10	5.1	33	77.890	140.893
915	2009/12/18	8:44:38	SZOH35	5.1	4	86.705	178.486
916	2011/4/14	7:35:51	IBRH13	5.1	2	658.233	536.271
917	2011/4/14	7:35:52	IBRH14	5.1	10	163.904	328.441
918	2011/4/14	7:35:54	IBRH16	5.1	22	199.494	185.855
919	2011/6/14	21:49:08	NMRH05	5.1	55	147.702	117.195
920	2012/1/23	20:45:53	FKSH12	5.1	58	155.902	183.009
921	2012/6/1	17:48:20	TCGH15	5.1	59	115.704	212.022

922	2014/9/3	16:24:20	TCGH07	5.1	6	280.865	247.580
923	2014/9/3	16:24:21	TCGH08	5.1	11	131.072	153.390
924	2015/2/6	10:25:15	TKSH05	5.1	9	488.920	418.788
925	2017/7/1	23:45:57	IBUH01	5.1	10	279.507	191.735
926	2017/7/1	23:45:59	SRCH09	5.1	30	133.594	72.816
927	2018/3/30	8:17:42	IBRH18	5.1	9	184.882	135.429
928	2018/3/30	8:17:45	IBRH12	5.1	51	160.712	104.745
929	2004/10/23	21:44:32	NIGH01	5.0	18	122.852	133.904
930	2004/12/30	22:29:58	MYGH04	5.0	32	104.342	107.045
931	2005/1/1	5:14:06	FKSH19	5.0	80	178.104	128.782
932	2005/7/28	19:15:45	GNMH06	5.0	30	136.388	123.695
933	2007/6/11	3:45:16	ISKH04	5.0	8	160.897	72.204
934	2009/12/17	23:45:25	SZOH35	5.0	5	180.204	299.607
935	2011/2/27	2:19:01	GIFH14	5.0	12	119.445	186.089
936	2011/3/30	22:19:15	IBRH16	5.0	54	128.948	160.478
937	2011/4/1	19:49:46	AKTH09	5.0	8	197.375	259.125
938	2011/4/1	19:49:47	AKTH08	5.0	13	160.818	218.614
939	2011/4/1	19:49:54	AOMH18	5.0	56	128.332	175.291
940	2011/4/19	23:10:33	IBRH16	5.0	75	181.335	261.376
941	2011/4/19	23:10:29	TCGH06	5.0	33	75.454	184.593
942	2011/4/19	23:10:30	IBRH17	5.0	47	58.470	74.673
943	2012/3/18	9:36:48	IWTH02	5.0	114	128.514	87.524
944	2015/6/4	4:34:16	KSRH01	5.0	7	168.650	205.473
945	2016/4/14	23:43:22	KMMH16	5.0	3	109.047	104.437
946	2016/4/19	20:47:06	KMMH07	5.0	10	141.039	209.784

Reference

[A-1] 吉敷祥一, 大河原勇太, 山田 哲, 和田 章, 免震構造用 U 字形鋼材ダンパーの繰り返し変形性能に関する研究, 日本建築学会構造系論文集, 第 73 巻, 第 624 号, pp.333-340, 2008.2

(Kishiki S et al. Experimental evaluation of cyclic deformation capacity of U-shaped steel damagers for base-isolated structures. Journal of Structural and Construction Engineering (Transactions of AIJ) 2008;73(624):333–340.)

[A-2] Miner MA. 1945. Cumulative damage in fatigue. Journal of Applied Mechanics 67:A159–A164.

[A-3] Tavernelli JF, Coffin JF Jr. Experimental support for generalized equation predicting low cycle fatigue. Journal of Basic Engineering, (Trans. ASME) 1962;84:533–41.

[A-4] Ene D, Kishiki S, Yamada S, Jiao Y, Konishi Y, Terashima M, Kawamura N. Experimental study on the bidirectional inelastic deformation capacity of U-shaped steel dampers for seismic isolated buildings. Earthquake Engineering & Structural Dynamics 2016;45(2):173–192.

[A-5] Kishiki S, Ene D, Yamada S, Terashima M, Konishi Y, Kawamura N. Deformation capacity of U-shaped damages subjected to random bi-directional loadings. Bi-directional characteristics of U-shaped steel dampers for base-isolated structures Part 2 (In Japanese). Journal of Structural and Construction Engineering (Transactions of AIJ) 2014;79(704):1457–67.

[A-6] Bommer J, Martinez-Pereira A. The effective duration of earthquake strong motion. Journal of Earthquake Engineering 1999;3(2):127–172.

[A-7] Arias A. A measure of earthquake intensity, In Seismic Design for Nuclear Power Plants, R. J. Hansen (ed.), Cambridge, MA, 1970, 438–483, The MIT Press.